1-D Modeling and optimization of a hybrid locomotive powertrain utilizing Hydrogen Fuel Cell and Battery Integration

MTech. Thesis

By Dhruv Rajesh Gavande (2302106001)



DEPARTMENT OF CEVITS INDIAN INSTITUTE OF TECHNOLOGY INDORE

May 2025

1-D Modeling and optimization of a hybrid locomotive powertrain utilizing Hydrogen Fuel Cell and Battery Integration

A THESIS

Submitted in partial fulfillment of the requirements for the award of the degree of Master of Technology

by

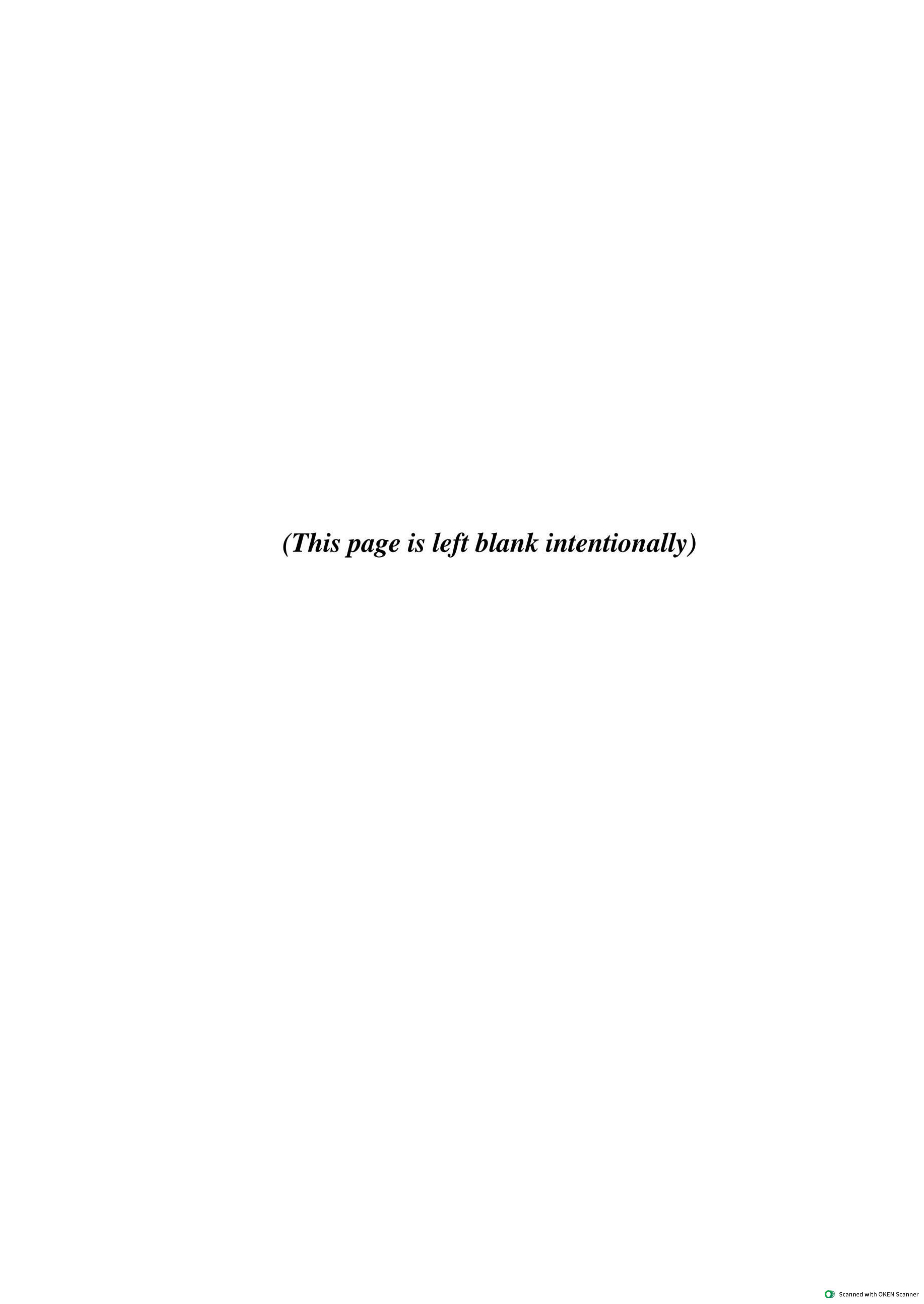
Dhruv Rajesh Gavande (2302106001)



Department of CEVITS

INDIAN INSTITUTE OF TECHNOLOGY INDORE

May 2025





INDIAN INSTITUTE OF TECHNOLOGY INDORE

CANDIDATE'S DECLARATION

I hereby certify that the work which is being presented in the thesis entitled, "1-D Modeling and optimization of a hybrid locomotive powertrain utilizing Hydrogen Fuel Cell and Battery Integration" in the partial fulfilment of the requirements for the award of the degree of MASTER OF TECHNOLOGY and submitted to the Department of CEVITS, Indian Institute of Technology Indore, is an authentic record of my own work carried out as a part of my internship at 'Wabtec Corporation'. The work presented in this thesis is original, except where references are provided, and has been conducted under the supervision of Dr. Devendra Deshmukh, Professor, Department of Mechanical Engineering, Indian Institute of Technology Indore and under guidance of professionals within 'Wabtec Corporation'. This thesis has not been submitted in part or full for any other degree or diploma at any university or institution. All sources of information and assistance received during this research have been duly acknowledged.

Signature of the student (Dhruv Rajesh Gavande)

This is to certify that the above statement made by the candidate is correct to the best of my/our knowledge.

Signature of the Supervisor

(Dr. Devendra Deshmukh)

Date:

Mr. Dhruy Rajesh Gayande has successfully given his M. Tech. Oral Examination

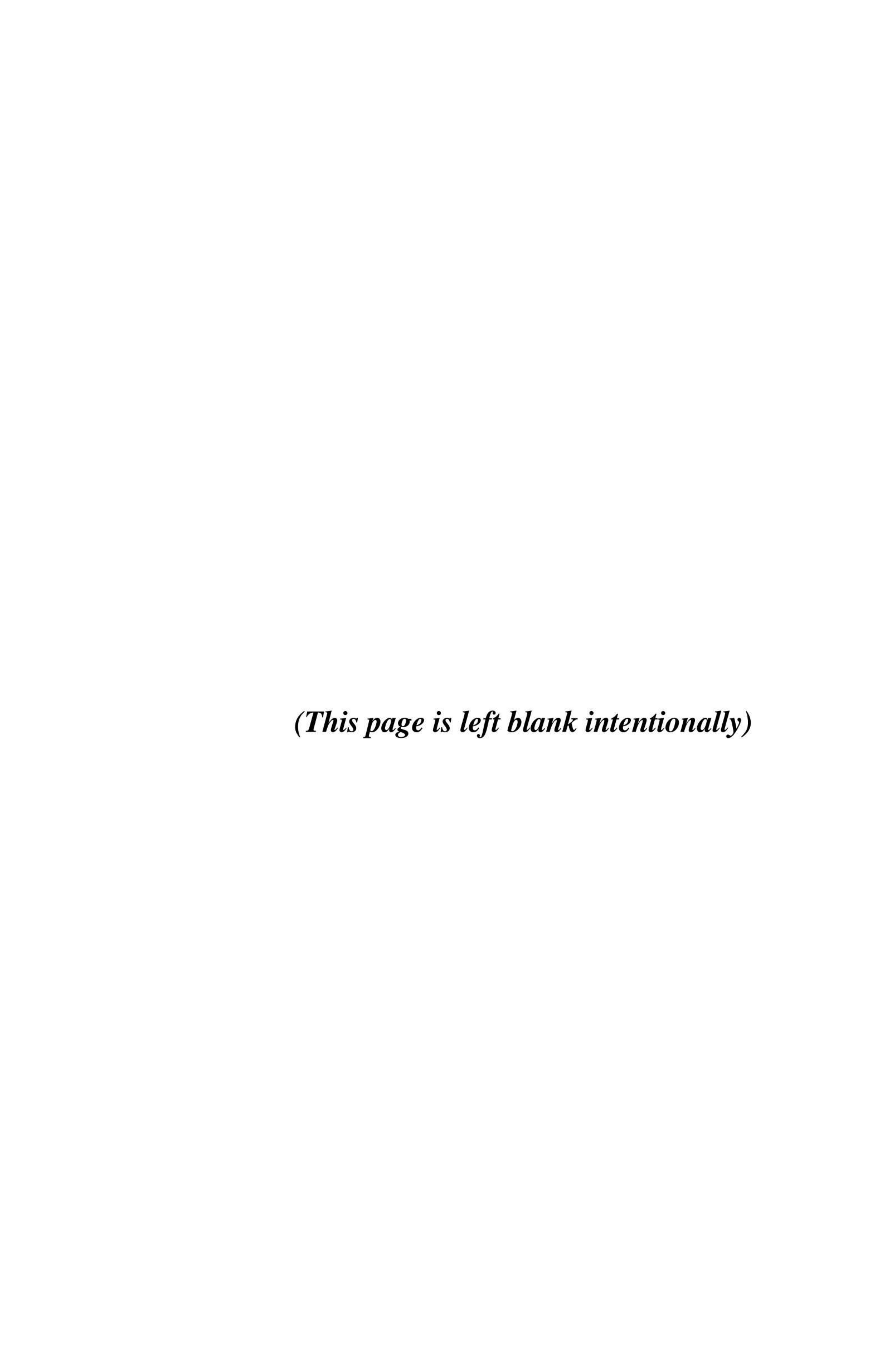
Mr. Dhruv Rajesh Gavande has successfully given his M. Tech. Oral Examination held on 8th May 2025

Signature(s) of the Supervisor(s) of M. Tech. thesis

Date:

Convener, DPGC

Date: 9.5.25



ACKNOWLEDGEMENT

My deep gratitude goes first to my supervisor, **Dr. Devendra Deshmukh**, who expertly guided me throughout my two years of Master of Technology. I was fortunate to have advisors who offered me the constant motivation and productive support that preceded this work to attain this form.

I would like to extend my sincere gratitude to 'Wabtec Corporation' for providing me with the opportunity to work on this project as part of my internship. The invaluable resources and supportive environment greatly contributed to the development of my research. I am especially grateful to Mr. Chandra Kesavan and Mr. Raseen Mohammed for their unwavering guidance, insightful feedback, and encouragement throughout this journey. Their expertise and mentorship have been instrumental in shaping the direction of this work

I cannot end my words without expressing my heartfelt thanks and admiration for my dear parents' blessings and efforts to maintain my morale throughout my project. I also want to express my sincere gratitude to everyone. who has assisted me during this duration in any way, whether directly or indirectly, during this project.

With Regards,

Dhruv Rajesh Gavande

Dedicated

to

my beloved

Parents

ABSTRACT

Sustainable transportation is the key research area today in which most of the industries are investing. In the railway industry, research has been inclined towards hybrid locomotives. This project focuses on design and optimization of a hybrid locomotive powertrain that incorporates 'Polymer Electrolyte Membrane Fuel cell' and 'Battery' as the power sources for propelling the locomotive. This will lead to environmental sustainability and reduced operational cost and. This report outlines the methodology and results of the project.

The proposed design in the project will be replacing the conventional Diesel-electric locomotive powertrain which utilizes the combination of diesel engine and alternator to provide electric power to the traction motor. The entire design will be a system level simulation in 'GT-ISE', a tool under the package of GT-Suite. The design starts with understanding the technical specifications provided as a baseline. This is followed by deriving energy balance algorithms or control logics through some literature survey and brainstorming sessions. GT-ISE was then used to create the physics-based model of Fuel cell and battery, implement the derived control logic and integrate this logic with the physics-based model. 'Design of Experiments (DOE)' is then carried out on the developed system level model. Optimum hardware configurations and corresponding control parameter values are obtained from these DOE outcomes.

The outcome of the simulation was the Fuel cell stack rating and battery pack rating required to cater the power demand at minimum total cost. This work provides valuable insights into the development of eco-friendly powertrain systems and contributes to the advancement of sustainable transportation technologies

TABLE OF CONTENT

A	ACKNOWLEDGEMENT	. j
A	ABSTRACT	V
]	TABLE OF CONTENT	vii
Ι	LIST OF FIGURES	xi
Ι	LIST OF TABLES	XV
ľ	NOMENCLATUREx	Vii
A	ACRONYMSx	ix
(Chapter 1	. 1
1	Introduction	1
1.1	Conventional Diesel-Electric locomotive layout	2
1.2	Fuel cell	3
	1.2.1 Working of a hydrogen fuel cell	3
	1.2.2 Types of fuel cell	4
	1.2.3 Fuel cell performance factors	5
1.3	Organization of thesis	. 8
1.4	Couplings for HEVs	. 7
1.5	Organization of the Thesis	9
(Chapter 2	10
2	Literature Review	10
	2.1 Objectives	11
(Chapter 3	12
3	Proposed powertrain layout	12
3.1	Introduction	12
	3.2 Type of hybrid powertrain operating modes	13
(Chapter 4	14

4 D	esign requirements	14
4.1	Problem statement	14
4.2	Technical requirements	14
Chapter	5	16
5 E	nergy balance algorithms	16
5.1	Types of energy balance algorithms	17
5.2	Algorithm 1 – Fuel cell power-based algorithm	19
5.3	Algorithm 2 – Fuel cell efficiency-based algorithm	21
5.4	Algorithm 3 - Battery State of charge (SOC) based algorithm	
Chapter	6	24
6 S	imulation model	24
6.1	0D vs 1D simulations	24
6.2	Introduction to GT-ISE	25
6.3	Mathematical model for Fuel cell power-based algorithm	26
	6.3.1 Templates used in simulation	30
6.4	Mathematical model for Fuel cell efficiency-based algorithm	31
6.5	Mathematical model for Battery SOC-based algorithm	32
6.6	Parameter values	
Chapter	7	34
7 D	Design of Experiments	34
7.1	Introduction to Design of Experiments	34
7.2	Methodology for Design of Experiments	35
7.3	Total cost calculations	36
7.4	DOE – FC Power-based algorithm	37
	7.4.1 Sensitivity analysis – FC power-based algorithm	41
7.5	DOE-FC efficiency-based algorithm	44

7.6	DOE-Battery SOC-based algorithm47
Chapte	r 8 51
8 1	Results from mathematical model51
8.1	Results-FC power-based algorithm51
8.2	Results-FC efficiency-based algorithm54
8.3	Results-Battery SOC-based algorithm56
8.4	Results comparison58
Chapte	r 9 60
9 1	FC physics-based model60
9.1	FC PEM template59
9.2	Results comparison – FC Mathematical model & FC physics-based model
Chapte	r 10 68
10	Conclusion & future scope68
10.1	Conclusion
10.2	Puture scope
REFER	ENCES71

List of Figures

Figure 1 Conventional diesel-electric locomotive layout	2
Figure 2 Hydrogen fuel cell	3
Figure 3 Polarization curve of fuel cell	7
Figure 4 Powertrain layout block diagram	8
Figure 5 Route map (Power demand curve)	. 15
Figure 6 Energy balance algorithms	17
Figure 7 Fuel cell power-based algorithm	19
Figure 8 Efficiency based algorithm flowchart	21
Figure 9 Variation of efficiency curve with temperature	21
Figure 10 Battery SOC based algorithm flowchart	22
Figure 11 Mathematical model for Fuel cell power-based algorithm	26
Figure 12 FC mathematical model	28
Figure 13 Battery and BMS model	29
Figure 14 Output power calculation subassembly	29
Figure 15 Efficiency to power conversion	32
Figure 16 Mathematical model – Battery SOC-based algorithm	32
Figure 17 DOE Methodology	. 35
Figure 18 Variation of minimum battery cells and total cost with no. of FC modules	39
Figure 19 Hydrogen Cons. variation with Upper & Lower	40
Figure 20 Percentage Energy deficit variation with Upper & Lower Power limit factors	41

Figure 21 Sensitivity analysis of hardware parameters for perc. energy deficit – FC power-based algorithm	42
Figure 22 Sensitivity analysis of control parameters for perc. energy	42
Figure 23 Sensitivity analysis of hardware parameters for total	43
Figure 24 Sensitivity analysis of hardware parameters for total	43
Figure 25 Sensitivity analysis of control parameters for	46
Figure 26 Sensitivity analysis of control parameters for total cost	46
Figure 28 Sensitivity analysis of control parameters for perc. energy deficit—Batte SOC-based algorithm	ery
Figure 29 Power demand vs power output	52
Figure 30 Battery SOC	52
Figure 31 Percentage of total energy delivered	53
Figure 32 Battery power request vs Max. allowed discharge power	53
Figure 33 FC efficiency	54
Figure 34 Power demand vs power output – FC efficiency-based algorithm	55
Figure 35 Battery SOC – FC efficiency-based algorithm	55
Figure 36 FC efficiency curve – FC efficiency-based algorithm	56
Figure 37 Power demand vs power output –Battery SOC-based algorithm	57
Figure 38 Battery SOC plot –Battery SOC-based algorithm	57
Figure 39 FC efficiency and FC power–Battery SOC-based	58
Figure 40 FC efficiency comparison	58

Figure 41 No. of battery cells comparison	59
Figure 42 Total cost comparison	59
Figure 43 FC physics-based model	61
Figure 44 FC physics-based model flow circuit	62
Figure 45 FC physics-based model power OP vs power demand	64
Figure 46 FC efficiency comparison	65
Figure 47 Hydrogen comparison – FC Mathematical Model vs FC physics-based model	65
Figure 48 Anode stoichiometric ratio	66
Figure 49 Hydrogen mass flow rate	66
Figure 50 Polarization curve obtained from the model	67

List of Tables

Table 1 Fuel cell efficiency	6
Table 2 Parameter values	33
Table 3 Hardware parameters and constraints	36
Table 4 Factors and their ranges – FC Power-based algorithm	38
Table 5 DOE1 optimum results – FC power-based algorithm	39
Table 6 Control parameters – FC power-based algorithm	40
Table 7 Final optimum configuration - FC power-based algorithm	41
Table 8 Factors and their ranges – FC efficiency-based algorithm	44
Table 9 DOE1 outcome – FC efficiency-based algorithm	45
Table 10 Control parameters – FC efficiency-based algorithm	45
Table 11 Final optimum configuration - FC efficiency-based algorithm	45
Table 12 Factors and their ranges – Battery SOC-based algorithm	47
Table 13 Final optimum configuration - Battery SOC-based algorithm	47
Table 14 Control parameters - Battery SOC -based algorithm	48
Table 15 Final optimum configuration - Battery SOC-based algorithm	48
Table 16 Results – FC power-based algorithm	51
Table 17 Results – FC efficiency-based algorithm	55
Table 18 Results - Battery SOC-based	56
Table 19 FC physics-based model parameters	61

NOMENCLATURE

Hydrogen pressure in bars P Density of hydrogen (kg/m³ ρ characteristic gas constant for hydrogen R hydrogen temperature in ⁰C Pipe cross sectional area for FC physics-based model A Di Inner diameter of the pipe in meters Velocity of hydrogen in pipe in m/sec Mass flow rate of hydrogen (kg/sec) ṁ hydrogen mass fraction in the incoming flow X Volumetric flow rate (kg/m³) Q

ACRONYMS

FC Fuel cell

AC Alternating current

DC Direct current

SR Stoichiometric ratio

SOC State of charge

DOE Design of experiments

LL Lower limit

UL Upper limit

CP Chargin power

DP Discharge power

PEMFC Proton exchange membrane fuel cell

Chapter 1

1.0 Introduction

In railway industry, diesel locomotives have been widely used for the freight or good transportation purpose owing to their better efficiency, high torque output and longevity. However, it is evident that diesel engines produce extensive number of harmful emissions, especially NOx. Owing to this, there has been wide research going on to derive an environmentally sustainable alternative for the diesel engines in locomotives.

Right from the initial stages wherein steam locomotives were used, the research regarding locomotive propulsion has come a long way. Today, almost all the transit or passenger trains employ electric locomotives i.e. Powered by electricity from overhead lines or a third rail. However, some of the reasons for which freight trains still employ diesel-electric locomotives are infrastructure limitations in rural areas, cost considerations, long-haul efficiency of diesel locomotives, etc. But due to government incentives, growing environmental awareness and advancement in technology, various greener powertrain alternatives like hybrid locomotives wherein a hybrid powertrain is used utilizing engine — battery combinations to propel the traction motor, battery electric locomotives, hybrid powertrain 'hydrogen fuel cell' — 'battery' locomotives have gained traction and are getting into limelight. Hydrogen fuel cell is the most sustainable of all the above-mentioned alternatives since these cells only give water vapor as a byproduct and no harmful chemicals. Moreover, hydrogen can be produced using renewable energy sources such as solar, wind or hydropower which makes the entire process sustainable and ecofriendly.

This research focuses on design and optimization of a hybrid locomotive that utilizes 'Hydrogen fuel cell' and 'battery' to produce electric power for traction motor which in turn drives the locomotive wheels.

In this section, we will delve into some general aspects of a fuel cell including its types, construction and working and explore the typical layout of a conventional diesel-electric locomotive.

1.1 Conventional Diesel-Electric locomotive layout

Traction motors are the main driving source for the locomotive wheels. Electric power is provided to these motors by diesel engine using an alternator.

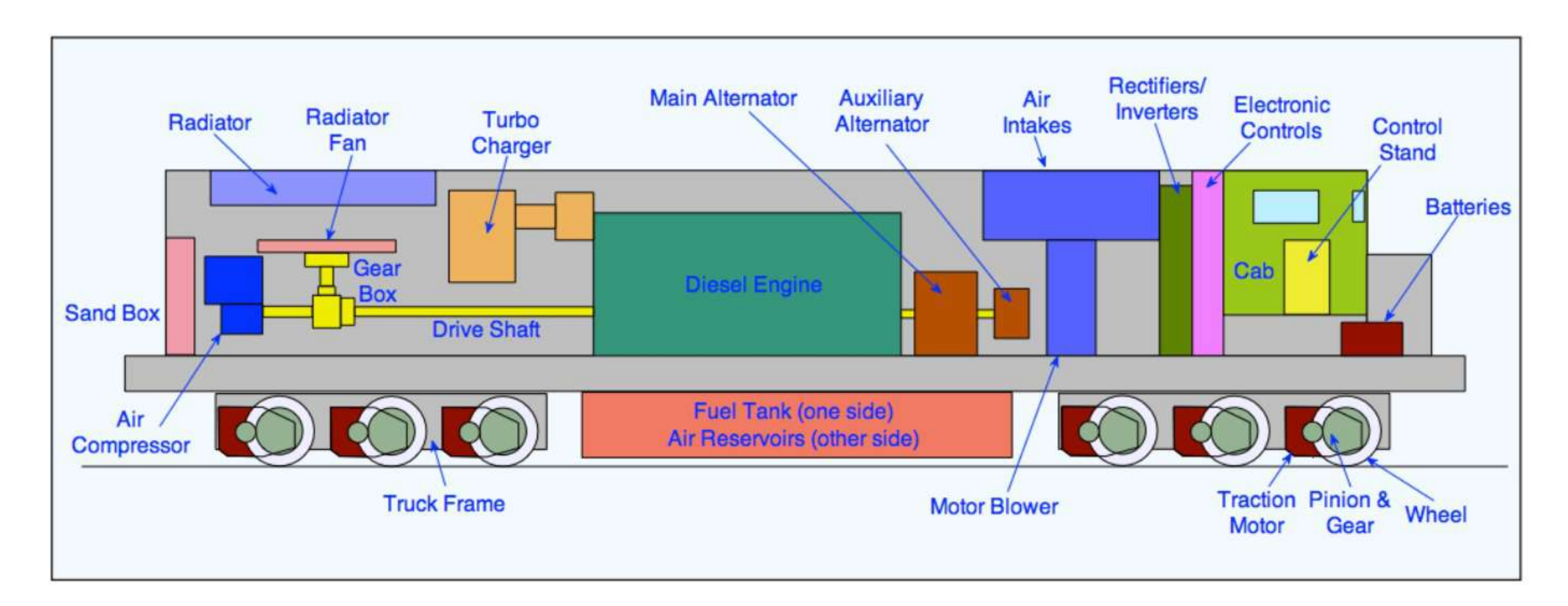


Figure 1 – Conventional diesel-electric locomotive layout [1]

The above figure represents this conventional layout. Diesel engine is mechanically coupled with an alternator. Alternator converts mechanical energy into electrical energy which is then supplied to the traction motors through various power electronic devices like rectifier, chopper or DC-DC converter and inverter. Layout also consists of other components like the air compressor, radiator, turbocharger but are not in the scope of this research.

The electric power from the alternator is processed in different ways depending on the type of alternator and traction motor:[1]

- 1. DC DC type where the DC generator supplies power to DC traction motors;
- 2. AC DC type where AC alternator output is rectified to supply it to DC motors
- 3. AC DC AC type where AC alternator output is rectified to DC and then is inverted to 3-phase AC for supplying it to the traction motors

1.2 Fuel cell

Fuel cell converts the chemical energy of a fuel into electrical energy. As a byproduct, we get is mainly the electricity, water and heat. It is noteworthy that fuel cells operate like batteries but are not energy storage devices. Fuel cell will continue to produce power until hydrogen is supplied to it.

1.2.1 Working of a hydrogen fuel cell

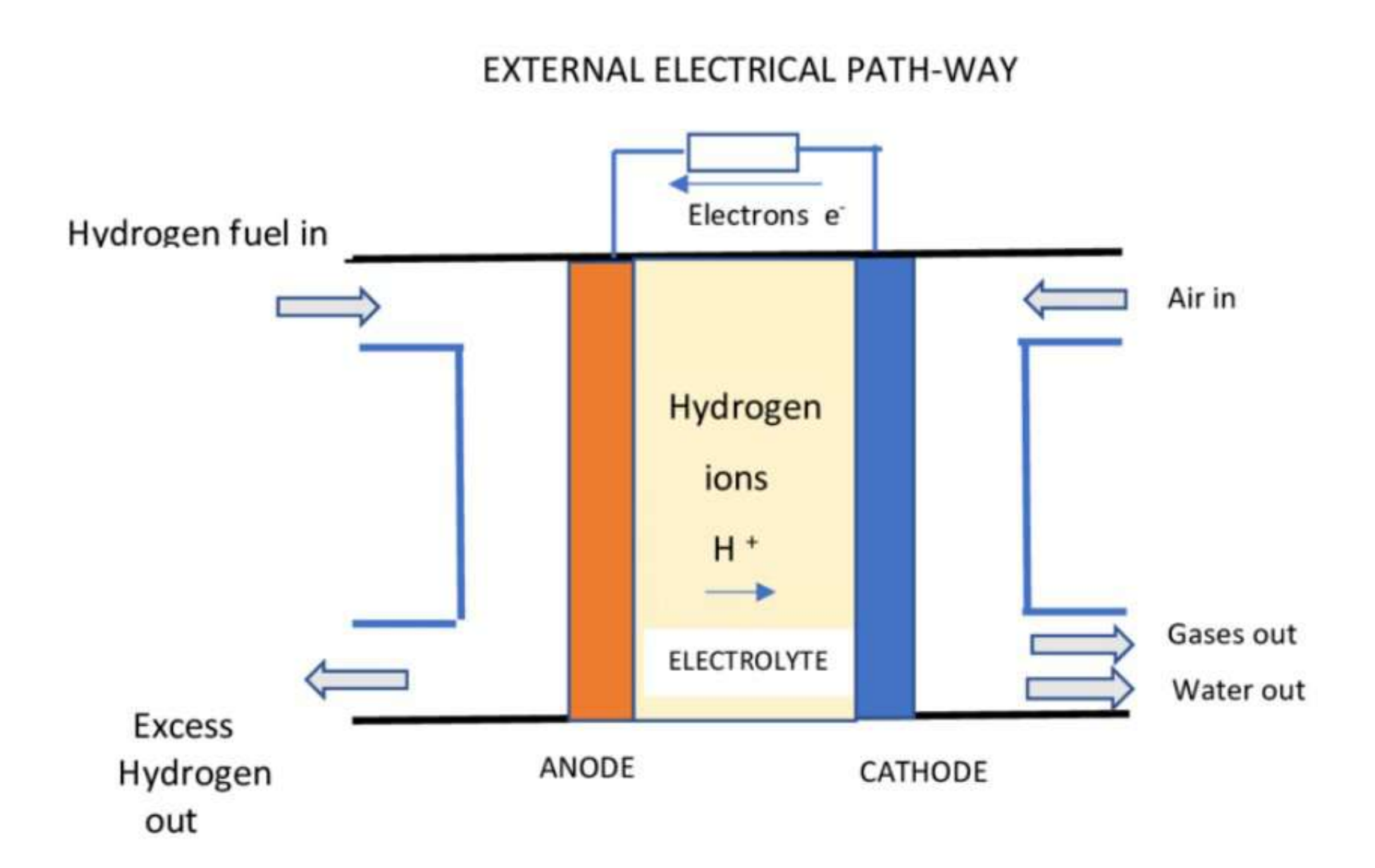


Figure 2 – Hydrogen fuel cell [2]

A fuel cell consists of two electrodes, negative electrode i.e. anode and positive electrode i.e. cathode with electrolyte in between. For a typical hydrogen fuel cell, hydrogen will be passed through the anode and oxygen through the cathode. Anode consists of a catalyst, generally Platinum which separates hydrogen molecules into protons and electrons. The electrons go through an external circuit, creating a flow of electricity. The protons migrate through the electrolyte to the cathode, where they unite with oxygen and the electrons to produce water and heat. The overall reaction can be given as follows -

$$2H_2 + O_2 \rightarrow 2H_2O$$

The net cell potential produced by this reaction is equal to the difference between the electrochemical potentials of the oxygen reduction reaction and the hydrogen oxidation reaction. Continuous removal of the reaction product keeps the system in a steady state.

1.2.2 Types of fuel cells [3]

In the domain of fuel cells, their classification primarily revolves around the type of electrolyte they utilize. This classification is instrumental in defining the specific electro-chemical processes within the cell, the necessary catalysts, the temperature range of operation, the type of fuel required, and other pertinent aspects.

Polymer electrolyte membrane fuel cell

Low operating temperature fuel cells (FCs) that use a polymer membrane as the electrolyte are known as polymer electrolyte membrane fuel cells PEMFCs are also known as proton exchange membrane FCs because the polymer membranes conduct H+ ions. The operating temperature of PEM fuel cells is comparatively low, at about 80°C. Low-temperature operation improves durability by reducing wear on system components and enabling them to start more quickly.

Direct methanol fuel cells

Because it employs a polymer membrane as an electrolyte, it is comparable to the PEM cell. Nevertheless, a fuel reformer is not required because the platinum-ruthenium catalyst on the DMFC anode can extract the hydrogen from liquid methanol. Thus, the name comes from the fact that pure methanol can be used as fuel.

Alkaline fuel cell

AFCs are typically powered by pure hydrogen and employ an alkaline electrolyte, such as potassium hydroxide in water. Although the original AFCs ran at temperatures ranging from 100 to 250 degrees Celsius, modern AFCs typically run at 70 degrees. A range of non-precious metals can be utilized as catalysts to accelerate the reactions at the anode and cathode because of the low operating temperature, which eliminates the need for a platinum catalyst in the system. The most common catalyst in AFC units is nickel. These cells provide comparatively high fuel to electricity conversion efficiencies, up to 60% in certain applications, because of the speed at which the chemical reactions occur.

Solid oxides fuel cell

The maximum operating temperature for solid oxide fuel cells is between 800 and 1,000 degrees Celsius, which is the highest of all fuel cell types. When converting fuel to electricity, they can achieve efficiencies of more than 60%; if the heat they generate is also captured, their total efficiency in converting fuel to energy can reach more than 80%. An additional benefit of the high operating temperature is that it improves reaction kinetics, negating the need for a metal catalyst. The high temperature does have certain drawbacks, though: these cells require protection to stop heat loss, they require sturdy, heat-resistant materials to be built, and they take longer to start up and reach operating temperature.

1.2.3 Fuel cell performance factors

Single cell voltage

Ideally, the reversible cell potential should be 1.23 Volts[4]. Practically, this voltage is not achieved even at open circuit due to irreversibility. Since a single cell doesn't generate enough voltage for most applications, multiple cells are connected in series to form a stack. The total voltage is the sum of all individual cell voltages.

Current density

The current density of a fuel cell refers to the amount of electric current generated per unit area of the fuel cell's active surface. It is typically measured in amperes per square centimetre (A/cm²). Current density is a critical parameter in fuel cell performance, as it influences the efficiency, power output, and operational characteristics of the cell.

Fuel cells operate within specific current density ranges to optimize performance. At low current densities, activation losses dominate, while at moderate densities, ohmic losses become significant. At high current densities, concentration polarization (mass transport losses) can occur, leading to reduced efficiency. Depending on the membrane material, current density varies from 0.75 A/cm² (conventional Nafion) to 2.25 A/cm² (for ZrO₂-Nafion)[5]

Operating temperature

Temperature has a significant impact on the performance and efficiency of a fuel cell.

Reaction kinetics - Higher temperatures enhance reaction rates, improving performance[6]

Proton conductivity - In PEMFCs, proton conductivity improves with temperature, up to a limit[7]

Ohmic losses - Increased temperature reduces electrical resistance, aiding current flow Gas diffusion - Higher temperatures improve gas diffusion, enhancing fuel and oxidant access[6]

Material constraints - Extreme temperatures can damage materials and reduce durability^[7] Values of operating temperatures depends on the type of membrane material and ranges from 50-80 °C for conventional Nafion to 120°C for Zr-O₂ – Nafion

Fuel cell efficiency[5]

Fuel cell efficiency =
$$\frac{\Delta G}{\Delta H} = \frac{Change\ in\ the\ Gibbs\ Free\ Energy}{Change\ in\ Enthalpy} = \frac{\Delta H - T * \Delta S}{\Delta H}$$

where T – Absolute temperature in Kelvin

 Δs – Change in the entropy

In simple terms, it is the ratio of the electrical energy produced by the fuel cell to the chemical energy supplied to it. Factors like fuel quality, operating temperature, load conditions, operating pressure, membrane material affect the efficiency of fuel cell

Typical efficiency values -

Fuel cell type	Efficiency (%)
PEMFC	50-60
Alkaline	70
Solid oxide	60
Molten carbonate	60-80 with cogeneration

Table 1 – Fuel cell

Polarization curve

The polarization curve of a fuel cell is a graphical representation of its performance, showing the relationship between the cell voltage and the current density. It provides

insights into the efficiency and losses within the fuel cell. The curve typically has three distinct regions

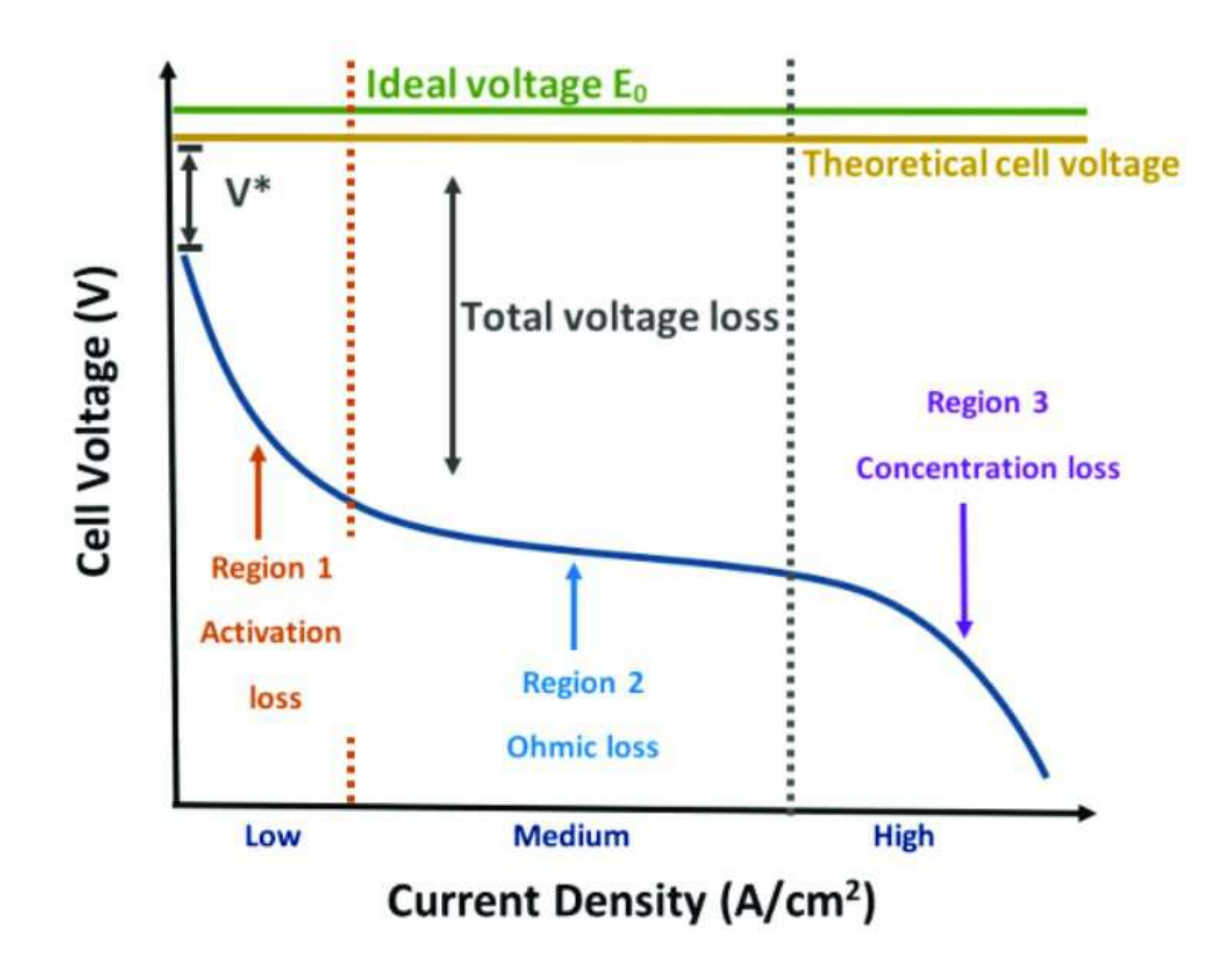


Figure 3 – Polarization curve of fuel cell[8]

The curve typically has three distinct regions:

- Activation polarization The energy needed to start the electrochemical reactions on the catalyst surface causes the voltage to decrease at low current densities.
- Ohmic polarization Resistance in the cell's constituents, such as the electrolyte
 and electrodes, causes the voltage to drop linearly with current at moderate current
 densities.
- 3. Concentration polarization As the reactant gases such as oxygen and hydrogen find it more difficult to effectively reach the reaction sites at high current densities, the voltage drop becomes more noticeable.

Owing to the polarization curve, it is always desired to operate the fuel cell in the 'Region 2' i.e. at moderate current densities or moderate load.

1.3 Organization of the thesis

In this section, an overview of the chapters included further in the report will be discussed.

Chapter 2 – Literature review

This chapter mentions the resources that were availed of during the research work.

This includes a jinx of journal, conference papers, websites along with how these helped in bridging the knowledge gap about various topics

Chapter 3 – Proposed hybrid powertrain

This chapter explains the hybrid powertrain layout using a rough schematic. It also explains about the type of hybrid that is to be designed i.e. plug-in-hybrid and its advantages

Chapter 4 – Design requirements

This chapter outlines the design requirements which are the foundation for the design. It presents a comprehensive set of technical specifications and functional constraints which serve as the guiding principles for the subsequent design and implementation phases

Chapter 5 – Energy balance algorithms

Focusing on the control logics, this chapter delves into the details of the algorithms developed for an efficient power split between the fuel cell and battery. The algorithm will be depicted in terms of flowchart and a detailed description of each case will be given

Chapter 6 – Mathematical simulation model

This chapter provides a brief on the simulation model created in GT-ISE. It also includes a short explanation on some of the important templates used in the model along with the values of important parameters in these templates

Chapter 7 – Design of Experiments

This chapter presents the DOE objectives and the methodology or steps that were followed. The outcomes of the DOE are discussed for each algorithm. The outcomes also include the sensitivity graphs which helps in identifying influential factors.

Chapter 8 – Results

Results from the optimum configuration of each algorithm are mentioned in tabular form in this chapter along with the time-variant plots of some important parameters

like the battery SOC, power output and efficiency. It is concluded with the comparison graphs of all the three algorithms and stating the best algorithm out of the three.

Chapter 9 – FC physics-based model

This chapter focuses on the physics-based model of FC. It highlights the important parameters of the model along with their values and includes some significant equations. It concludes by depicting the plots obtained from this physics-based FC model.

Chapter 10 – Conclusion and future scope

This chapter summarizes the key findings and contributions of the research, highlighting how the objectives were achieved. Additionally, potential directions for future research and possible enhancements are discussed to extend the scope of the current work.

Chapter 2

2. Literature Review

During the research, various journals, conference papers and websites were availed of to get the best insights available in the field of fuel cells and locomotives. This section cites the resources used along with their significance in overcoming the knowledge barrier during the research.

David Murray-Smith in his work "A Review of Developments in Electrical Battery, Fuel Cell and Energy Recovery Systems for Railway Applications" describes the current state of the railway industry's short-term energy storage systems, hydrogen fuel cells, and batteries. This helped to understand the basic chemistry and working of a fuel cell

The official website of the U.S Department of Energy provides great insights about the types, advantages and application of fuel cells

Vijay Ramani's "The Polymer Electrolyte fuel cell" mentions about the chemical reactions in a fuel cell, operating temperatures and operating voltage. This helped in deciding the hardware configurations of fuel cell.

Alessandro Franco's "Optimum design of bipolar plates for separate air flow cooling system of PEM fuel cells stacks" discusses about thermal management of PEM fuel cells. This article helped in understanding various performance factors of a fuel cell.

"The Operating Parameters, Structural Composition, and Fuel Sustainability Aspects of PEM Fuel Cells: A Mini Review" by Muhammad Tawalbeh, Suma ALarab, Amani Al-Othma - sustainability of different fuels for proton exchange membrane fuel cells is covered in this paper. This study primarily aided in the comprehension of how variables such as temperature and relative humidity impact fuel cell efficiency.

The paper "A Self-Validating Method via the Unification of Multiple Models for Consistent Parameter Identification in PEM Fuel Cells" by Luis Blanco, Luis

Ordonez, Sergio Pena mentions about Mathematical models used for simulating the electrochemical phenomena of proton exchange-membrane (PEM) fuel cells. This paper helped in gaining insights about the polarization curve of a fuel cell

"Optimal energy management strategies for hybrid electric vehicles: A recent survey of machine learning approaches" by Julakha Jahan Jui, Mohd Ashraf Ahmad, M.M. Imran Molla, Muhammad Ikram Mohd Rashid explains the various types of energy balance algorithms available and the discrete features of each. Study of this journal helped to form a strong foundation for such algorithms before building them

'PEMFC Lifetime and Durability - an overview is an article that puts limelight on various aspects of fuel cell like the voltage, current density, cost and life cycle. It also provides some insights into the degradation mechanisms of FC. From this research perspective, the literature was helpful for obtaining practical values of some important FC parameters.

'Fuel Cell Systems Explained' by James Larminie and Andrew Dicks helped in understanding the physics and mathematics behind calculations of hydrogen and air mass flow rates for a fuel cell.

2.1 Objective

The entire research work has been jolted down into few objectives which helped in breaking down the whole project into small tasks.

- Understanding the design requirements which helps to know the technical constraints and boundaries within which the research must be carried out. This will work as a foundation for the entire research
- 2. Developing energy balance algorithms or control logic using literature survey and brainstorming sessions with experienced personnels.
- Implement the control logic in the simulation tool 'GT-ISE' and integrate this algorithm with the mathematical model of fuel cell and physics-based battery model.
- Perform Design of Experiments using the system model and obtain optimum values of hardware parameters and control parameters using constraints and cost function

Finalize the algorithm giving minimum cost function and integrate the algorithm
with the physics-based Fuel cell model and tune the model parameters to match
the results obtained from mathematical Fuel cell model

Chapter 3

3. Proposed Powertrain layout

3.1 Introduction

The proposed locomotive powertrain design consists of a fuel cell and battery as the primary electric power source for the traction motor. Before reaching the motors, power is transferred to the power electronic circuitry. This consists of a chopper i.e. DC-DC converter and an inverter. Moreover, there is a controller in between which has the control algorithm fed into it. The fuel cell and battery power can be controlled using this controller.

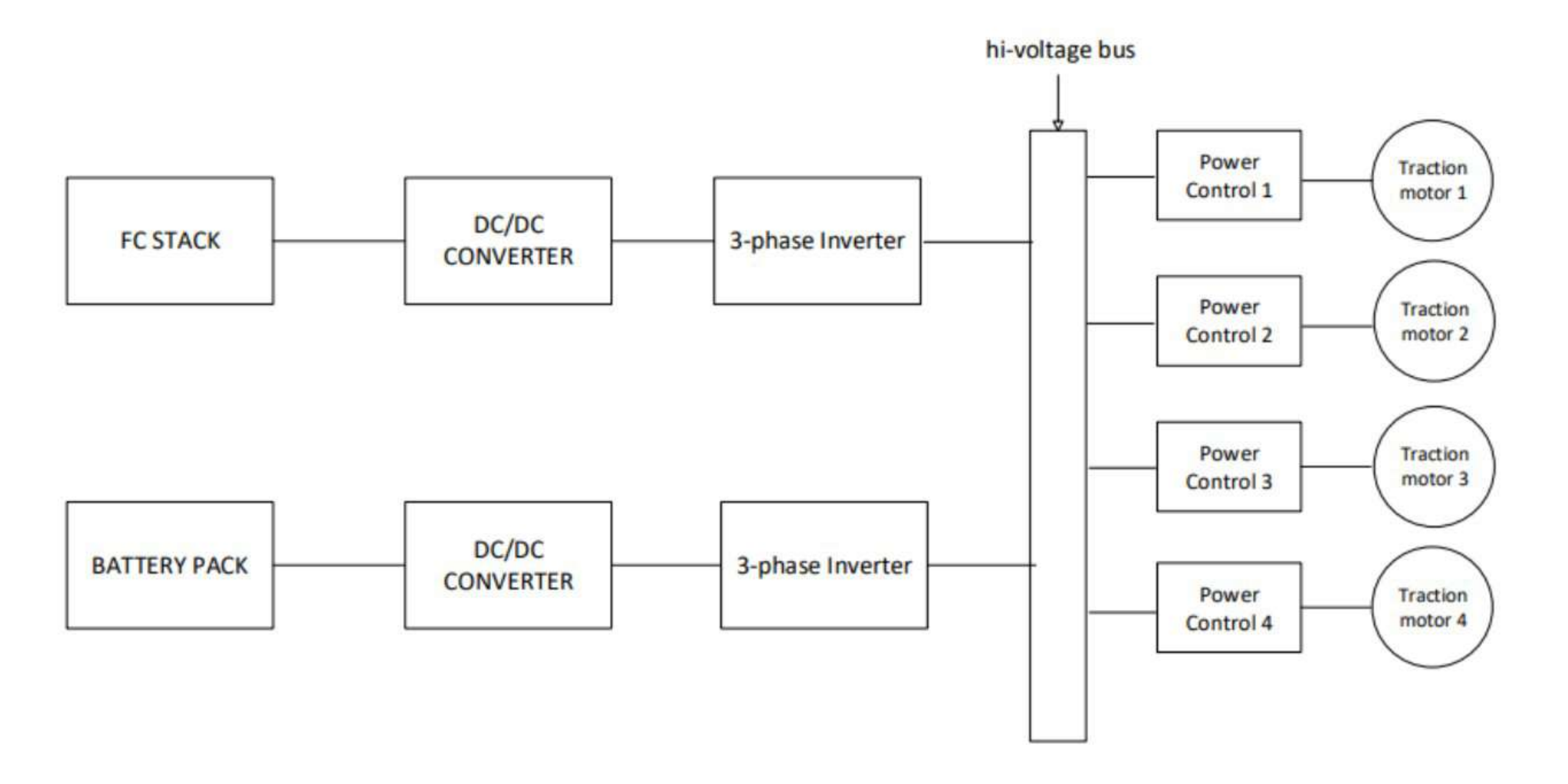


Figure 4 – Powertrain layout block diagram

Before the controller, there is a busbar that basically divides the power and distributes to the further circuitry. Purpose of the chopper is to convert the produced DC voltage into a higher voltage (using a boost converter) or a lower voltage (using a buck

converter). Also, a chopper stabilizes the fluctuating voltage which is necessary for good performance of the traction motor.

For AC traction motors, the DC supply must be converted into a three phase AC supply. A 3 – phase inverter will produce a 3-phase AC supply at required frequency. Further, the power from busbar can also be given to auxiliary components either directly or after rectifying it. Traction motors then drive the wheel through bull gear – pinion pair for final torque multiplication.

3.2 Type of hybrid powertrain operating modes -

In any hybrid vehicle based on the way the battery is charged, there are two types of operating modes –

1. Charge sustaining mode

Initial and final State of Charge (SOC) of the battery is same. This is ensured by ensuring that the energy supplied by the battery is equal the energy given to the battery i.e. the net energy must be zero. The energy is given to the battery by the primary source. i.e. in our case it is the fuel cell. This model is generally employed in hybrids where battery size is relatively small. Energy balance for such hybrids is difficult because the net energy of battery is always to be taken care of.

2. Charge depleting mode

As the name suggests, the battery initial and final SOC are not the same. A plug-in-hybrid follows this model. In case of a locomotive where the journey time and distance is fixed, it is desired that by the end of the journey, the battery ends at its set lower limit i.e. the entire battery capacity is utilized.

In this research, plug-in-hybrid i.e. charge depleting model has been designed. Once the journey is completed, the battery will be charged from an external charging station before commencing for the next trip. Electricity being cheaper as compared to the hydrogen fuel, plug-in-hybrid proves out to be a better option. This is because in case of a charge sustaining model, a large amount of fuel has to be utilized for charging the battery itself which will increase the fuel consumption which in turn will increase the total operating cost. Moreover, plug-in-hybrid gives the freedom to design a large battery pack which increases the flexibility of energy balance algorithms.

Chapter 4

4. Design Requirements

This section serves as a crucial framework, outlining the technical and functional requirements that guided the development of the proposed solution. It provides a detailed description of the essential parameters, constraints, and objectives established to meet the problem statement effectively.

4.1 Problem statement

Design of a hybrid 'fuel cell +battery' powertrain for retrofitting an existing dieselelectric locomotive into a hydrogen powered locomotive. Predict optimum power split between fuel cell and battery to meet the power demand with minimum cost

4.2 Technical Requirements

1. Fuel cell type and size -

Type – Proton exchange membrane fuel cell (PEMFC)

Baseline Power output = 480 kW

2. Battery requirements -

Baseline power output = 800 Kw

Baseline energy rating desired = 400 kW-hr

Battery SOC should be 90% at start and 40% at the end of the trip

Battery should have the option to be charged by the fuel cell

3. Operating temperature -

Temperature range = 6° C to 50° C

4. Drive cycle -

Distance of the route map = 90 km

Maximum power demand = 1517 KW

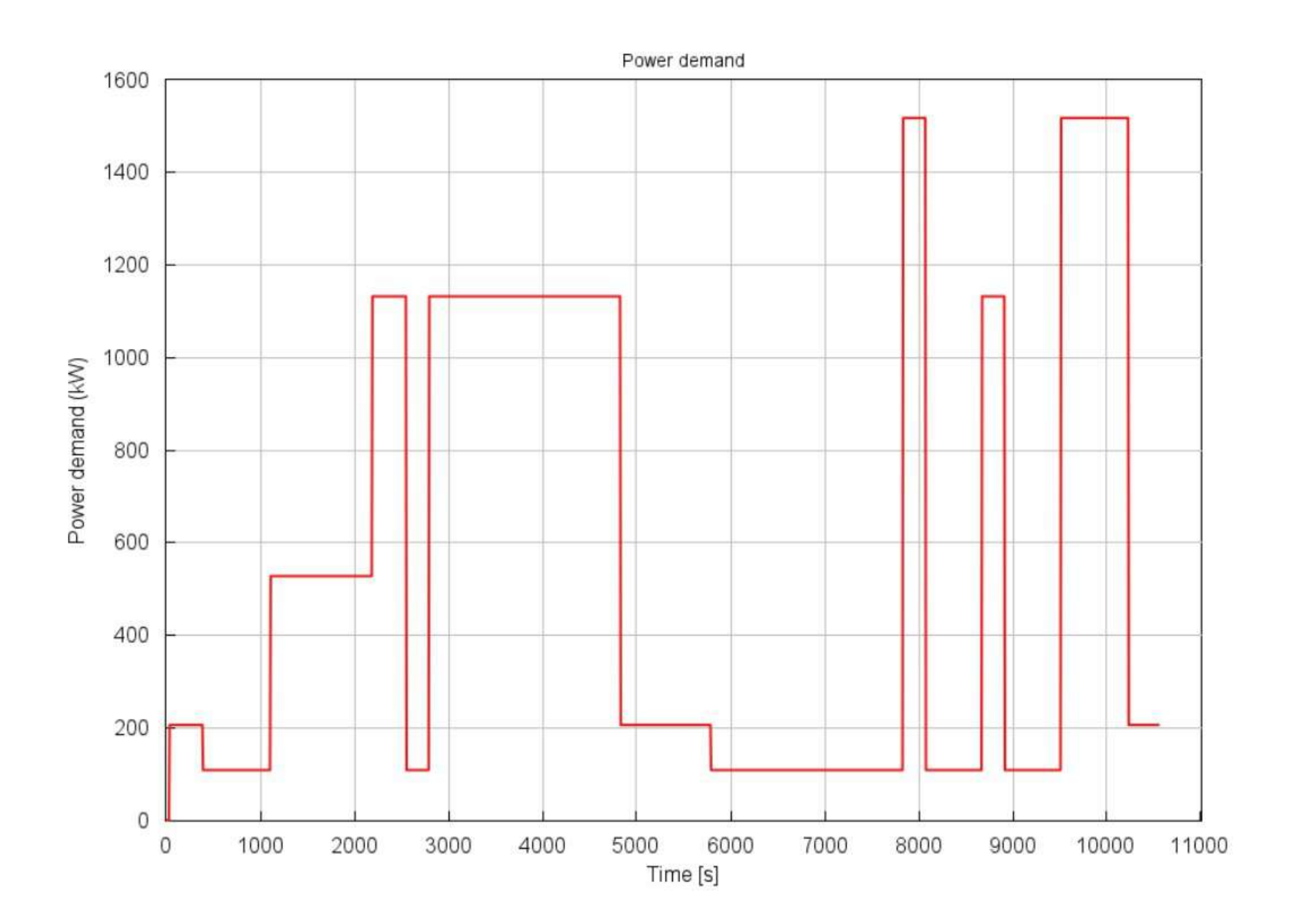


Figure 5 – Route map (Power demand curve)

The locomotive is assumed to travel at an average speed of 30 kmph throughout the journey.

The design requirements mentioned above serve as the foundational criteria that guide the development and evaluation of the proposed solution

Chapter 5

5. Energy balance algorithms

Energy balance algorithm is a control logic that splits the power demand between the available power sources. These algorithms are designed to manage the distribution and utilization of energy across various power sources, such as internal combustion engines, batteries, supercapacitors, and fuel cells. By ensuring a seamless balance between energy generation, storage, and consumption, they contribute to reducing fuel consumption, minimizing emissions, and enhancing overall system efficiency.

In hybrid locomotives, energy balance algorithms are integral to the energy management system (EMS). They enable real-time decision-making by analysing factors such as load demand, state of charge (SOC) of energy storage devices, and operational constraints. These algorithms often incorporate predictive models and optimization techniques to anticipate energy needs and allocate resources efficiently. For instance, during acceleration, the algorithm may prioritize energy from batteries or supercapacitors for quick response, while relying on fuel cells or engines for sustained power during cruising.

The development of energy balance algorithms involves addressing challenges such as dynamic load variations, regenerative braking, and the integration of multiple energy sources. Advanced control strategies, such as model predictive control (MPC) and fuzzy logic, are commonly employed to enhance the adaptability and robustness of these algorithms. Additionally, simulation tools and real-world testing are used to validate their effectiveness under diverse operating conditions.

This chapter delves into details of the various types of energy balance algorithms. Furter, it mentions various algorithms that have been derived and employed as a part of research. All the algorithms have been obtained using extensive literature survey and brainstorming.

5.1 Types of Energy Balance Algorithms

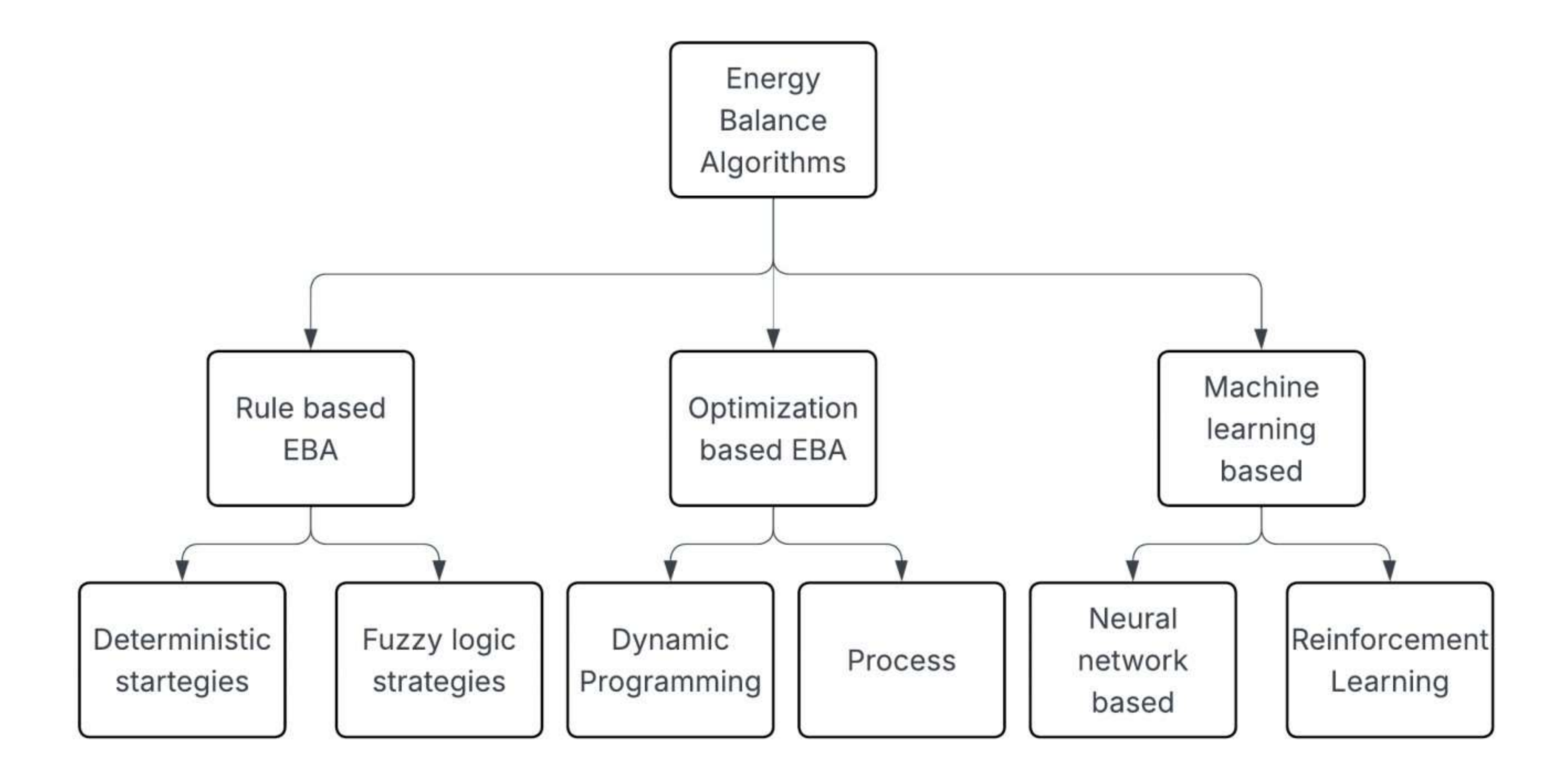


Figure 6 – Energy balance algorithms

Rule-Based Algorithms[9]

To control energy flow, these rely on preset guidelines and thresholds. Although they are easy to use, they might not always provide the best results. A set of rules that codify the expertise of engineers or subject matter experts is necessary for rule-based EMSs to operate. These rules are frequently derived from system dynamics, vehicle specifications, and engineering concepts. Every rule explains a specific circumstance or state, and the action that goes with it details the control command or method of implementation. The rule-based EMSs continuously monitor the vehicle's operating parameters while it is in motion, including the battery's level of charge, speed, and engine load. The action linked to the first rule that satisfies the requirements is performed after comparing the predefined rules with the current situation. Higher priority rules usually take precedence over lower priority rules in this hierarchical or priority-based process.

Deterministic strategy - A deterministic strategy in a rule-based energy balance algorithm refers to a predefined set of rules that govern energy distribution without relying on probabilistic or adaptive methods. This approach ensures consistent and predictable energy management based on fixed conditions

Fuzzy logic[9] - A computational method called fuzzy logic uses imprecise or uncertain data to simulate human reasoning. Fuzzy logic permits degrees of truth, which makes decision-making more adaptable and flexible than traditional binary logic, which relies on rigid true or false values.

Optimization based strategies[9]

These algorithms do not provide output simply based on a certain rule. Rather, the output will be something that satisfies the rule as well as is the most optimum value possible.

Dynamic Programming –

Mathematical optimization technique dynamic programming serves as an instrumental tool for addressing intricate problems by dissecting them into their constituent, less complex subproblems. Its efficacy is particularly pronounced for problems characterized by overlapping subproblems and optimal substructure, a property that allows the resolution of larger problems to be constructed from the solutions of their smaller counterparts. This method operates under the principle of optimality, asserting that an optimal solution to a problem encompasses optimal solutions to its subproblems.

Model Predictive Algorithm - Predicts future energy demands and adjusts accordingly.

Machine learning based algorithms[9]

Using real-time feedback and historical data, learning-based approaches use machine learning algorithms to learn and modify energy management strategies. The ability of these algorithms to learn from their past experiences and apply that knowledge to develop patterns for producing output in future scenarios makes them like humans. Both supervised and unsupervised machine learning are possible. In supervised learning, training data is created by pairing target data with input data that has been expressed as a feature. The most common applications of supervised learning are in HEV energy balance algorithms.

Reinforcement learning – Although the target data is not explicitly provided, the model is trained to maximize the reward it receives through a variety of experiences, making it a form of semi-supervised learning.

Energy balance algorithms used in this research work follow deterministic strategy.

5.2 Algorithm 1 – Fuel cell power-based algorithm

In this algorithm, power is split between fuel cell and battery by comparing the power demand with the limits that are set on the power output of the fuel cell

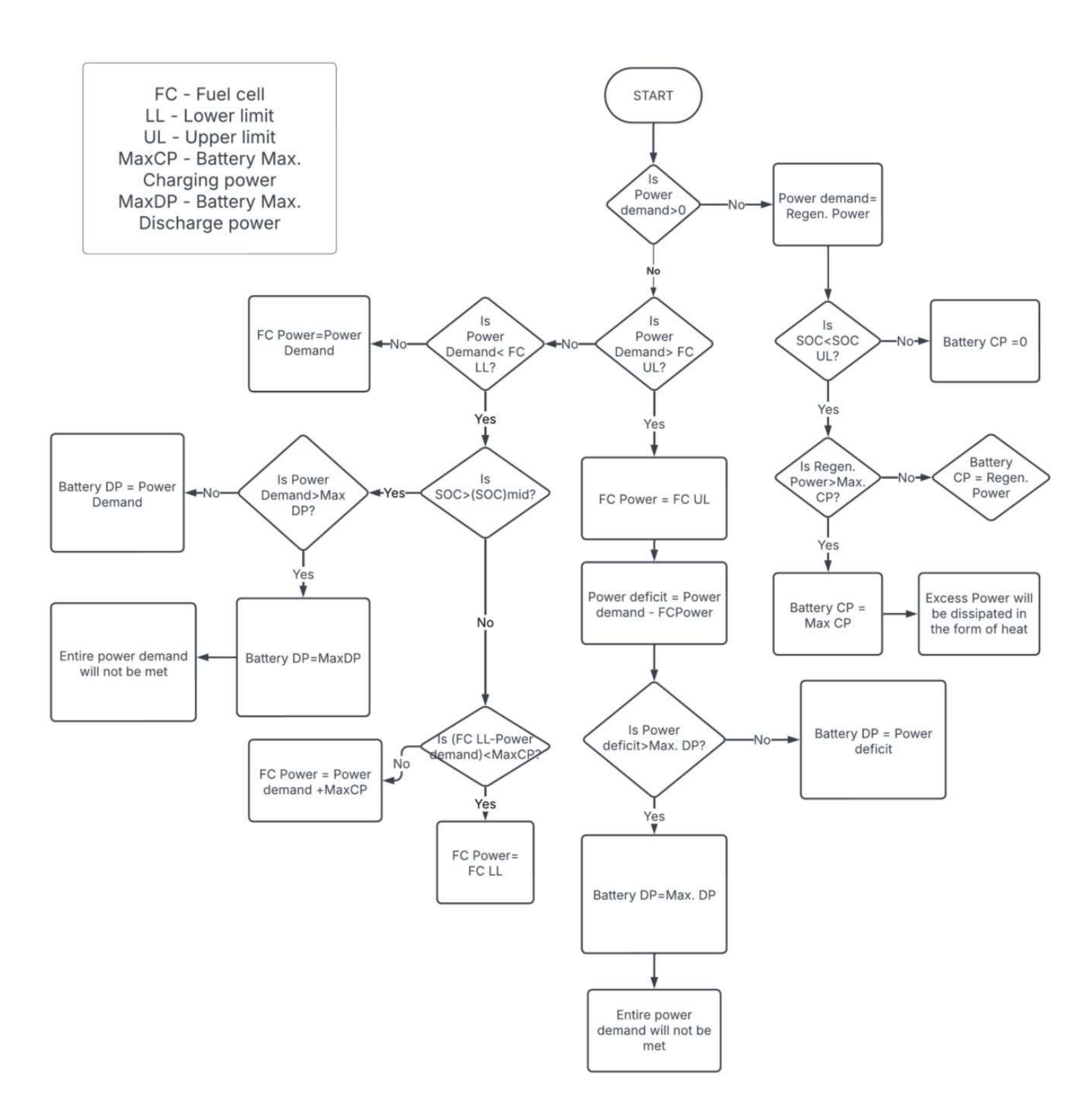


Figure 7 – Fuel cell power-based algorithm

The algorithm can be broken down into two sections. The first section is the dynamic braking mode whereas the second section is the motoring mode.

The power demand will be obtained as an input to the algorithm at each timestep. The power demand will be processed in such a way that if the value is negative, it means that power is produced through dynamic braking. This is the regenerative power and can be used to charge the battery. Before giving this power to the battery for charging, the algorithm will check if the charging power is less than the maximum allowable charging power. If it is not, then only the maximum allowable power will be sent as an input to the battery for charging. This maximum allowable power for charge and discharge is obtained through the Battery power limiter – a template in GT-ISE. Any excess regenerative power which cannot be utilized to charge the battery will be going to the grid and dissipated in the form of heat.

The second section is for the motoring mode. Initially, the instantaneous battery SOC is checked. If it is equal to the set lower limit which is 40 %, then battery cannot be discharged further. So, the entire power demand will be fulfilled by the fuel cell. On the contrary, if SOC is above the set lower limit, then the fuel cell power limits will come into picture.

If the power demand is greater than the set upper power limit of fuel cell, then fuel cell will be restricted to produce power equal to its upper power limit. The remaining power will be supplied by the battery provided that the demand power from battery is less than the maximum allowable discharge power. If not, then there will be some power deficit which cannot be met.

In second case, if the power demand is between the upper and lower limits of the fuel cell, then the entire power demand will be met by fuel cell itself, and the battery will neither charge nor discharge.

The final condition left is that the power demand is less than the set lower limit of the fuel cell. In this case, whether power demand is met by battery or fuel cell depends on the battery instantaneous SOC. If the SOC is above set limit, then the battery has enough energy to provide the power. Hence, battery will deliver the entire power demand. On the other hand, if the battery SOC is less than the set limit, then fuel cell will meet the power demand. It will produce power equal to power demand plus an additional amount of power which can be used to charge the battery

5.3 Algorithm 2 – Fuel cell efficiency-based algorithm

In this algorithm, the power demand is split between fuel cell and battery based on the efficiency limits set on the fuel cell. This algorithm is a good option if the target is to keep the efficiency within a certain limit, especially the lower limit.

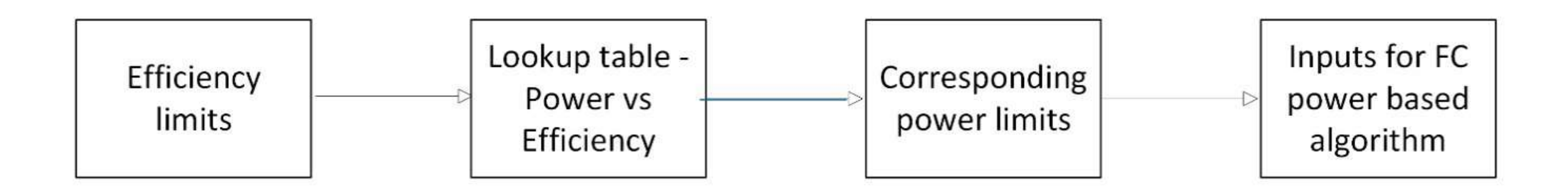


Figure 8 – Efficiency based algorithm flowchart

The set efficiency limits are given as an input to the lookup table which has efficiency as the X variable and power as the Y variable. From this lookup table, corresponding power limits are obtained. The algorithm is then similar to the power-based algorithm now as the inputs are in terms of power. So, the same logic as discussed in the previous sections will be followed.

The lookup table is obtained by first running a simulation with only fuel cell as the power source. Now this run will be at two different temperatures -6° C and 50° C.

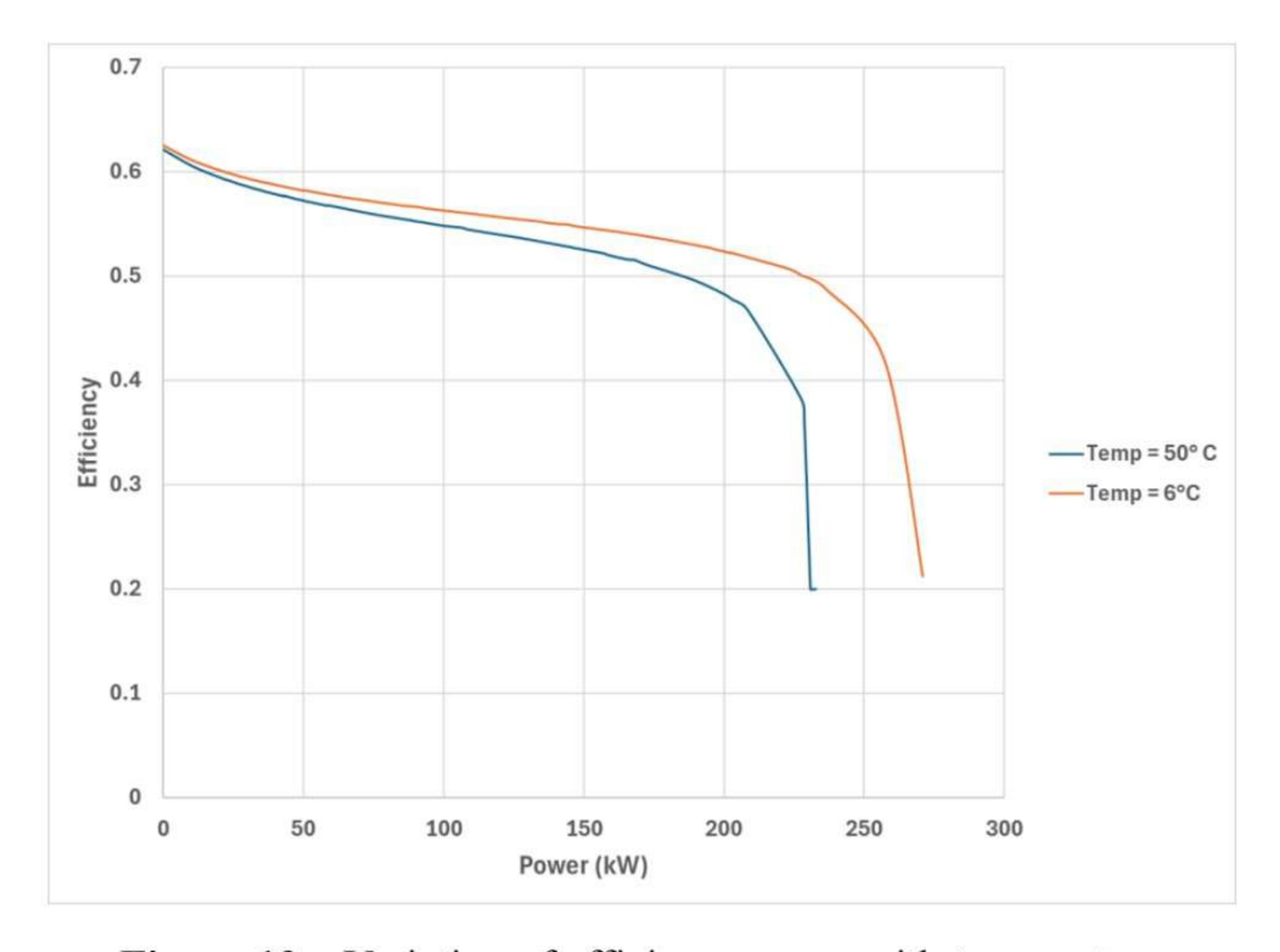


Figure 10 – Variation of efficiency curve with temperature

In the above figure, it can be observed that at a given power, efficiency of the fuel cell is more at a lower temperature as compared to that of a higher temperature.

5.4 Algorithm 3 - Battery State of charge (SOC) based algorithm

In this algorithm, the power output from battery and fuel cell i.e. the power split is determined based on instantaneous battery SOC. The main crux of this logic is to use the battery according to its available energy.

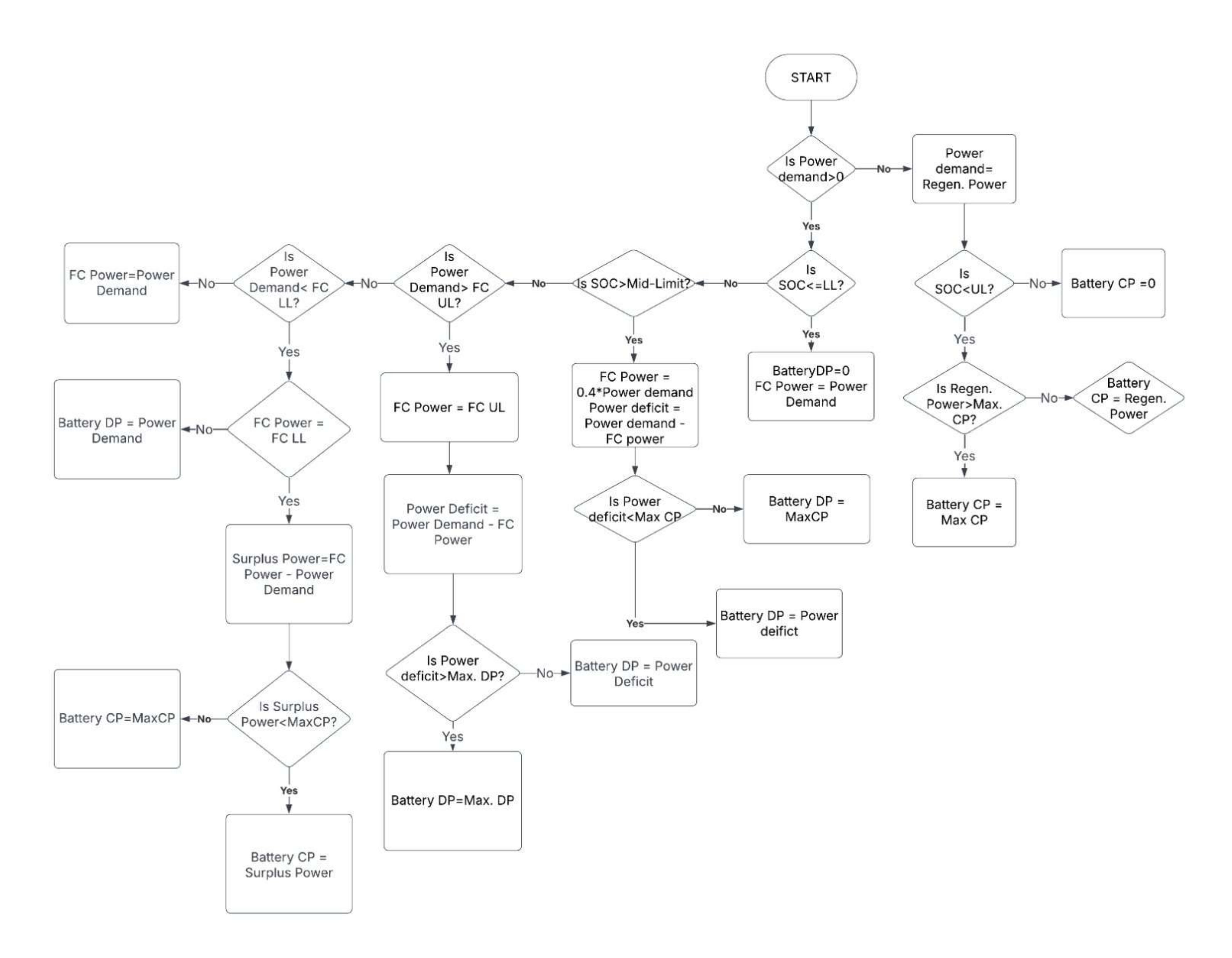


Figure 10 – Battery SOC based algorithm flowchart

The above figure depicts the logic in the form of a flowchart. As stated earlier, the objective of the algorithm is to maximize the utilization of the battery.

Similar to the previous algorithm, this is divided into two sections as well – Regenerative or dynamic braking mode and the motoring mode. Regenerative braking mode determines if the battery can take the incoming power for charging. If not, then the power goes to the grid where it is dissipated in the form of heat.

In the motoring mode, the logic first checks if the SOC is equal to lower limit. If yes, then the battery cannot be further discharged. The entire power demand is met by the fuel cell. However, if the power demand is greater than the maximum power that can be produced by the fuel cell, then fuel cell is restricted to maximum power and the entire power demand will not be met.

If the SOC is greater than the set mid-limit, then battery has enough energy to deliver. In this case, fuel cell will produce power equal to 40% of the power demand if it is less than the maximum power that can be produced by fuel cell. Else, it will produce power equal to the maximum power. Battery will provide power equal to the power deficit provided that the BMS allows it.

Finally, if the above two cases are not triggered, SOC is between lower and mid-limit. In this case, the same logic as in the first algorithm will be implemented i.e. the power split will take place based on the power limits of the fuel cell. Whenever the power demand is above upper limit, the fuel cell produces power equal to its upper limit and the deficit is met by the battery. If the power demand is within the limits of fuel cell, it will be completely met by the fuel cell. Power demand when comes out to be less than the lower limit, the power split depends on the battery SOC again.

All the algorithms mentioned in this chapter were tested on the given route map and the cost function of these algorithms were compared to obtain the best algorithm. The algorithms were implemented as mathematical models in GT-ISE which will be shown in the coming chapter.

Chapter 6

6 Simulation model

This chapter describes the system level model made in GT-ISE. It will describe the subsystems included in the model. Moreover, the chapter includes a section which illustrates the types of system level simulations.

6.1 0D vs 1D simulations

0D simulations

These are lumped parameter models where the system is represented by averaged properties rather than spatial variations. In short, these simulations include only time-variant parameters. For example, a battery model might use 0D simulations to analyse overall performance during a drive cycle. 0D simulations can be characterized by following-

- 1. Less complex systems
- 2. Small simulation time required
- 3. Less computational power required

Examples of these simulations can be found in cases of mathematical modelling wherein the physical models are represented using mathematical equations. Another uses case can be in a Map-based engine model in which the important engine parameters are correlated using a lookup table. 0D simulations do not include fluid circuits or thermal circuits.

1D simulations

These simulations include spatial variations of parameters along with time variations. They include fluid or thermal circuits. Lumped analysis is not valid in these simulations. These can be characterized by following -

- 1. Relatively complex systems
- 2. More computational time required

A simple example can be a flow through pipe where convection heat transfer takes place between the fluid and the pipe walls. Here the temperature will be varying along the pipe length which can be analysed using 1-D simulation. This type can also be understood by another example where one wants to measure the piston position with respect to TDC as the crank rotates.

6.2 Introduction to GT-ISE

GT-ISE, part of the GT-SUITE software by Gamma Technologies, is a versatile simulation environment designed for multi-physics and system-level modelling. It is analogous to other tools like Simulink. The tool consists of various templates which can include a map-based model of complex systems like engine, controls template like that of a PI controller, template representing Boolean logics like the 'If-Then Else' template, electrical templates like DC busbar, switches, DC-DC converters and many more. An entire system can be represented and simulated in the form of interconnected block(templates). Some of the significant features of GT-ISE can be jolted down as follows -

Integrated Simulation Environment: GT-ISE serves as the interface for building and managing simulation models. It allows users to create models step-by-step and control the settings of individual components, such as cylinders, pipes, combustion systems, and more.

Multi-Physics Capabilities: It supports simulations across various physical domains, including fluid dynamics, acoustics, thermal analysis, mechanical systems, and chemical kinetics.

Model Fidelity: GT-ISE enables seamless adjustment of model fidelity, from 0D (lumped parameter models) to 1D (detailed spatial resolution). This flexibility is crucial for balancing computational efficiency and accuracy

Embedded 3D CFD and FE Modelling: Users can perform computational fluid dynamics (CFD) and finite element (FE) thermal/structural modelling within the same environment, integrating boundary conditions from the surrounding system.

Optimization and Design of Experiments (DOE): It includes tools for design optimization, exploring trade-offs among objectives, and calibrating models to measured data.

GT-ISE is widely used in industries like automotive, aerospace, and energy for tasks such as engine performance analysis, thermal management, and powertrain optimization.

6.3 Mathematical model for Fuel cell power-based algorithm

The control algorithm explained in previous sections was implemented in GT-ISE using the various templates available. This logic is then connected with the battery and fuel cell mathematical models. These subassemblies will be explained in this section.

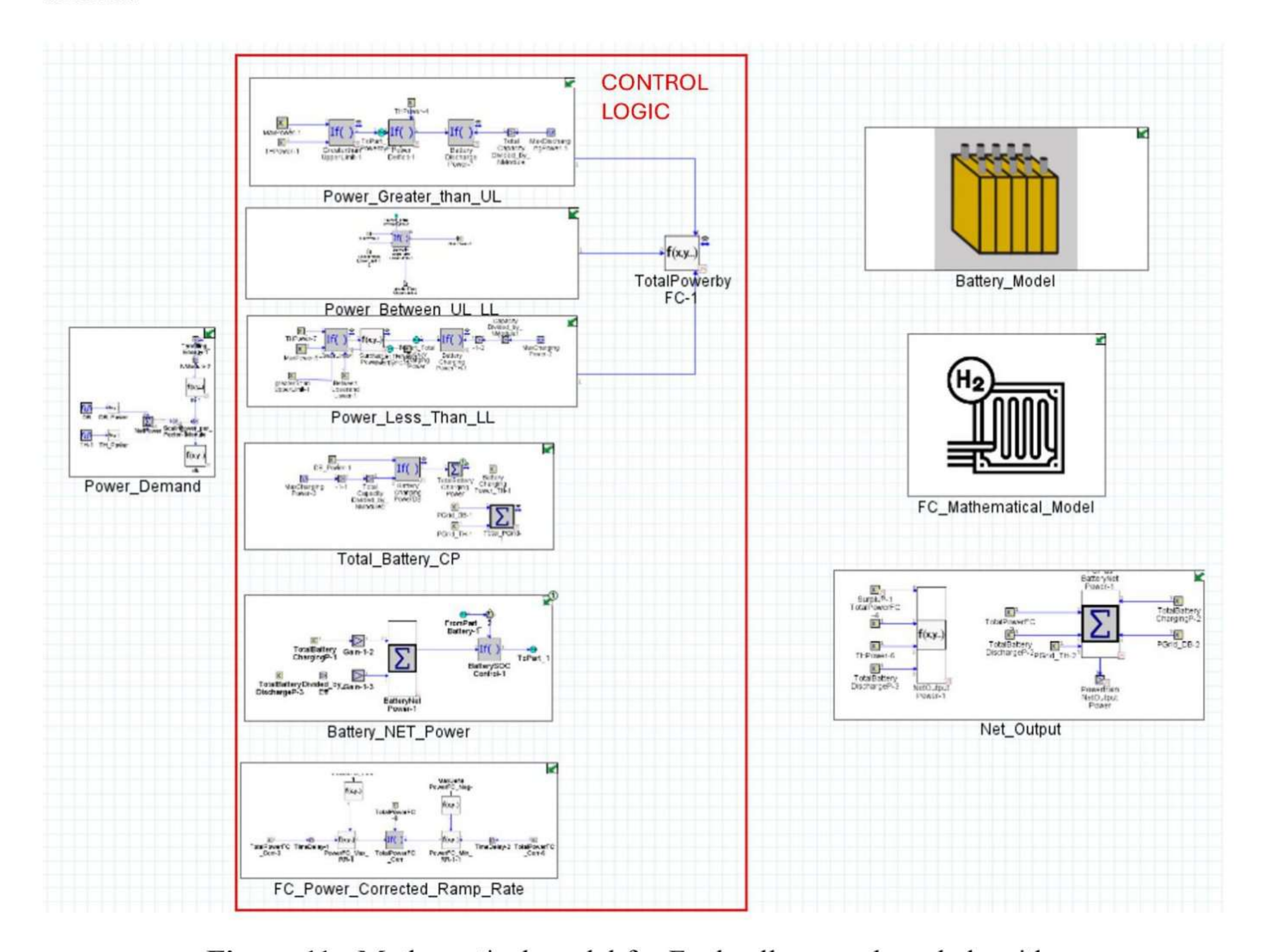


Figure 11 - Mathematical model for Fuel cell power-based algorithm

The above figure shows the simulation model prepared in GT-ISE. It can be divided into five main sections -

- 1. Power demand estimation
- 2. Control logic
- 3. Fuel cell mathematical model
- 4. Battery and Battery Management system model
- 5. Output calculations

Each section or assembly has its own subassemblies with each carrying out a significant function. The subassemblies involved are explained below -

- 1. Power demand estimation subassembly In this subassembly, the route map output is segregated as throttling/motoring power and regenerative power. These powers are then used in the control logic. It is noteworthy that the power demand is divided by the number of fuel cell modules. This is because the mathematical model of fuel cell for calculating the maximum power is on basis of one module of fuel cell. Each module contains approximately 300 cells
- 2. Fuel cell maximum power producing capacity This calculates the maximum power that can be produced by fuel cell per module. It is a mathematical model which was obtained by using DOE and neural network.
- 3. Fuel cell power estimation subassembly Receiving motoring power as the input, this will estimate the power to be produced by the fuel cell according to the logic as explained in the previous chapter. The logic will be divided into three possible cases -
- Case 1 Power demand greater than the set upper power limit
- Case 2 Power demand lesser than the set lower power limit
- Case 3 Power demand between upper and lower power limit

Fuel cell load will be calculated in each of the case and added to get the total power required.

- 4. Fuel cell corrected power based on ramp rate The fuel cell power value obtained from the previous subassembly is corrected based on the maximum ramp rate of the fuel cell. Ramp rate is the maximum allowable power increment or decrement per second for the fuel cell.
- 5. Battery power calculations This subassembly will calculate the battery discharge and charging power based on the fuel cell power output obtained from the previous subassembly. The power deficit after considering the power output from fuel cell is the desired discharge power from the battery. Similarly, any excess power produced by the fuel cell and the one coming from regenerative braking will sum up to obtain the charging power of the battery. Battery net power is calculated using these charge and discharge powers. The logic to keep battery SOC between the set limits is also included in this calculation.

6. Fuel cell efficiency and hydrogen consumption – This subassembly consists of mathematical models for calculating the fuel cell efficiency and in turn the hydrogen consumed. The fuel cell efficiency model was obtained using DOE and neural network on a physical fuel cell model.

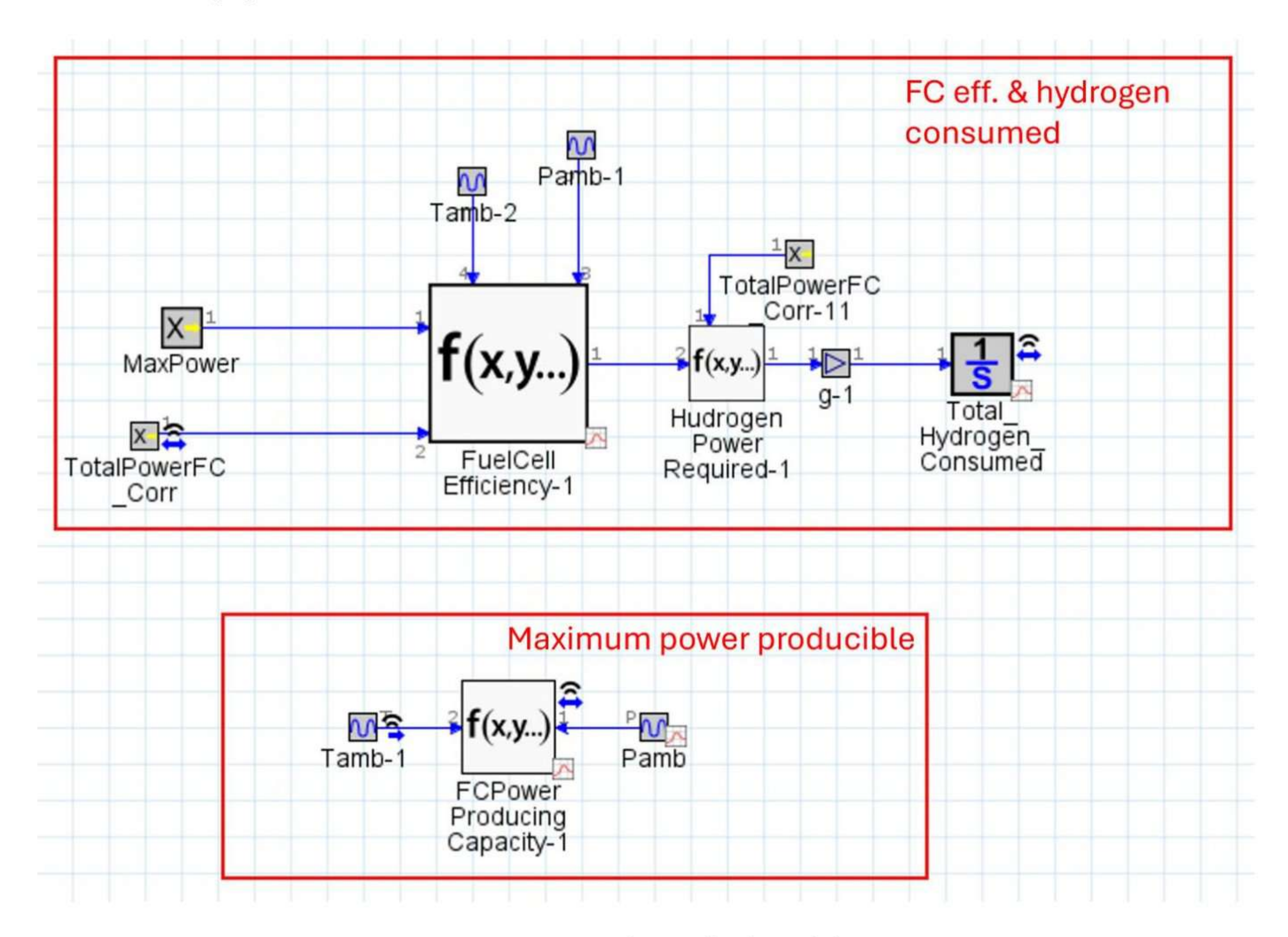


Figure 12 – FC mathematical model

7. Battery and battery management system - This subassembly receives input from the battery net power calculation subassembly. It consists of physics-based battery and BMS model. The BMS model is represented by a template named 'Battery power limiter'. In these templates, various electrochemical parameters are to be defined (some can be left as default). From the 'Battery' template, various output plots like the battery SOC, battery terminal power, battery temperature, voltage and current can be obtained. Similarly, the 'battery power limiter' template gives the instantaneous maximum charging and discharging power possible which is dependent on the maximum and minimum voltage limits and the provided maximum C-rate and battery

capacity values. These power limits provided are used in the battery net power subassembly to limit the battery net power.

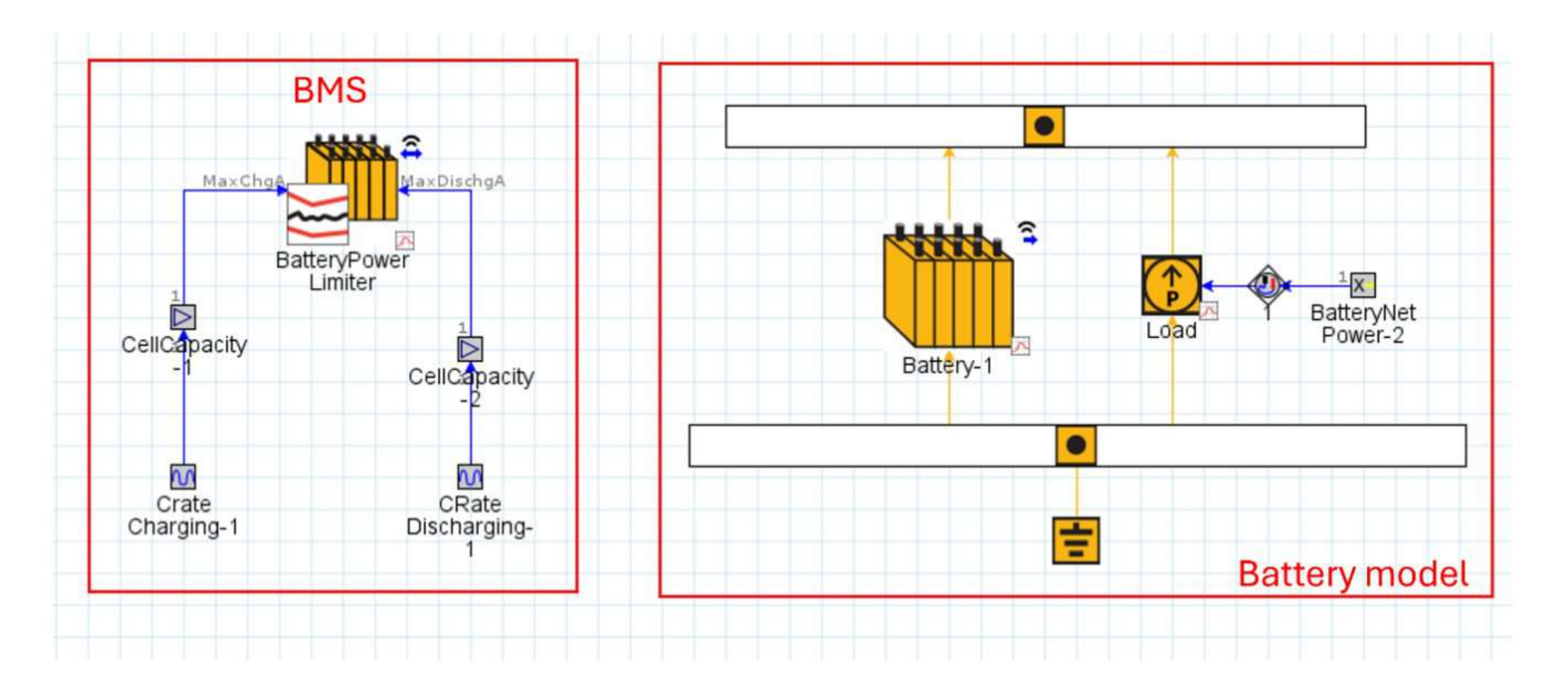


Figure 13 – Battery and BMS model

8. Output calculations – This subassembly calculates the net powertrain output, total cost, energy deficit and the percentage contribution of battery and fuel cell in the total power. Total cost and the energy deficit will be explained in the upcoming chapter on DOE.

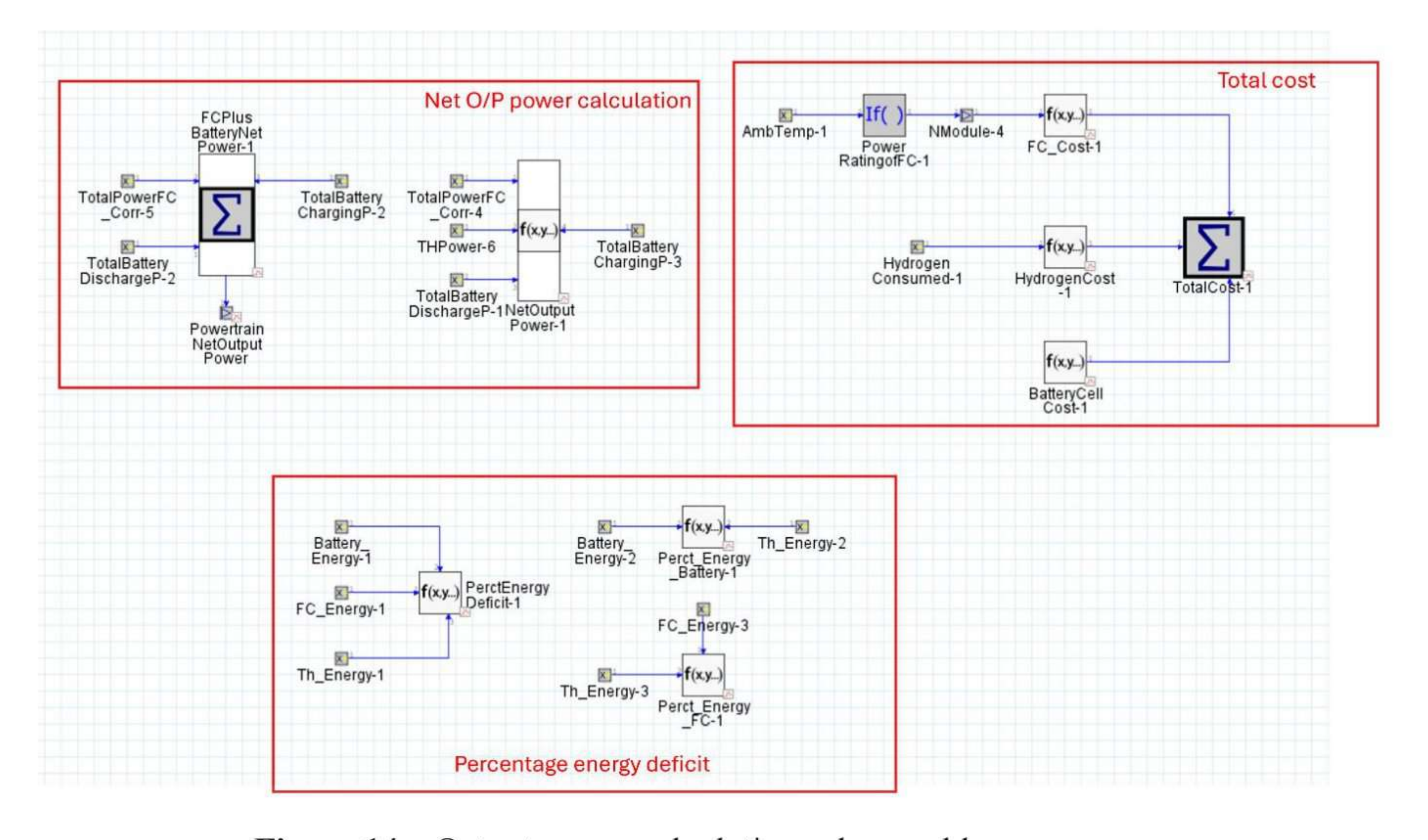


Figure 14 – Output power calculation subassembly

6.3.1 Templates used in simulation

The simulation in GT-ISE is an assembly made from interconnected templates. The important templates used in the simulation will be explained in this section.

- If then Else This template is used to implement conditional programming into a
 model. Using 'If-Then-Else' logic, one can create a number of conditional
 statements that determine a particular output. This is the most widely used
 template in this research work for implementation of the control logic.
- 2. Math equation This template performs mathematical calculations on an input signal(s) from a mathematical expression typed by the user to compute the output signal. If logic can also be employed in this template
- Receive signal This template is used to wirelessly connect the output of one template to the input of another template. It helps in making the model look less congested and reduces the simulation runtime
- Signal generator used to define a time variant property in the form of a table.
 Can also be used to output instantaneous simulation time.
- 5. Battery This template defines resistive or Thevenin electrical-equivalent battery models, consisting of open-circuit voltage, internal resistance, and optional R-C branches for electrical dynamics. The template can be used as a standalone model that works with power requests, or as a part of an electrical circuit within GT-SUITE. The default calculation for SOC is commonly referred to as "Coulomb Counting" where the current through the battery is integrated with respect to time to calculate a change in charge, which is translated to SOC. The template consists of following folders each containing battery parameter options -
 - 1. Main Consists of three sections -

Battery definition - defines the basics of the battery like number of cells in series, number of cells in parallel and cell capacity;

Initialization – Defines initial SOC of the battery

Battery load – defines how the load on the battery is defined

2. Circuit parameters – Consists of three sections -

Circuit parameters defined with cell data – used to define the open circuit voltage during charge and discharge and the internal resistance

Thevenin RC branches – allows RC branches to be defined in the battery equivalent circuit

Efficiency – Used to define the coulombic efficiency

3. Advanced – Includes six sections -

Hysteresis – This section defines how the battery template will change between using the charging or discharging characteristics given in the "Circuit Parameters" folder

SOC Model – defines how SOC value is calculated

Aging model - This section defines the attributes for capacity aging, resistance increase, and initializing as an aged cell

Equivalent model – defines whether the battery model will be solved by Thevenin or Norton circuit

- 4. Cell thermal model defines how the thermal aspects of battery will be calculated.
- 6. Power source This template acts as an electrical power source or sink. For e.g. it can be used as a source to charge the battery by giving a positive value as an input or can be used as a sink to discharge the battery by giving it a negative power value as an input
- 7. Battery power limiter This template is used to limit the power output from and power input into the battery. It taken in parameters like maximum current during charging and discharging, maximum voltage during charging and discharging and some instantaneous parameters referred from the battery model.
- Node electrical This template is used to model an ideal junction of two or more electrical branches. From a modelling standpoint it is considered a node of common electrical potential.

6.3 Mathematical model for Fuel cell efficiency-based algorithm

This mathematical model is like that of the power-based algorithm model with an exception of the lookup table. This lookup table converts the efficiency limits into power limits.

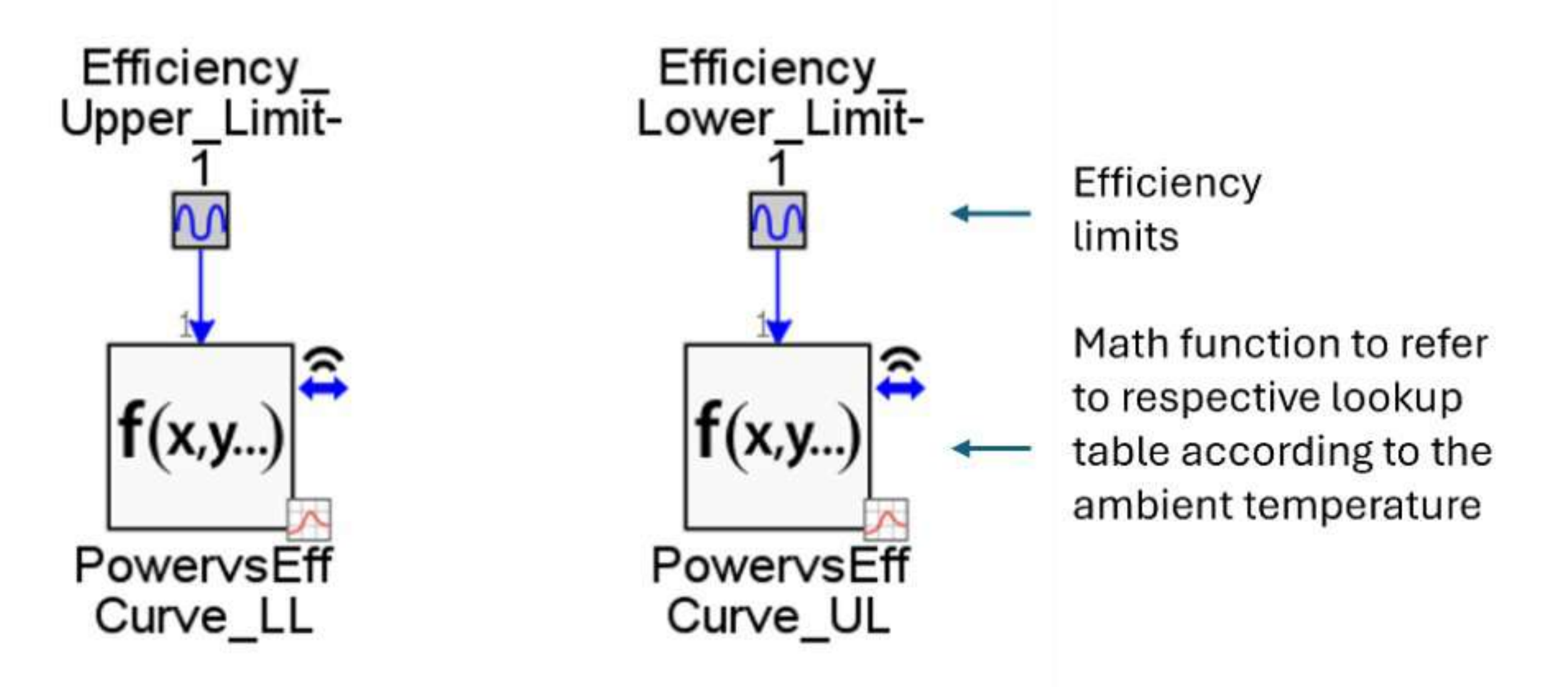


Figure 15 – Efficiency to power conversion

6.5 Mathematical model for Battery SOC-based algorithm

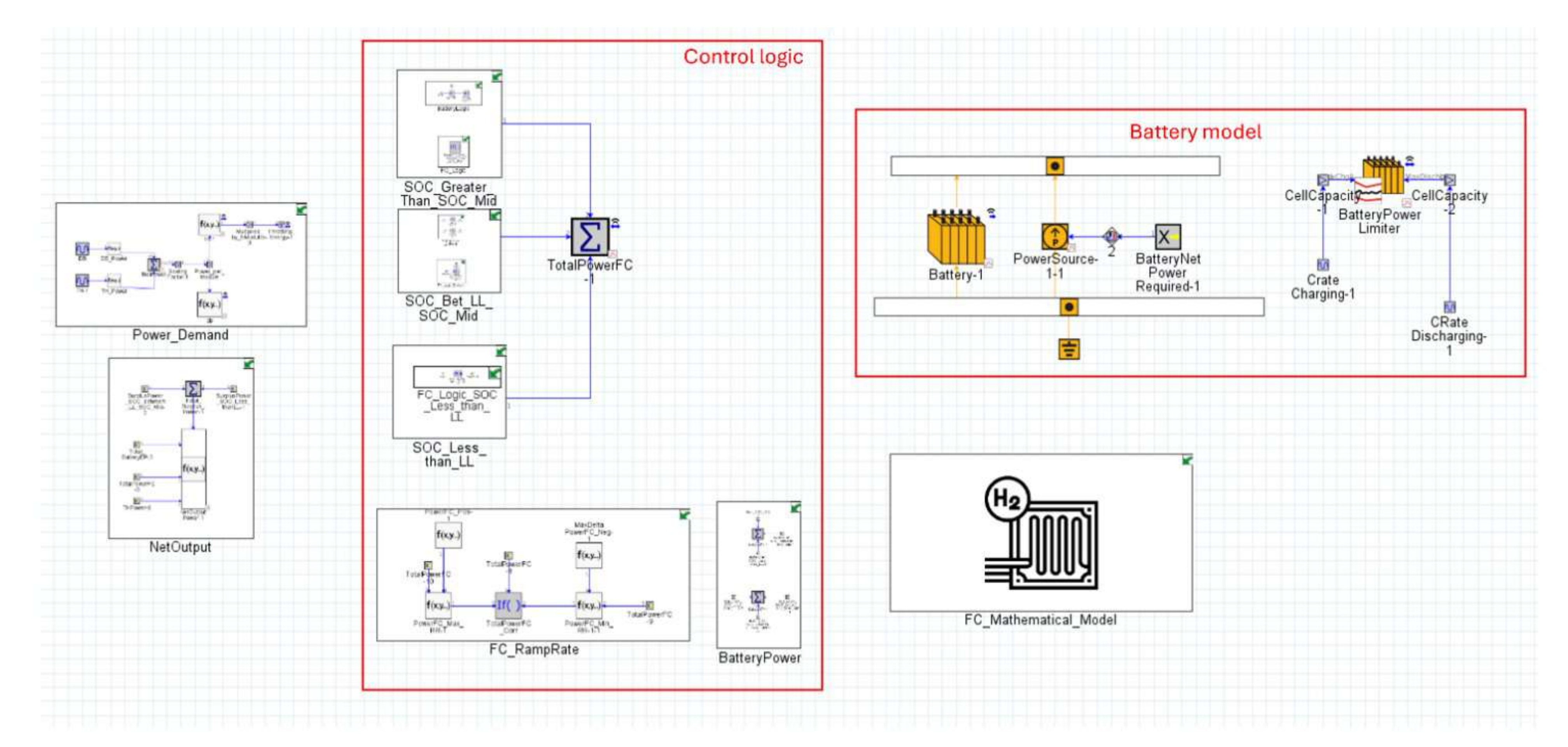


Figure 16 – Mathematical model – Battery SOC-based algorithm

The entire model as seen in the above figure is divided into five sections viz. control logic, power demand, battery model, FC mathematical model and the net output calculations.

The control logic is further subdivided into five subassemblies. The top three subassemblies calculate the power to be produced by the fuel cell in different scenarios as explained in the algorithms section earlier. Each of the three subassembly represents either one of the three possible cases. The other two subassemblies are for calculating the battery net power and the fuel cell corrected power

6.6 Parameter values

Each template in GT-ISE is build using some mathematical relations and so they require parameter values to be provided as inputs. Some of the important parameters of various templates will be mentioned in this section. It is important to note that some parameters are variable parameters which are varied in the DOE. So these parameters will have different values for each algorithm and will be mentioned about in the next chapter. In this section, only the parameters with same value for each algorithm will be mentioned in this section

Template/Subassembly	Parameter	Value
3i	Initial SOC	0.9
	Cell capacity	100 A-hr
Battery	Load type	Electrical connection
	Open circuit voltage @ SOC=0.9	4.1 Volts
	Imposed battery temperature	300 K
	Equivalent model type	Thevenin
	Max charging voltage limit per cell	4.2 Volts
Battery power limiter	Max discharging voltage limit per	2 Volts
	cell	
	Max C-rate during charging	2
	Max C-rate during discharge	1.5
FC corrected power	FC ramp rate	10 kW/sec
Power demand	Motor efficiency	90%
	Power electronic devices efficiency	95%
FC mathematical model	Hydrogen Calorific value	143 MJ/kg
Run setup	Simulation duration	10560 seconds
	Max integration time step	0.1 seconds

Table 2 – Parameter values

Chapter 7

7. Design of Experiments

7.1 Introduction to Design of Experiments

DOE can be referred to as a process of intentionally altering a system's or process's input variables through a series of tests and analysing the effects on response variables. Both computer simulation models and physical processes can benefit from this strategy. DOE will only apply to computer simulation models in the context of this study.

For performing DOE on the prepared simulation models, GT-ISE has a unique tool. For every active case in Case Setup, a DOE is a table or matrix of simulations that will run. A factor is what happens when a parameter in a DOE is changed. A particular set of factor values that are changed in the DOE is called an experiment.

GT-ISE provides various options for DOE type which are explained below.

- 1. Full factorial A Full-Factorial DOE indicates that all possible combinations of factors will be sampled. For this type, it is necessary to define the range of each factor, as well as the number of levels for each.
- 2. Full factorial discrete Full-Factorial Discrete differs from Full Factorial in that instead of giving a range and number of levels, the user explicitly defines each value to be run for each fact
- 3. D-optimal D-Optimal is a partial factorial sampling method that reduces a Full Factorial DOE to a fewer number of experiments using a polynomial fitting equation
- 4. D-optimal Latin hypercube D-Optimal Latin Hypercube is similar to the D-Optimal method but uses Latin Hypercube sampling instead of Full Factorial sampling to begin the reduction process. This DOE type requires the user to enter the ranges of each factor, the number of experiments, and to select a fitting equation.
- 5. Latin hypercube Latin Hypercube is a random sampling method with some logic to prevent clusters of points that are too near each other. It sampling consists of dividing the range of each factor into several equal-sized ranges or "bins". Then factor values are randomly placed in each bin

'Full factorial' DOE will be used in this research work.

7.2 Methodology for Design of Experiments

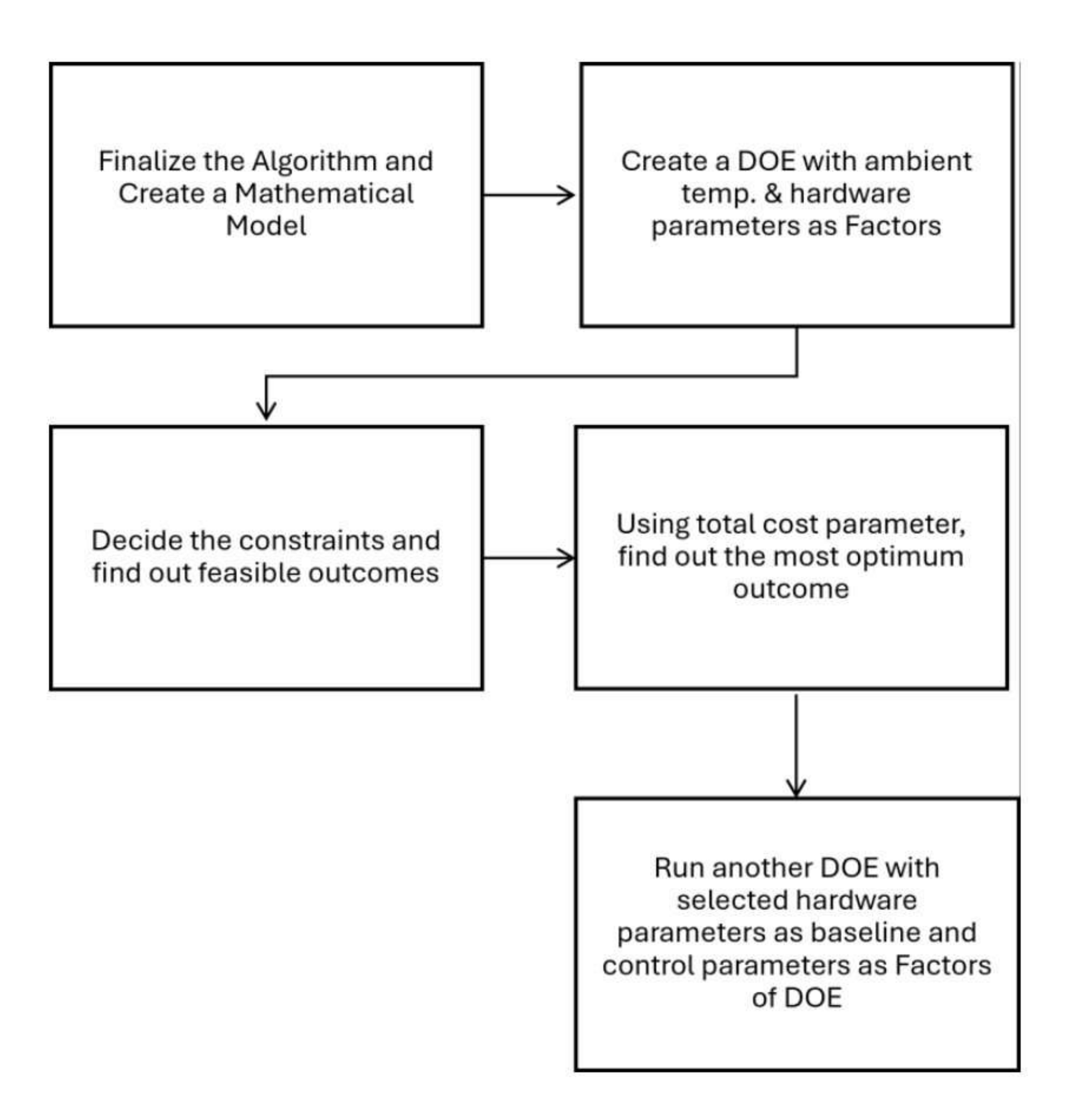


Figure 17 – DOE Methodology

The above flowchart describes the roadmap followed for conducting DOE in this research work. The first step was to create a mathematical model of the algorithm. The DOE was conducted in two steps – DOE1 and DOE2. In the DOE1, ambient temperature and hardware parameters were used as factors (parameters to be varied in the DOE). DOE 2 was conducted with control parameters like power and SOC limits as the factors

Objective of DOE 1 was to find out the minimum number of total battery cells required for each configuration of fuel cell. Configuration here refers to the number of fuel cell modules in the fuel cell stack. The main objective of the design was to satisfy all the powertrain performance requirements but with minimum total cost. So, to satisfy the performance requirements, some constrains had to be set. These constrains are mentioned in the Table 3 below. It is desired that the locomotive should complete its journey within the stipulated time. Owing to this, a constraint on percentage energy

deficit was setup. Similarly, to keep the battery SOC within limits, SOC constraint was setup.

Objective of the DOE 2 was to determine the most optimum values of the control parameters for the optimum hardware configurations obtained from DOE1. The three hardware parameters and the two constraints will be common for all the three algorithms (only the parameters and not their values) but the control parameters will be different for each.

Hardware parameters	 No of FC Modules No of Battery cells in series No of Battery cells in Parallel
Constraints	1. Percentage Energy deficit (<7%) 2. SOC (>40%)

Table 3 – Hardware parameters and constraints

After running DOE1, the feasible outcomes were filtered out using the two constraints. After obtaining the feasible outcomes, the optimum of them were determined using the cost function. This in our case is the 'Total cost'. Optimum outcome is the one which gives minimum cost function. So, for each fuel cell configuration an optimum hardware configuration was determined. In DOE2, each control parameter was varied for each local optimum obtained from DOE1 and then the outcome with least total cost was regarded as the global optimum configuration.

7.3 Total cost calculation

As mentioned in the previous section, total cost is the cost function used in the DOE of this research work which is to be minimized. It is a summation of four costs which will be explained in this section. All the costs calculated are on per kilometre basis to keep a common yardstick for comparison.

Fuel cell (FC) cost
 This is the hardware cost of a PEMFC.

Assumptions - FC life in hours = $8000^{[10]}$

FC cost per KW = $15000 \text{ Rs/-}^{[11]}$

Drive cycle distance = 90 kms

Drive cycle duration = 3 hours

Calculations -

FC life in kms
$$= \frac{FC \ life \ in \ hours}{drive \ cycle \ duration \ in \ hours} \times drive \ cycle \ distance$$

$$= \frac{8000 \times 3600}{10560} \times 90$$

$$= 240000 \ kms$$
FC cost per km
$$= \frac{FC \ initial \ cost}{FC \ life \ in \ kms}$$

$$= \frac{(FC \ cost \ per \ kW) \times (Power \ rating)}{240000}$$

FC cost per km =
$$\frac{15000 \times Power \, rating}{240000}$$

The above equation is used for obtaining the fuel cell initial cost for all the iterations based on the power rating.

2. Hydrogen cost -

This is the operating cost of hydrogen and will be incurred in every cycle Assumption -

- 1. Hydrogen cost per kg = 170 Rs/- [12]
- 2. Drive cycle distance = 90 kms

Calculations -

Hydrogen cost per km =
$$\frac{Hydrogen\ cost\ per\ kg \times hydrogen\ consumed\ per\ cycle}{Drive\ cycle\ distance}$$
Hydrogen cost per km =
$$\frac{170 \times hydrogen\ consumed\ per\ cycle}{90}$$

The above equation is used to calculate hydrogen fuel operating cost for various values of hydrogen consumed in every iteration

3. Battery cost -

Assumptions -

Type of battery – Lithium ion NMC

Battery cost per kW-hr = 13000 Rs/- [13]

Battery life in cycles = 4000

Calculations -

Battery cost per km =
$$\frac{\text{Battery cost per kW-hr} \times \text{Battery energy rating}}{\text{Battery life in cycles} \times \text{kms per cycle}}$$

$$= \frac{13000 \times \text{Battery energy rating}}{4000 \times 90}$$
Battery cost per km =
$$\frac{13000 \times \text{Battery energy rating}}{360000}$$

4. Electricity cost for charging battery -

Assumptions -

- 1. Electricity tariff for commercial purpose (above 15 KW) per unit = 8 Rs/-
- 2. Drive cycle distance = 90 kms
- 3. Battery will be charged after each cycle of 90 kms from 40% SOC to 90% SOC Calculations -

Electricity cost per km =
$$\frac{(Electricity per unit tariff) \times (0.5 \times Battery energy rating)}{Drive cycle distance}$$
Electricity cost per km =
$$\frac{4 \times Battery \ energy \ rating}{90} \ Rs/-$$

The above equation gives the cost for charging the battery for a given battery energy rating

7.4 DOE – FC Power-based algorithm

Factors	Range
Ambient temperature	6^{0} C
	50 ⁰ C
No. of FC modules	Min-4
	Max - 6
Battery cells in series	Min - 150
	Max - 300
Battery cells in parallel	Min – 7
	Max - 9

Table 4 – Factors and their ranges – FC Power-based algorithm

As explained in the previous sections, DOE1 was first conducted for finalizing the hardware configurations. Above Table4 depicts the factors and their ranges that were varied in the DOE1. After DOE, the minimum number of battery cells possible for each of the fuel cell configuration obtained is shown in the table below. —

No of FC Modules	FC Rating in kW (@Tamb=50° C)	Minimum battery cells possible	Battery Energy Rating in kW-hr	Total cost per km (Rs/-)
4	860	2360 (295S,8P)	990	243
5	1075	1400 (210S,7P)	615	246
6	1290	1050 (150S,7P)	440	249

Table 5 – DOE1 optimum results – FC power-based algorithm

It is important to note that the above results are the outcomes obtained from configurations which are feasible (meeting the constraints) at both the ambient temperature values ensuring that the locomotive performs at any extreme ambient conditions. Also, the values of upper and lower power limits are kept as constant and equal to 0.8 times the FC maximum power and 0.2 times FC maximum power respectively. In the minimum battery cells column, the value inside the bracket depicts the number of cells in series and parallel arrangement. Arranging cells in series adds to the voltage whereas parallel arrangement adds to the overall current.

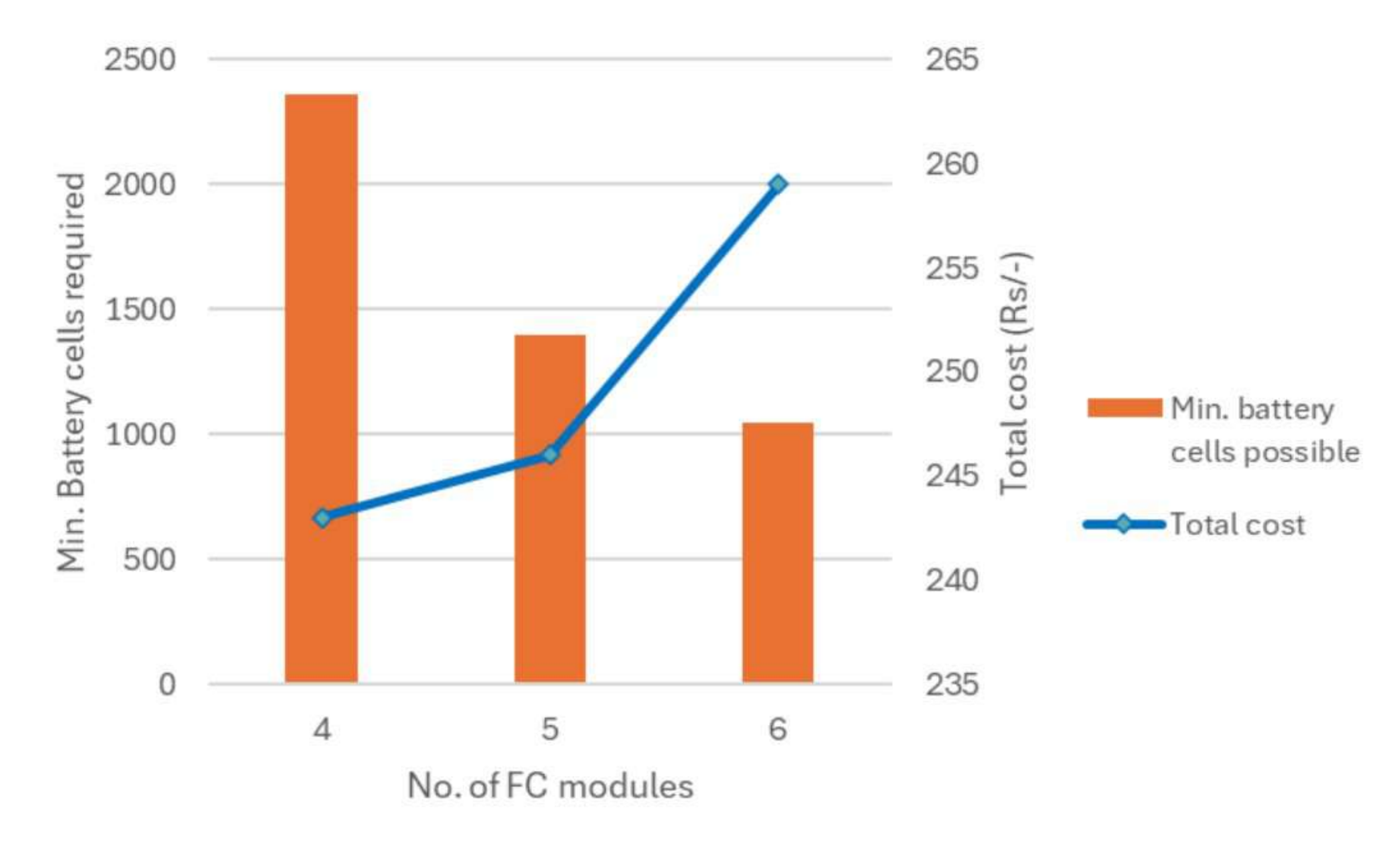


Figure 18 – Variation of minimum battery cells and total cost with no. of FC modules

The above figure shows the behaviour of 'minimum no. of battery cells' possible and 'total cost' with variation in the number of FC modules. It can be readily observed that as the number of FC modules increases, the number of min. battery cells possibly goes

on decreasing. This is because we are calculating the battery load based on the power deficit calculated after subtracting FC output from power demand. So, when the FC capacity increases, the load on the battery decreases and thus the battery rating required goes on decreasing. On the contrary, the total cost can be seen increasing with the no. of FC modules because of the high sensitivity of total cost towards FC initial cost & hydrogen consumption. So, even though the battery cells required are decreasing, the total cost is increasing.

DOE2 was conducted on the above configuration obtained through DOE1. Table below shows the control parameters that were varied in this DOE along with their range

Control parameter	Range
FC upper power limit	Min - 0.6*(FC max. power capacity)
	Max - 0.8*(FC max. power capacity)
FC lower power limit	Min – 0.2*(FC max. power capacity)
	Max - 0.3*(FC max. power capacity)

Table 6 – Control parameters – FC power-based algorithm

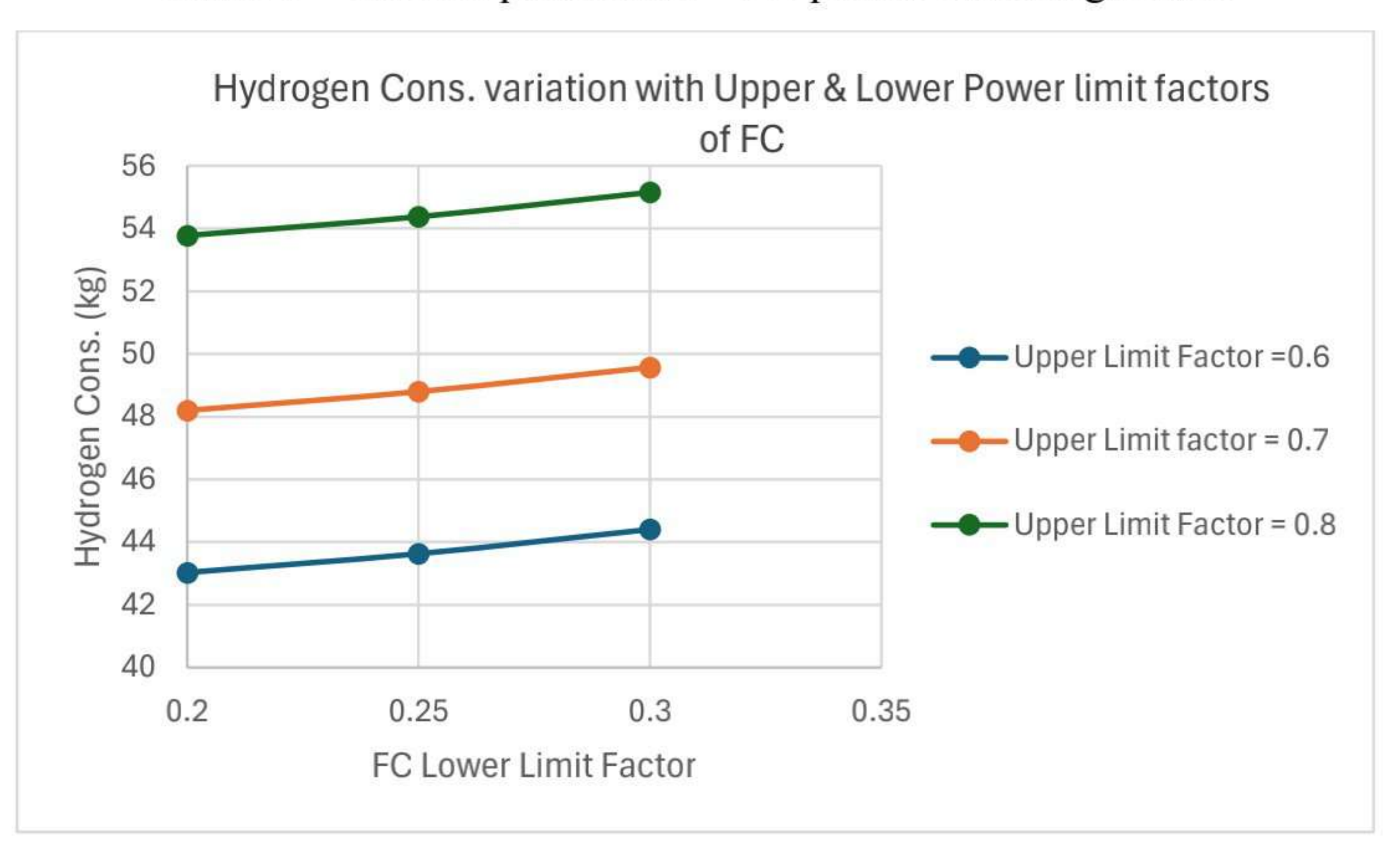


Figure 19 – Hydrogen Cons. variation with Upper & Lower Power limit factors of FC

FC power limits are the control parameters that were varied in DOE2. These limits are in terms of gain of FC's maximum power producing capacity which vary with the ambient temperature.

Figure 19 above shows the variation of hydrogen consumption with FC's upper and lower power limit. It is seen that an increase in both the limits leads to an increase in the hydrogen consumption. However, the upper power limit has a higher sensitivity on

hydrogen consumption that the lower power limit. This is because whenever there is an increase in the upper limit of the fuel, it directly means that the FC will operate at higher power bandwidth and in turn the hydrogen consumption increases since the FC efficiency with a higher slope at higher power values. However, at lower power levels, efficiency drop with increase in power is relatively lesser.

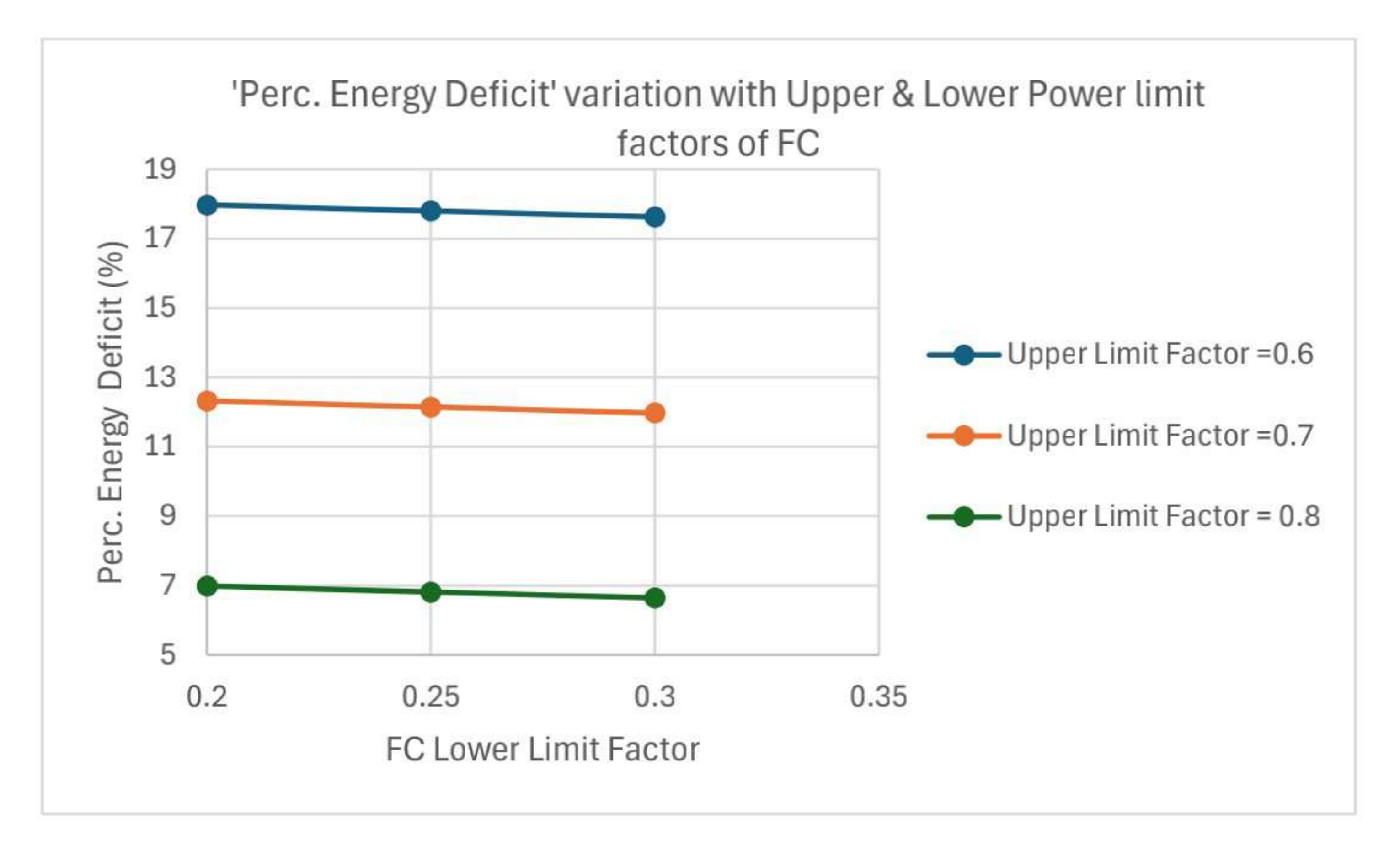


Figure 20 – Percentage Energy deficit variation with Upper & Lower Power limit factors

The above figure shows the behaviour of 'percentage Energy deficit' with change in the power limits of FC. It is seen that with increase in the power limits, the percentage energy deficit decreases. Sensitivity of upper limit is very high as compared to that of the lower limit.

The final optimum configuration after running DOE2 are shown in the table below.

Parameter	Value
No of FC Modules	4
FC max Power rating (@Tamb=50 ⁰ C)	860 kW
Cells in series	290
Cells in parallel	8
Total battery cells	2360
Battery energy rating	990 kW-hr
FC upper power limit	0.8 * (Max Power producible by FC)
FC lower power limit	0.2 * (Max Power producible by FC)

Table 7 – Final optimum configuration - FC power-based algorithm

7.4.1 Sensitivity analysis – FC power-based algorithm

Sensitivity analysis is the study of how the variation in the model inputs attributes to change in the model responses or outputs. Motivations for performing sensitivity analysis include the following -

- 1. Determining the most important factors on a model output.
- 2. Determining factors that have zero or negligible influence on a response.
- 3. Identifying relationships among factors and responses to better understand a model and ideally develop better models. This section includes the sensitivity analysis of various hardware configuration and control parameters used in the DOE on the responses that are significant to this research work.

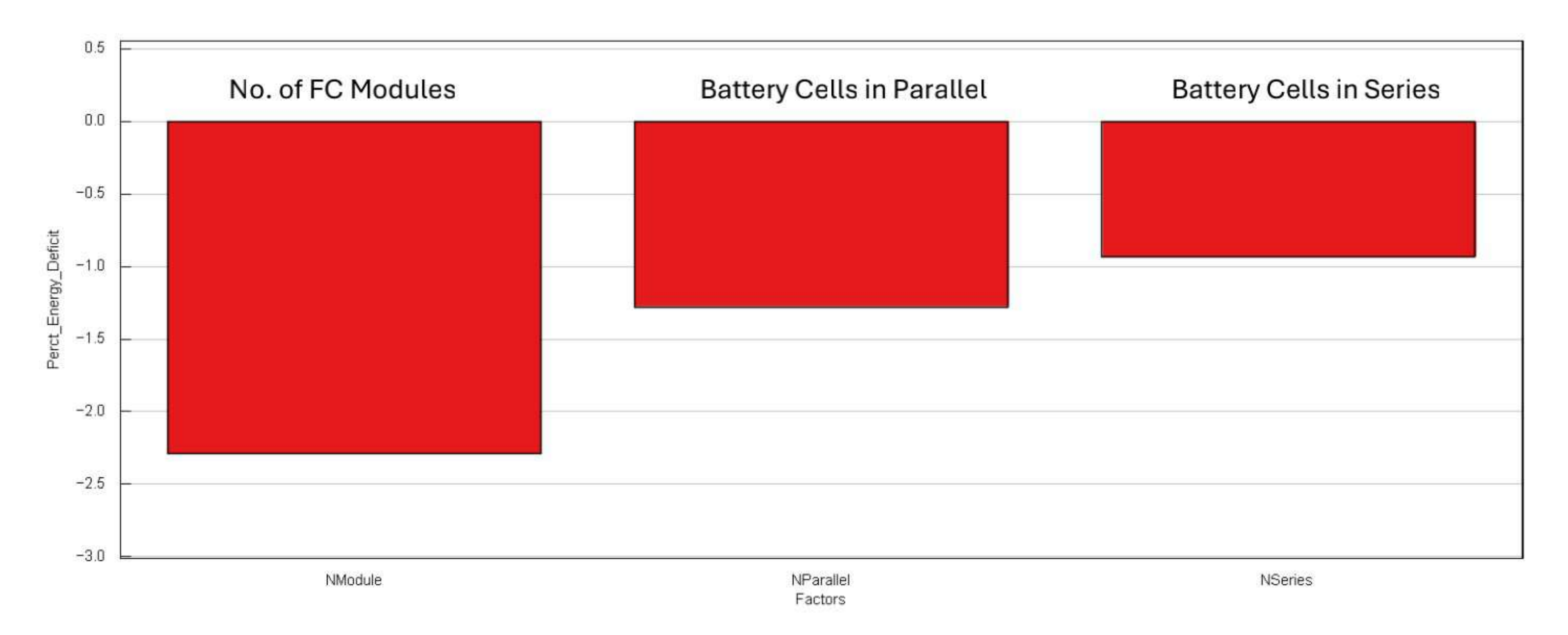


Figure 21 – Sensitivity analysis of hardware parameters for perc. energy deficit – FC power-based algorithm

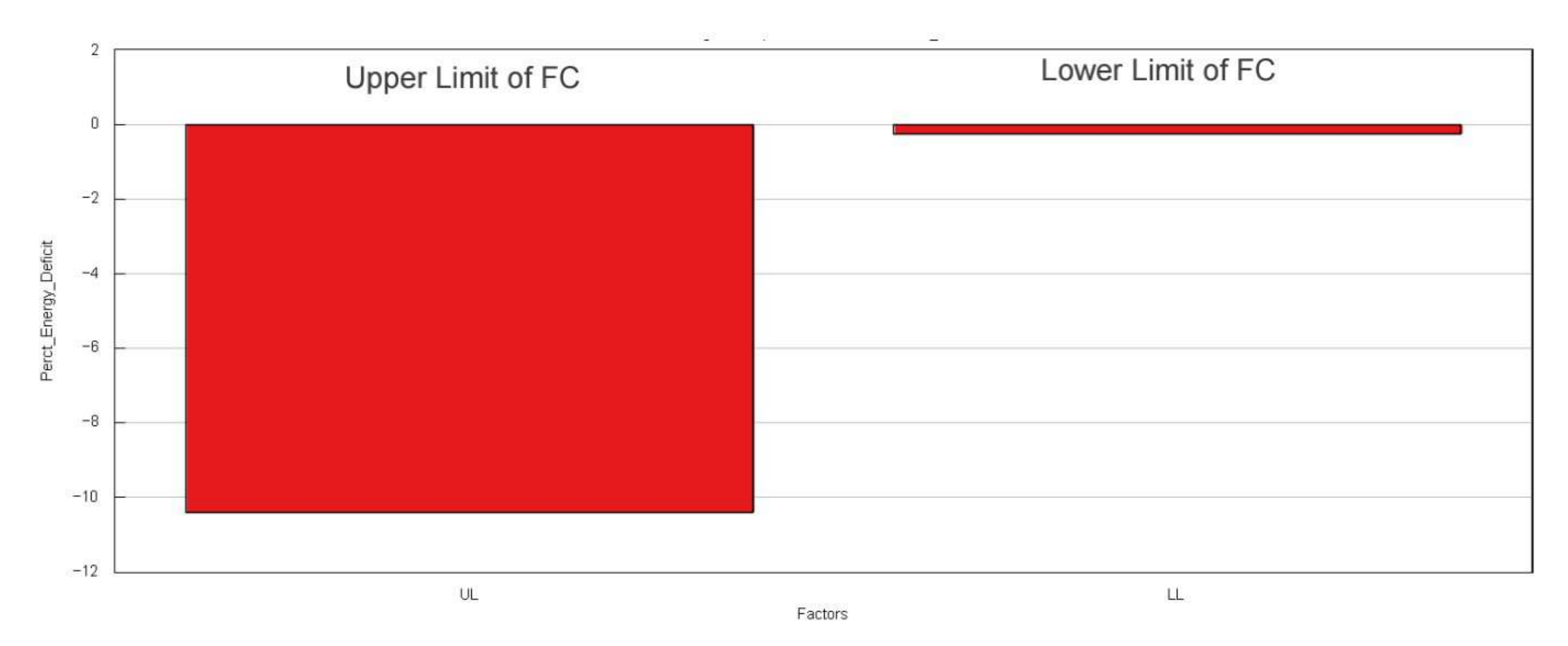


Figure 22 – Sensitivity analysis of control parameters for perc. energy deficit – FC power-based algorithm

Figure 21 & figure 22 shows the sensitivity analysis of 'perc. energy deficit' towards various hardware configurations(no. of FC modules, battery cells in series and cells in parallel) and control parameters (FC upper and lower power limit). From the Figure 21, it is seen that all the three hardware parameters are inversely related to the percentage energy deficit which means that an increase in any of the three parameters results in a decrease in the percentage energy deficit. Moreover, no. of FC modules is the factor for which the perc. energy deficit has the highest sensitivity followed by battery cells in parallel and battery cells in series respectively.

From the Figure 22, it can be inferred that percentage energy deficit has a very high relative sensitivity towards the FC upper power limit as compared to the lower power limit for which it has almost negligible sensitivity.

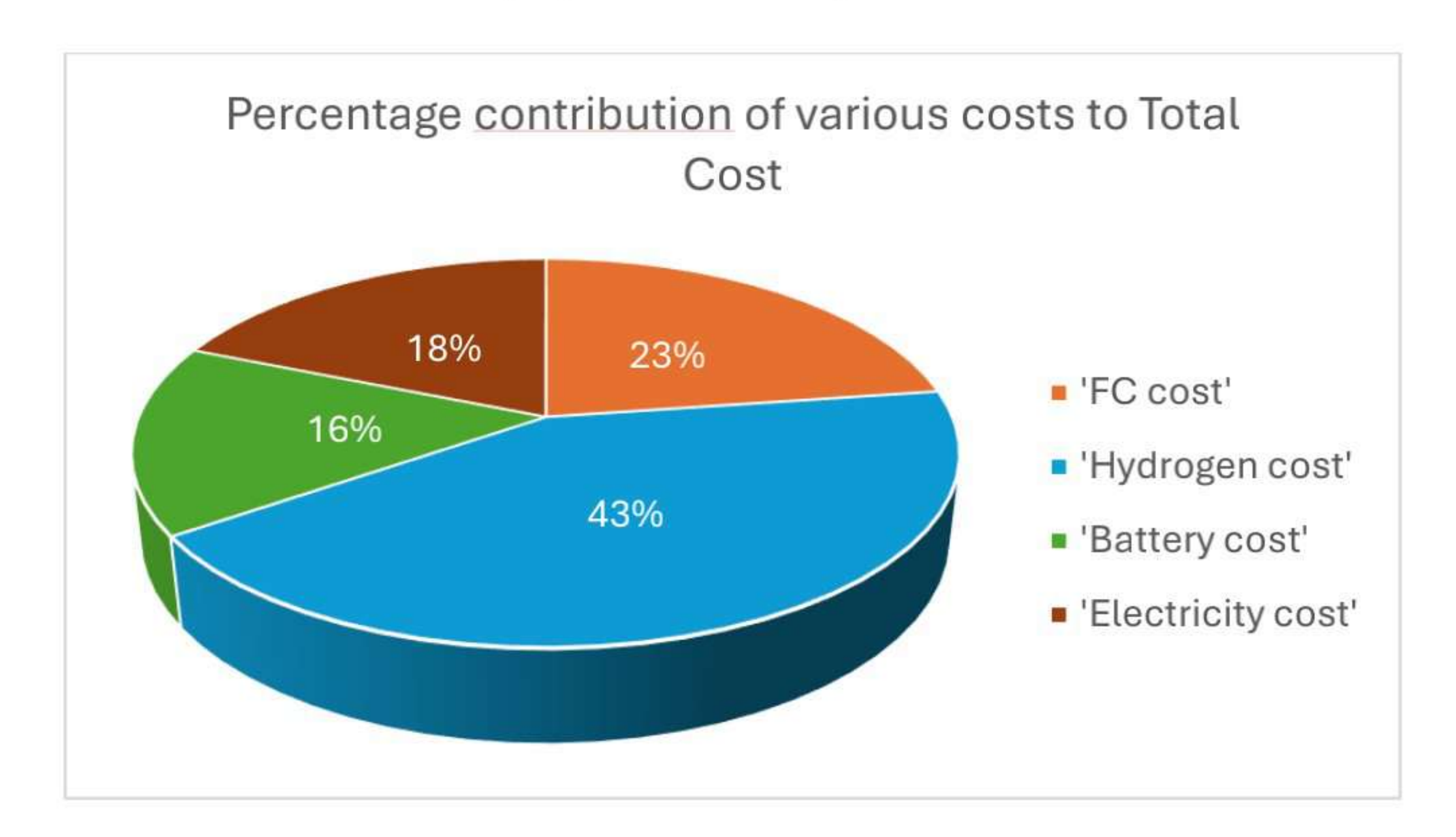


Figure 23 – Sensitivity analysis of hardware parameters for total cost– FC power-based algorithm

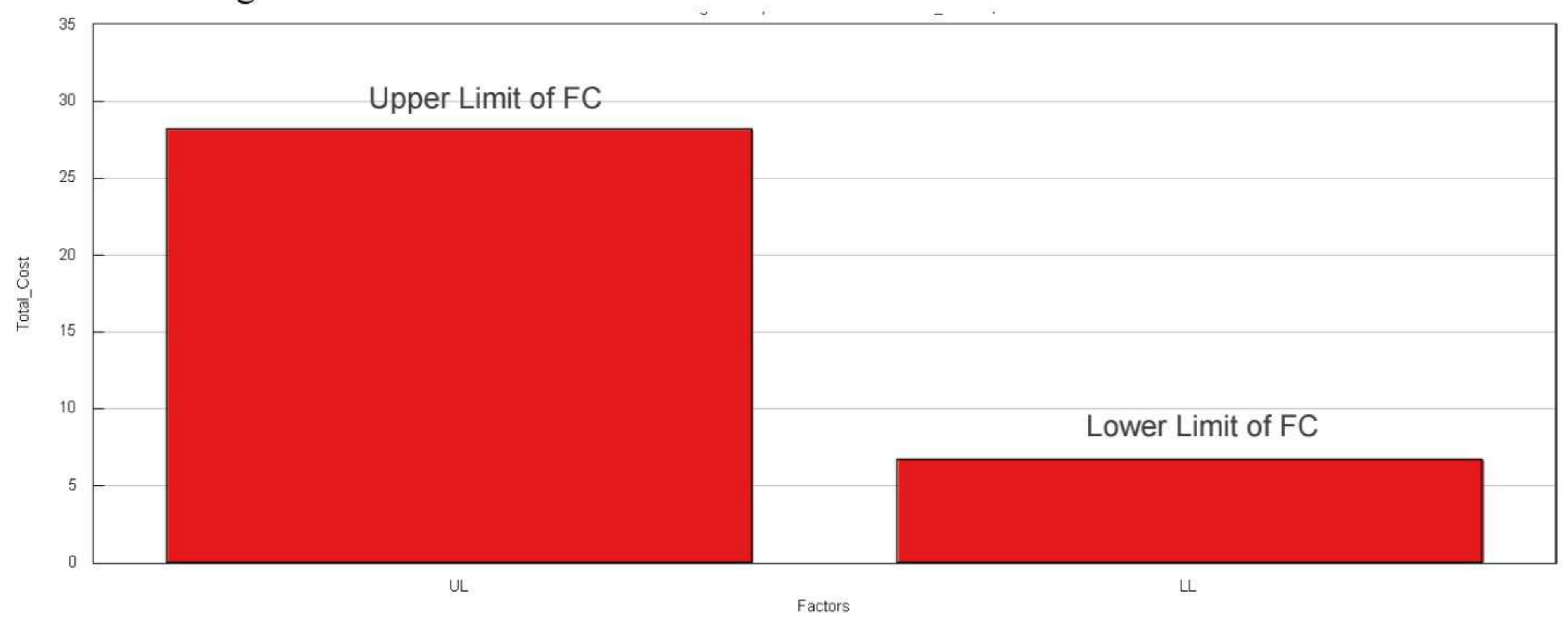


Figure 24 – Sensitivity analysis of hardware parameters for total cost– FC power-based algorithm

Figure 23 depicts the sensitivity of 'total cost' towards various hardware parameters in terms of percentage contribution to the total cost. The chart is obtained for results from the first configuration i.e. with 4 number of FC modules. It is seen that the highest percentage contribution is of hydrogen cost. This is followed by the fuel cell cost, electricity cost and the battery cost in order respectively. So, 66% of the total cost is related to fuel cell and 34% is from the battery. It can be inferred from this that even a unit change in the number of FC modules will result in a large variation in the total cost because hydrogen consumption and FC modules are related to each other.

Figure 24 shows sensitivity of total cost towards the FC power limits. It is seen that the total cost has a higher sensitivity towards upper limit as compared to the lower limit. This is because operating in higher power bands results in lower efficiencies and hence higher hydrogen consumption and total cost.

7.5DOE – FC efficiency-based algorithm

This section will provide details about the DOE conducted on the FC efficiency-based algorithm. The constraints and cost function for filtering feasible outcomes and finding optimum parameters will be the same as in the previous algorithm. Hardware parameters used are also the same except the range of these factors which is mentioned in the table below.

Factors	Range
Ambient temperature	6^{0} C
	50 ⁰ C
No. of FC modules	Min – 4
	Max - 6
Battery cells in series	Min - 200
	Max - 300
Battery cells in parallel	Min – 10
	Max - 13

Table 8 – Factors and their ranges – FC efficiency-based algorithm

No of FC Modules	FC Rating in kW (@Tamb=50° C)	Minimum battery cells possible	Battery Energy Rating in kW-hr	Total cost per km(Rs/-)
4	860	3900 (300S,13P)	1638	275
5	1075	3180 (265S,12P)	1336	279
6	1290	2585 (235S,11P)	1086	287

Table 9 –DOE1 outcome – FC efficiency-based algorithm

Table 9 shows the outcomes obtained after running DOE1 on the model. It is seen that the one with minimum modules i.e. 4 modules is giving the minimum total cost. In DOE2, the control parameters were varied for each of the configuration obtained above. Table below shows these control parameters along with their ranges

Control parameter	Range
FC upper efficiency limit	Min – 59%
	Max - 60% (3 levels)
FC lower efficiency limit	Min – 53%
	Max - 56%

Table 10 – Control parameters – FC efficiency-based algorithm

Parameter	Value
No of FC Modules	4
FC max Power rating (@Tamb=50 ⁰ C)	860 kW
Cells in series	270
Cells in parallel	13
Total battery cells	3510
Battery energy rating	1474 kW-hr
FC efficiency upper limit	60%
FC efficiency lower limit	53%

Table 11 – Final optimum configuration - FC efficiency-based algorithm

Table 11 depicts the optimum value of all the parameters which are significant inputs for the model. Again, it is important to note that the results obtained are the most optimum outcomes from the outcomes which were commonly feasible at both the ambient temperatures.

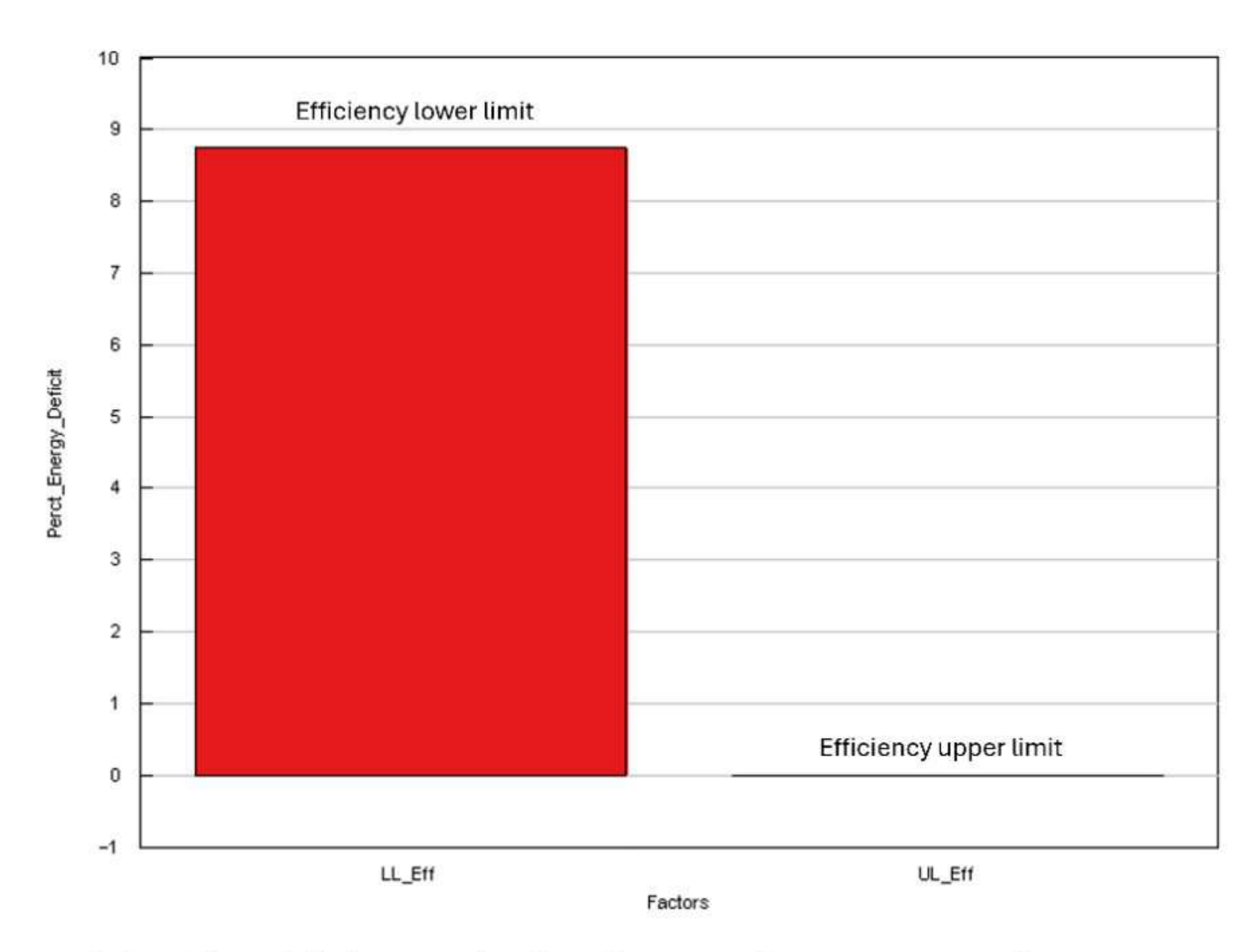


Figure 25 – Sensitivity analysis of control parameters for perc. energy deficit– FC efficiency-based algorithm

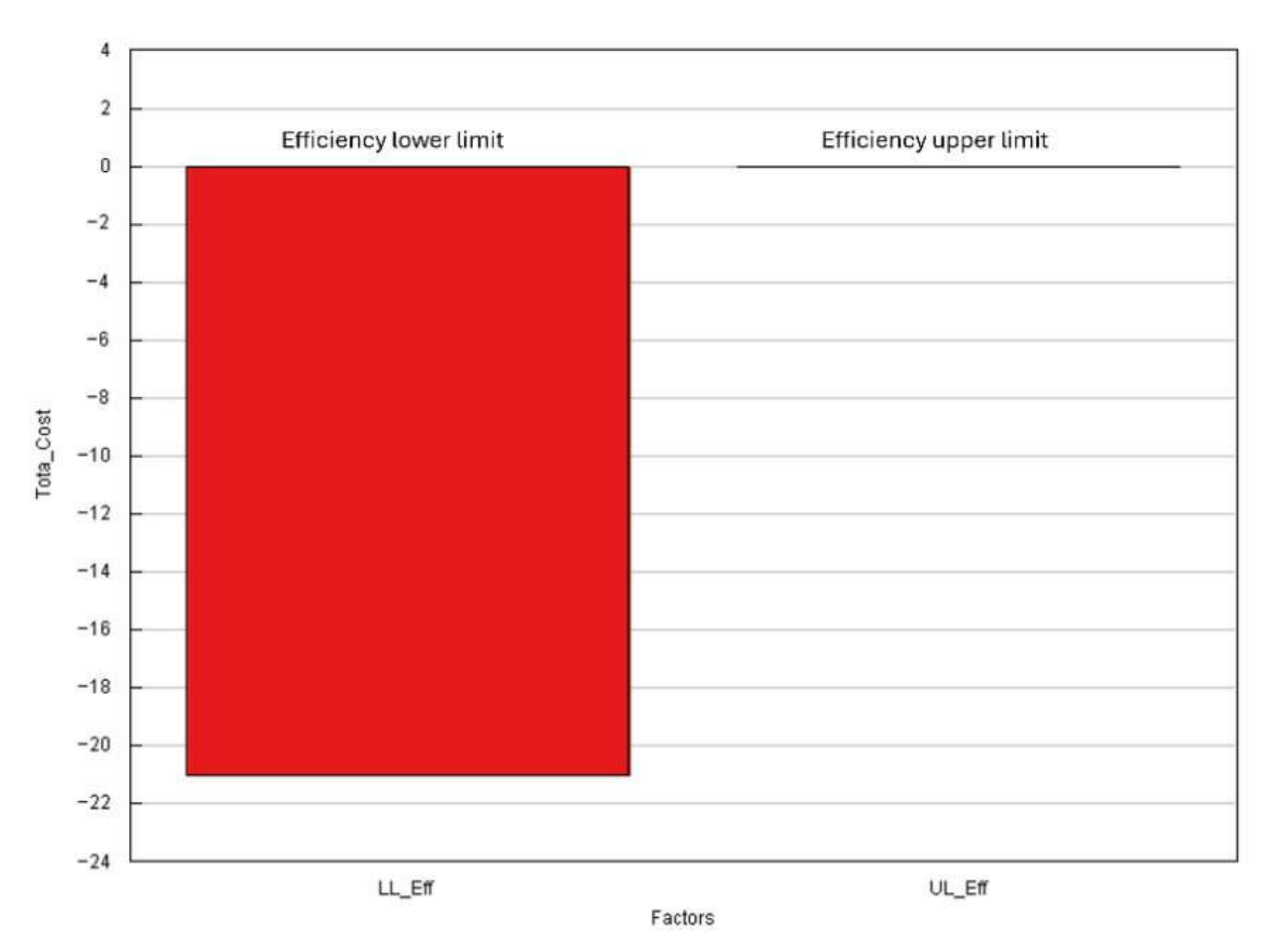


Figure 26 – Sensitivity analysis of control parameters for total cost – FC efficiency-based algorithm

Figure 25 and figure 26 illustrates the sensitivity of percentage energy deficit and total cost towards the FC efficiency limits. From figure 25, it can be seen that the energy deficit has a very high relative sensitivity towards lower efficiency whereas it has a negligible sensitivity for upper efficiency limit. It can be further inferred that an increase of lower efficiency from 54% to 56% leads to an increase of percentage energy deficit by around 9% i.e. percentage energy deficit increases by 3% per unit

increase in the lower efficiency limit. This is because as the lower efficiency limit is increased, the upper power limit of FC decreases which in turn increase the battery load. So, for a given battery size, the probability to have energy deficit increases.

From figure 26, it can be inferred that the lower efficiency is again the factor for which total cost has high sensitivity. It is seen that these two are inversely related. Every unit increase in the lower efficiency limit leads to a reduction in total cost by around 7 Rs/-

7.6 DOE-Battery SOC-based algorithm

For the third algorithm, same factors were varied in DOE1 as that for previous algorithms. The control parameters which were varied later in DOE2 are kept at some constant value during DOE1. The upper and lower power limit were kept at 0.8 times FC maximum power and 0.2 times FC maximum power respectively whereas the SOC lower and middle limit were kept at 40% and 60% respectively. The ranges of hardware parameters have been shown in the table below –

Factors	Range
Ambient temperature	6 ⁰ C 50 ⁰ C
F252	50° C
No. of FC modules	Min-4
	Max - 6
Battery cells in series	Min - 200
	Max - 300
Battery cells in parallel	Min – 5
	Max - 10

Table 12 – Factors and their ranges – Battery SOC-based algorithm

No of FC Modules	FC Rating in kW (@Tamb=50° C)	Minimum battery cells possible	Battery Energy Rating in kW-hr	Total cost per km (Rs/-)
4	860	2700 (270S,10P)	1218	262
5	1075	1320 (220S,6P)	554	269
6	1290	1000 (200S,5P)	420	263

Table 13 – Final optimum configuration - Battery SOC-based algorithm

Table 13 shows the minimum battery cells possible for each of the FC configuration so that they can be the basis for DOE2. It can be seen from the third configuration that even though the number of FC modules were increased, drastic fall in the number of battery cells caused an overall decrease in the total cost is less for the third configuration than that for the second one. The cells were not decreased further keeping in mid that this would lead to a very low voltage at the battery terminals.

Control parameter	Range
SOC middle limit	Min - 0.6
	Max - 0.7
SOC lower limit	Min - 0.4
	Max - 0.5
FC upper power limit	Min - 0.6*(FC max. power capacity)
	Max - 0.8*(FC max. power capacity)
FC lower power limit	Min – 0.2*(FC max. power capacity)
	Max - 0.3*(FC max. power capacity)

Table 14 - Control parameters - Battery SOC -based algorithm

Above table shows the ranges between which the control parameters were varied for each of the configuration obtained from DOE1. The results obtained from this DOE are shown in the table below

Parameter	Value
No of FC Modules	4
FC max Power rating (@Tamb=50 ⁰ C)	860 kW
Cells in series	270
Cells in parallel	13
Total battery cells	3510
Battery energy rating	1474 kW-hr
FC efficiency upper limit	60%
FC efficiency lower limit	54%

Table 15 – Final optimum configuration - Battery SOC-based algorithm

As seen in the previous algorithms, configuration with minimum fuel cells is giving the optimum outcome. To analyse the effects of various parameters, sensitivity analysis was carried out just like that for other algorithms. The sensitivity graphs for energy deficit and total cost have been shown below

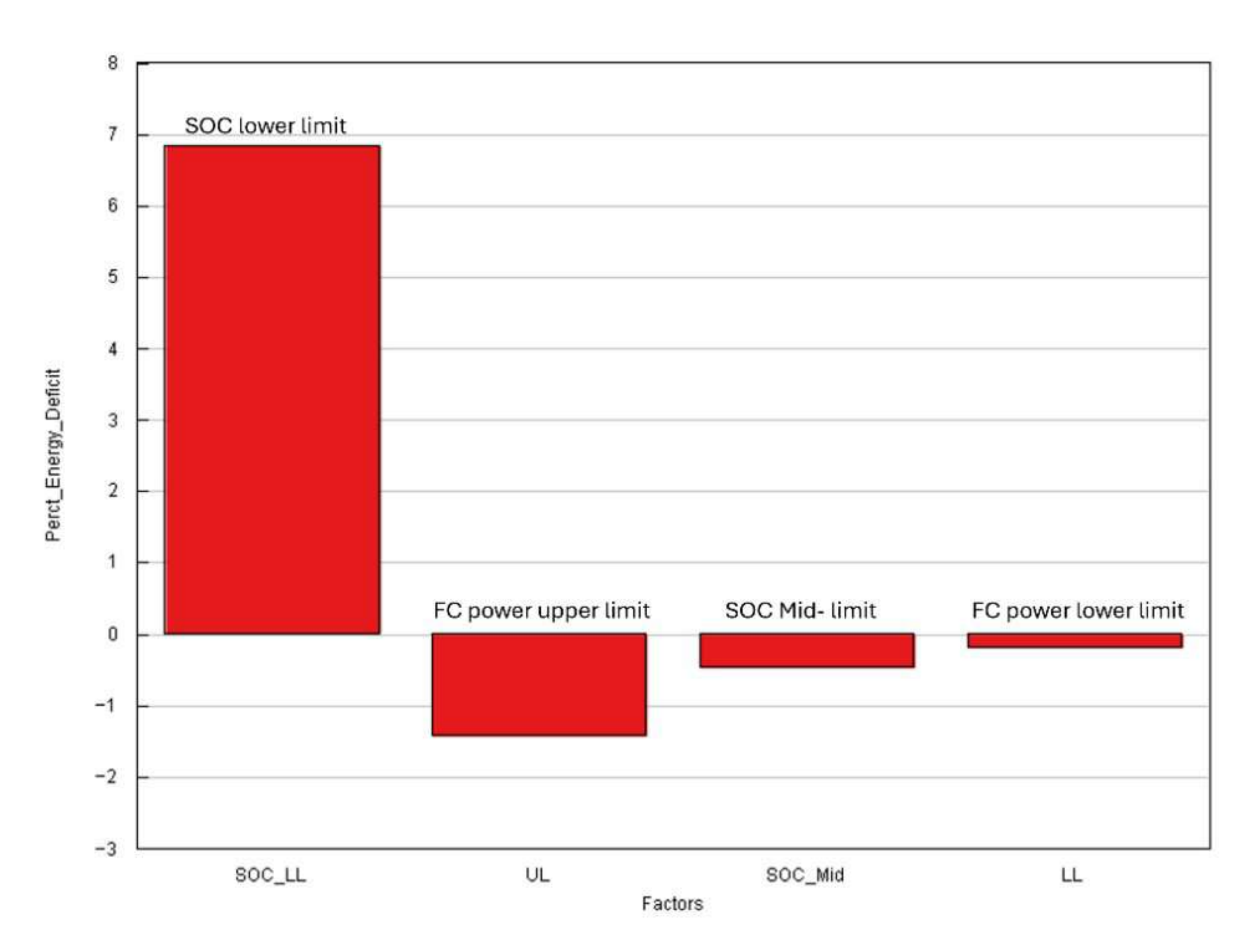


Figure 27 – Sensitivity analysis of control parameters for perc. energy deficit—Battery SOC-based algorithm

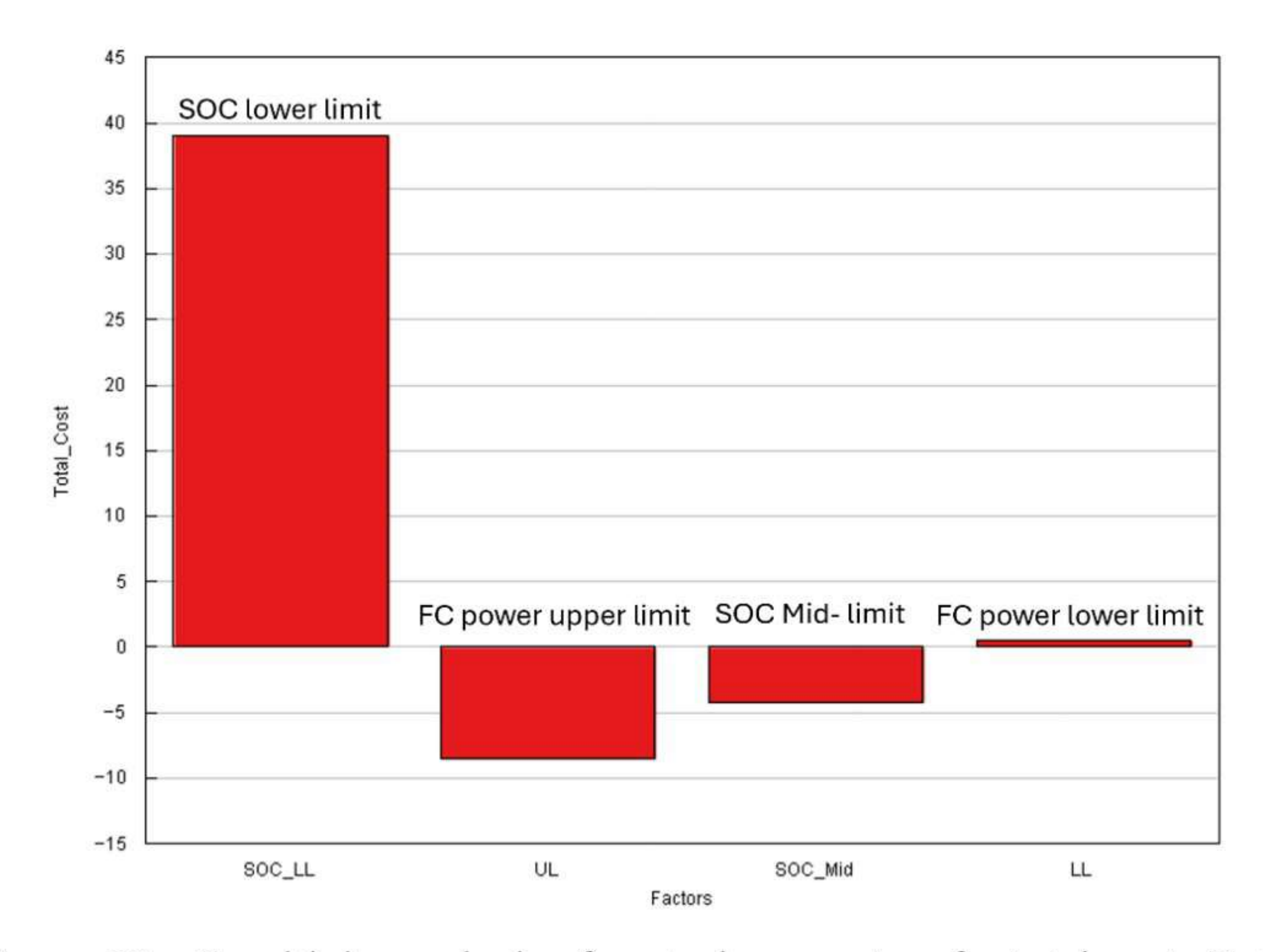


Figure 28 – Sensitivity analysis of control parameters for total cost– Battery SOC-based algorithm

From the figure 27, it is seen that the energy deficit has highest sensitivity towards lower SOC limit and least or negligible for FC lower power limit. SOC lower power limit is directly related to the energy deficit whereas other three parameters are inversely related. It can be inferred from the graph that every 10% increase in the

SOC lower limit leads to an increase in the percentage energy deficit by around 7 units. On the contrary, for SOC mid-limit, an increase of 10% leads to 0.5 units decrease in the percentage energy deficit. This is because according to the logic, the percentage contribution of battery is very high till SOC reaches its mid-limit. Hence, when we increase the SOC mid-limit, the time for which the battery delivers large amount of energy decreases which means that the battery has more energy to deliver at other cases. Thus, there is a decrease in the energy deficit. In case of FC upper power limit, increasing its value leads to a decrease in the energy deficit since this reduces the battery load and in turn chances of battery getting replenished before time.

From the figure 28, it can be observed that the total cost has highest sensitivity towards SOC lower limit and lowest towards FC lower power limit. This is because according to the control logic, when the battery reaches to its lower SOC limit, entire power must be given by the FC. Thus, increasing the lower SOC limit results in the battery reaching to its lower limit earlier and thus leading to more hydrogen consumption which in turn leads to higher total cost. In case of FC upper power limit, increase in its value reduces the battery load in case where the SOC is between lower and middle value. Hence, the phenomenon of battery reaching its lower limit gets postponed leading to a reduced hydrogen consumption and overall total cost.

This leads to the end of the chapter on DOE. The next chapter will be describing the results obtained from the configurations finalized in the DOE.

Chapter 8

Results

After obtaining the optimum values for control parameters and hardware configurations, simulation was run with this parameter and the corresponding plots were obtained for the algorithm which gives minimum total cost using the simulation post processing tool 'GT-Post'. This chapter shows these results along with graphs for the three algorithms. Moreover, it shows comparison of few important outputs of all the three algorithms in the graphical form.

8.1 Results – FC power-based algorithm

The simulation was carried out for two different ambient temperatures – 6° C and 50° C. The values shown in the table below are at these two temperatures.

Parameter	Value (@T=6 ⁰ C)	Value (@T=50°C)
Hydrogen consumption	58 kg	53 kg
Hydrogen cost per km	109 Rs/-	100 Rs/-
FC cost per km	65 Rs /-	53 Rs /-
Battery cost per km	36 Rs /-	36 Rs /-
Total energy demand	5811 MJ	5811 MJ
Electricity cost per km	44 Rs /-	44 Rs /-
Percentage of total energy	75.27%	65.68%
delivered by FC		G S
Percentage of total energy	24.62%	27.53%
delivered by battery		
Percentage energy deficit	0.13%	6.79%

Table 16 – Results – FC power-based algorithm

It can be inferred from the table above that the percentage energy deficit is critical at 50°C. This is because at this temperature, the maximum power producing capacity of fuel cell is lesser due to which the upper power limit of the FC is lower leading to a higher battery load. So, for a given battery size the percentage energy deficit comes out to be more at this temperature. On the other hand, the cost and hydrogen consumption are more at 6°C because the upper power limit is higher at this temperature. The total energy and the individual component energy was calculated by integrating the corresponding power curves. Battery cost and the electricity cost are

constant for both the temperatures because these values are only dependent on the hardware configurations which are same for both the temperatures.

The plots that are shown below are at 50°C.

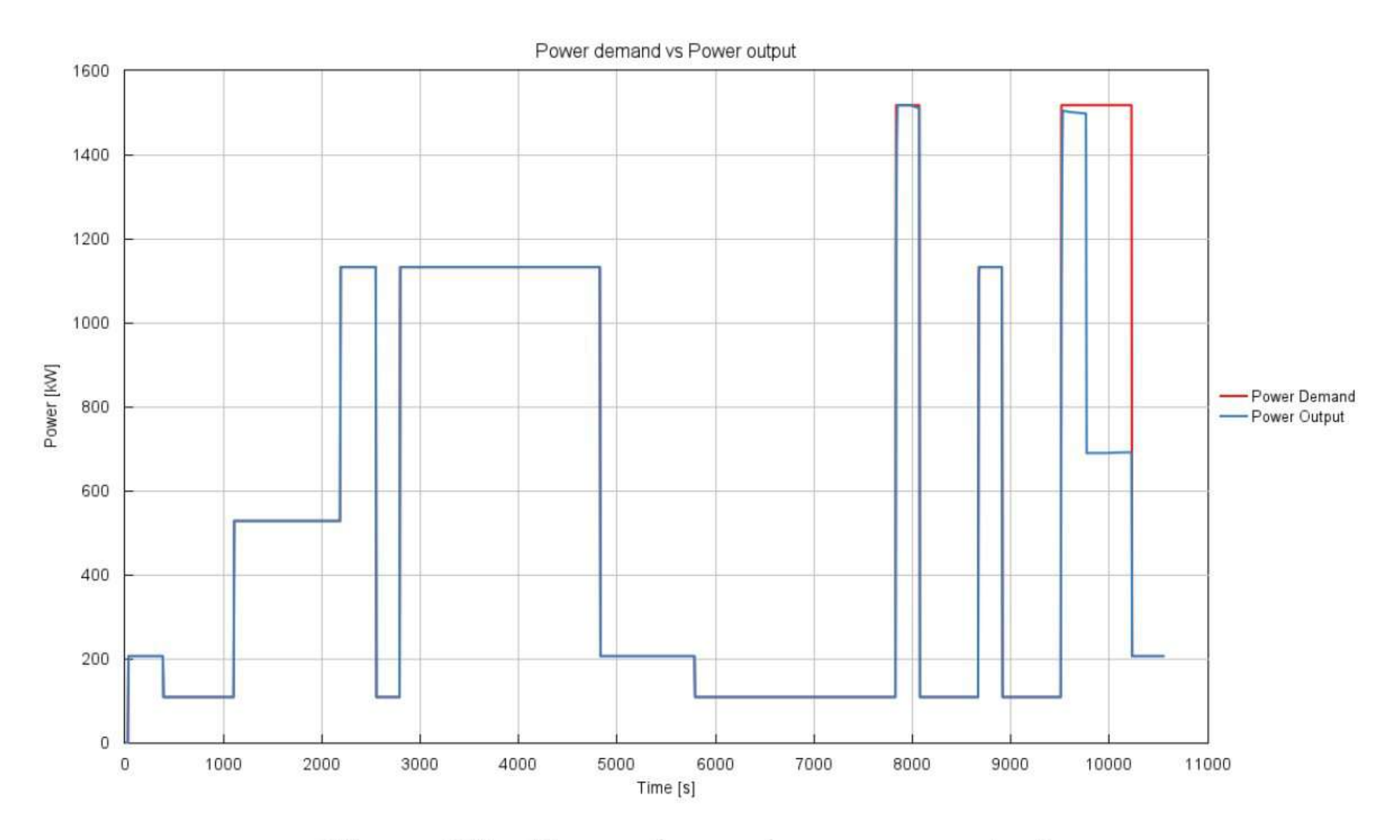


Figure 29 – Power demand vs power output

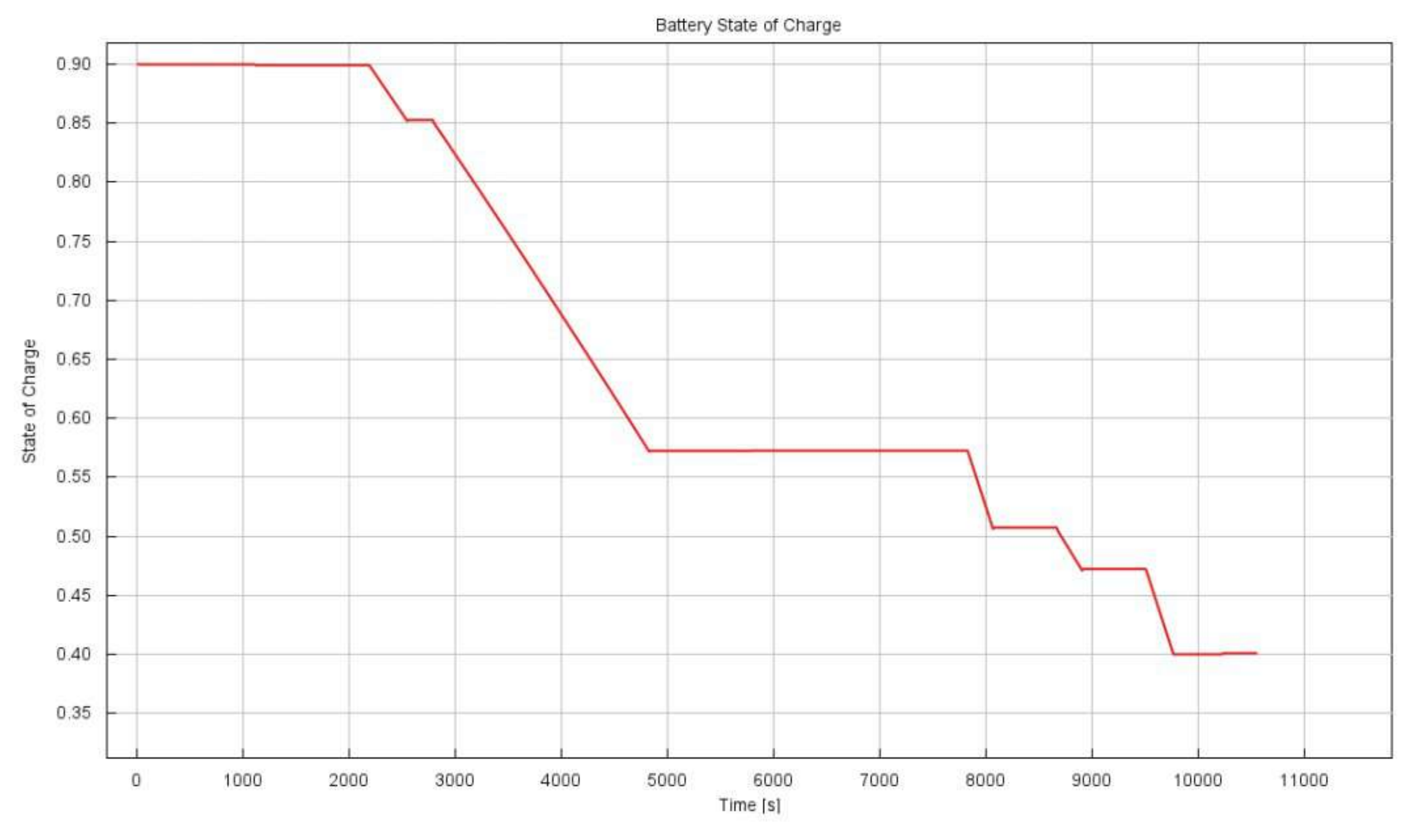


Figure 30 – Battery SOC

The Figure 29 above depicts the power demand vs power output curve. Power output is the summation of the power outputs from battery and FC. It can be seen that the power demand is very nicely met for most of the time except between 9500 and 10500 seconds where there is a certain amount of power deficit due to the battery

reaching its lower limit. Figure 30 shows the battery SOC profile for the entire run. The battery starts at an initial SOC of 90 % and ends at lower limit of 40% which ensures the full battery capacity utilisation.

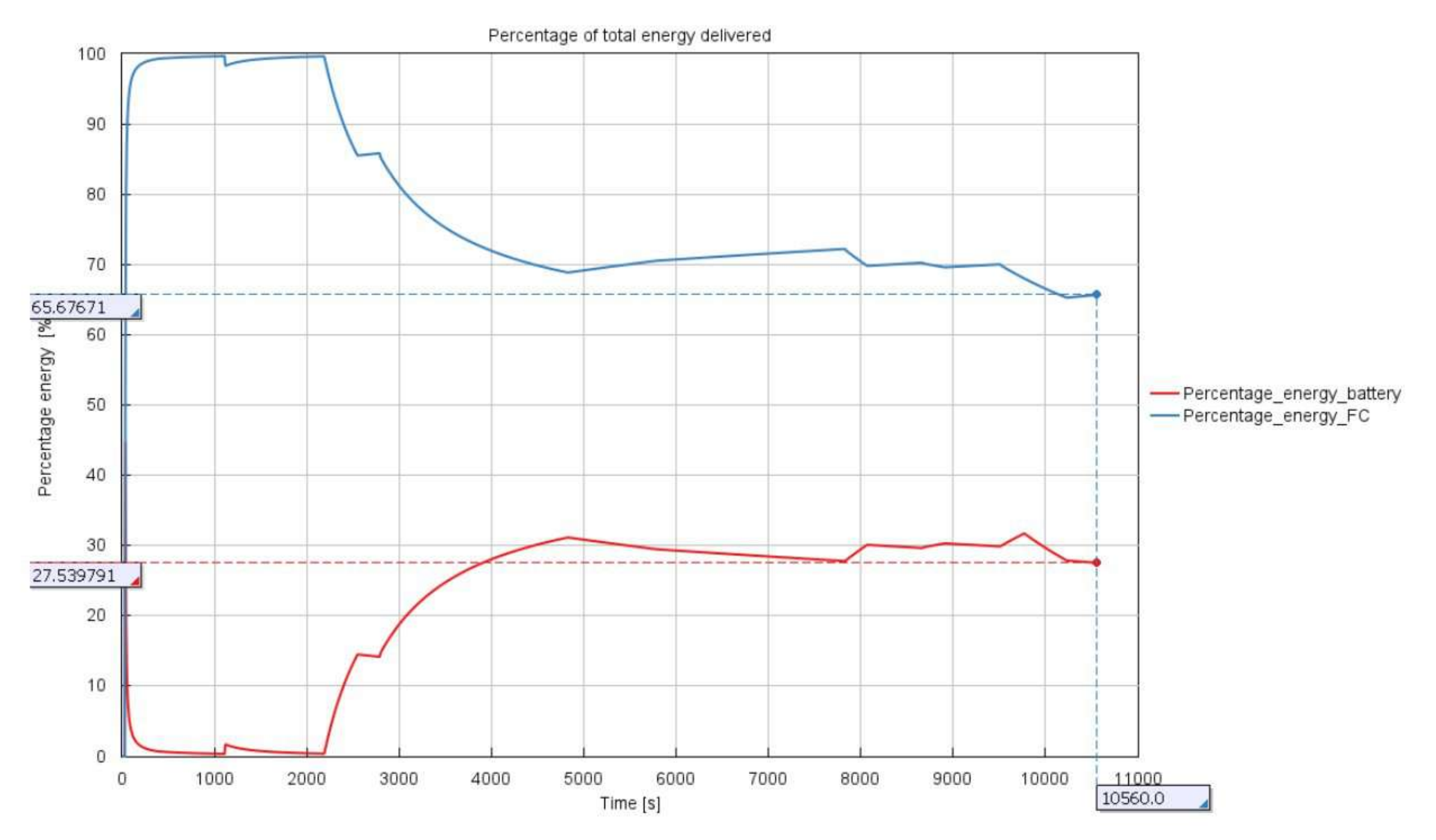


Figure 31 – Percentage of total energy delivered

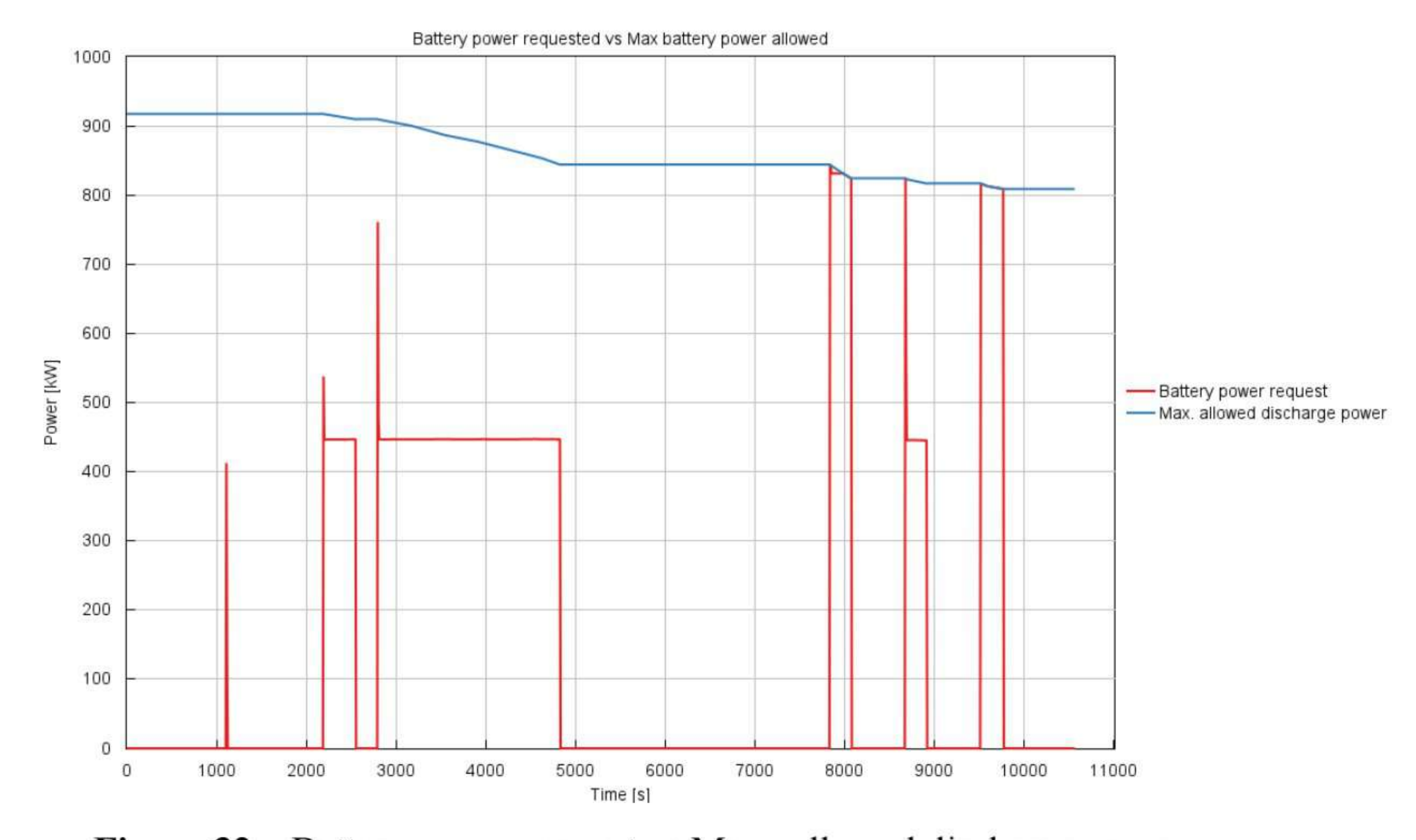


Figure 32 – Battery power request vs Max. allowed discharge power

Figure 31 shows the percentage of total energy delivered by battery and fuel cell. This plot were obtained by integrating the power curves of battery and FC. The FC is contributing more than battery and at the end, FC cumulatively contributes around 66% of the total energy demand and battery around 27% of the energy demand. Figure 32 compares the power demand from the battery and the maximum power allowed to be discharged from the battery at each time instant. The maximum discharge power is obtained from the battery power limiter. If the power demand goes above the maximum discharge power, then it will lead to power deficit i.e. the power demand will not be met. Hence in the logic, the battery power request has been restricted to maximum discharge power if the difference between power demand and FC output power goes above it. This will contribute to net power deficit.

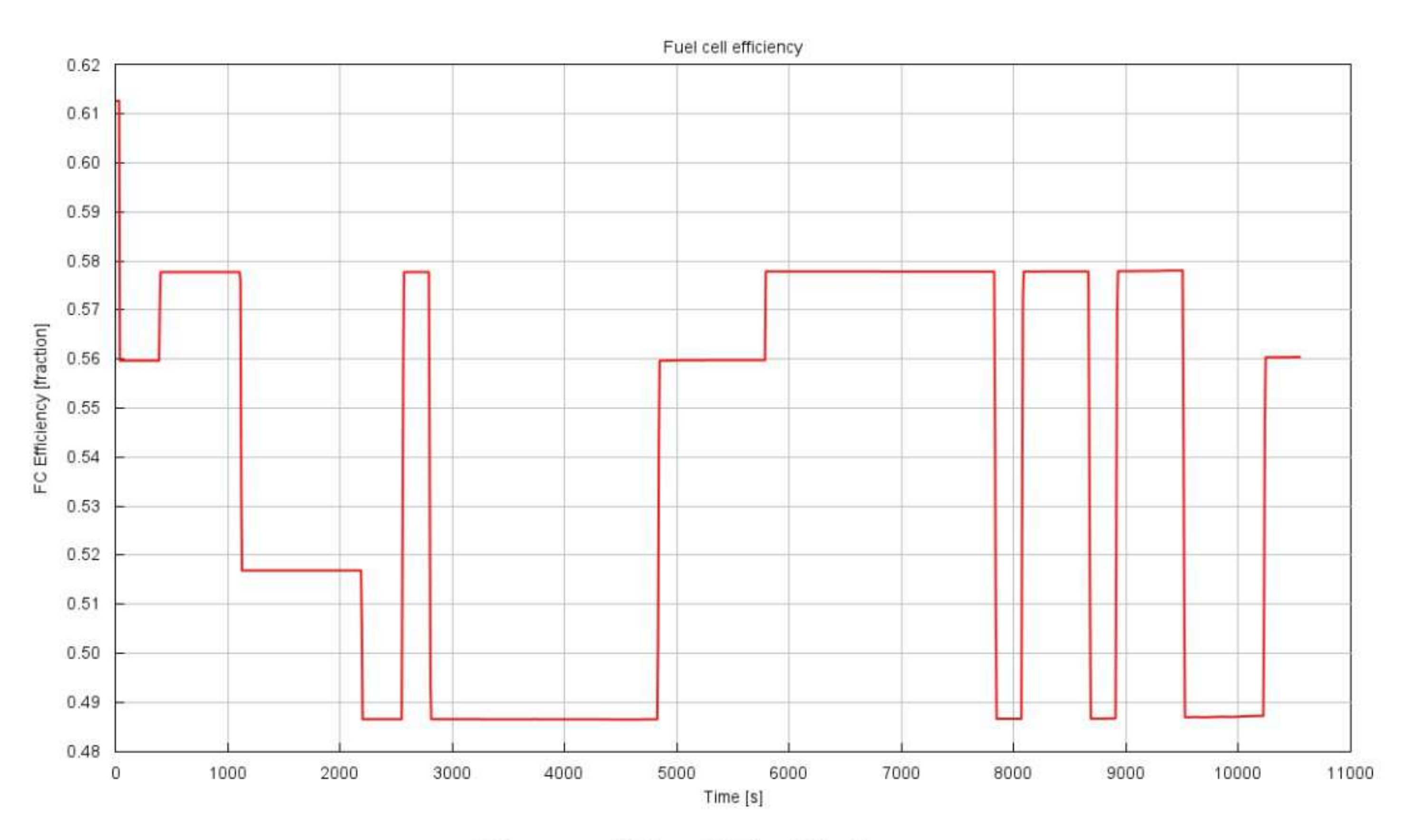


Figure 33 – FC efficiency

Figure 33 shows the FC efficiency curve. It is obtained from the mathematical model for FC efficiency which takes in maximum power, power output, ambient temperature and ambient pressure as the input. It is observed that the efficiency varies between 48.5% and 58%.

8.2 Results – FC efficiency-based algorithm

Parameter	Value (@T=6°C)	Value (@T=50°C)
Hydrogen consumption	53 kg	36 kg
Hydrogen cost per km	99 Rs/-	68 Rs/-
FC cost per km	65 Rs /-	53 Rs /-
Battery cost per km	59 Rs /-	59 Rs /-
Total energy demand	5811 MJ	5811 MJ

Electricity cost per km	73 Rs /-	73 Rs /-
Percentage of total energy	70.10%	48.11%
delivered by FC		
Percentage of total energy	29.80%	45.41%
delivered by battery		
Percentage energy deficit	0.10%	6.48%

Table 17 – Results – FC efficiency-based algorithm

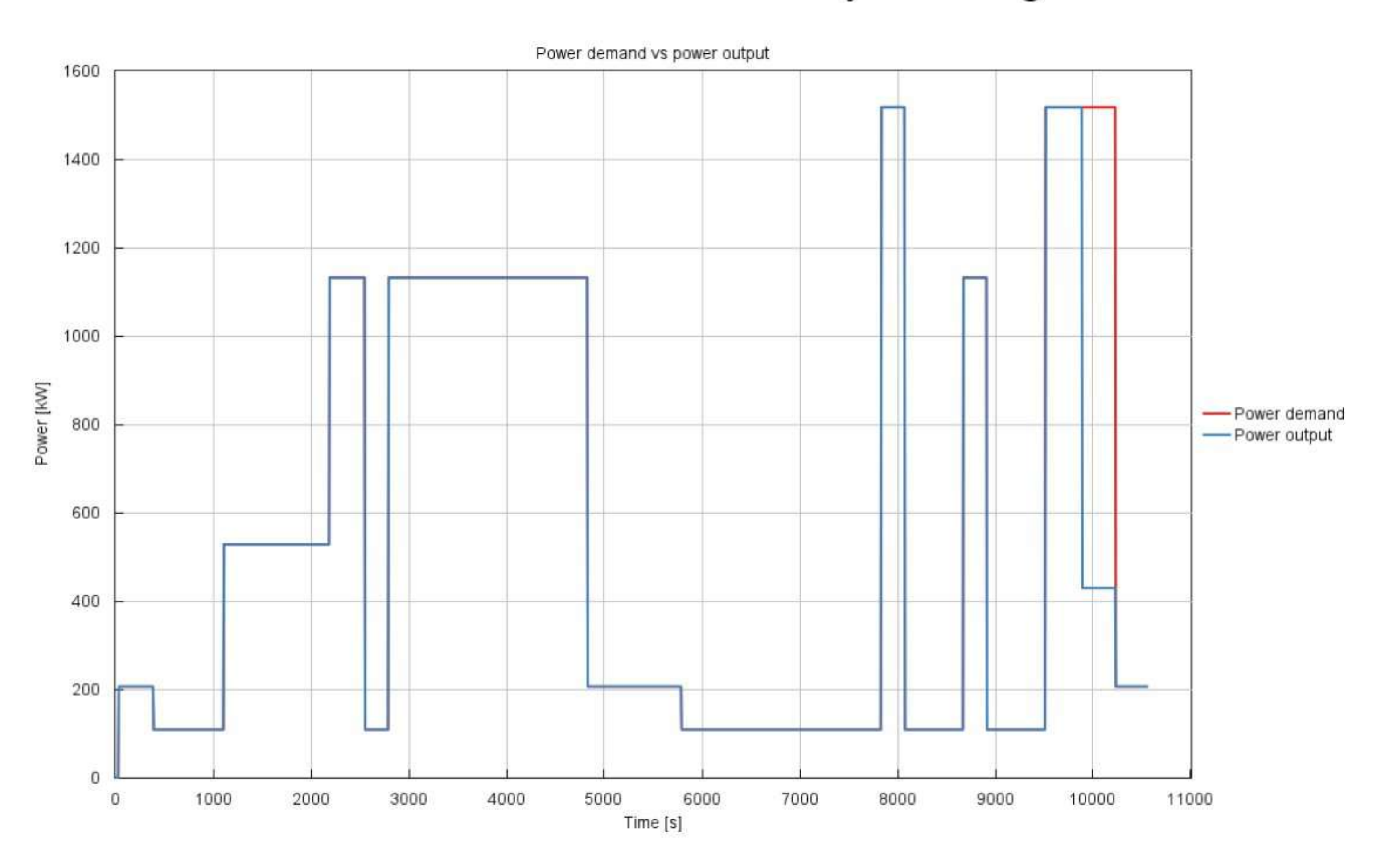


Figure 34 – Power demand vs power output – FC efficiency-based algorithm

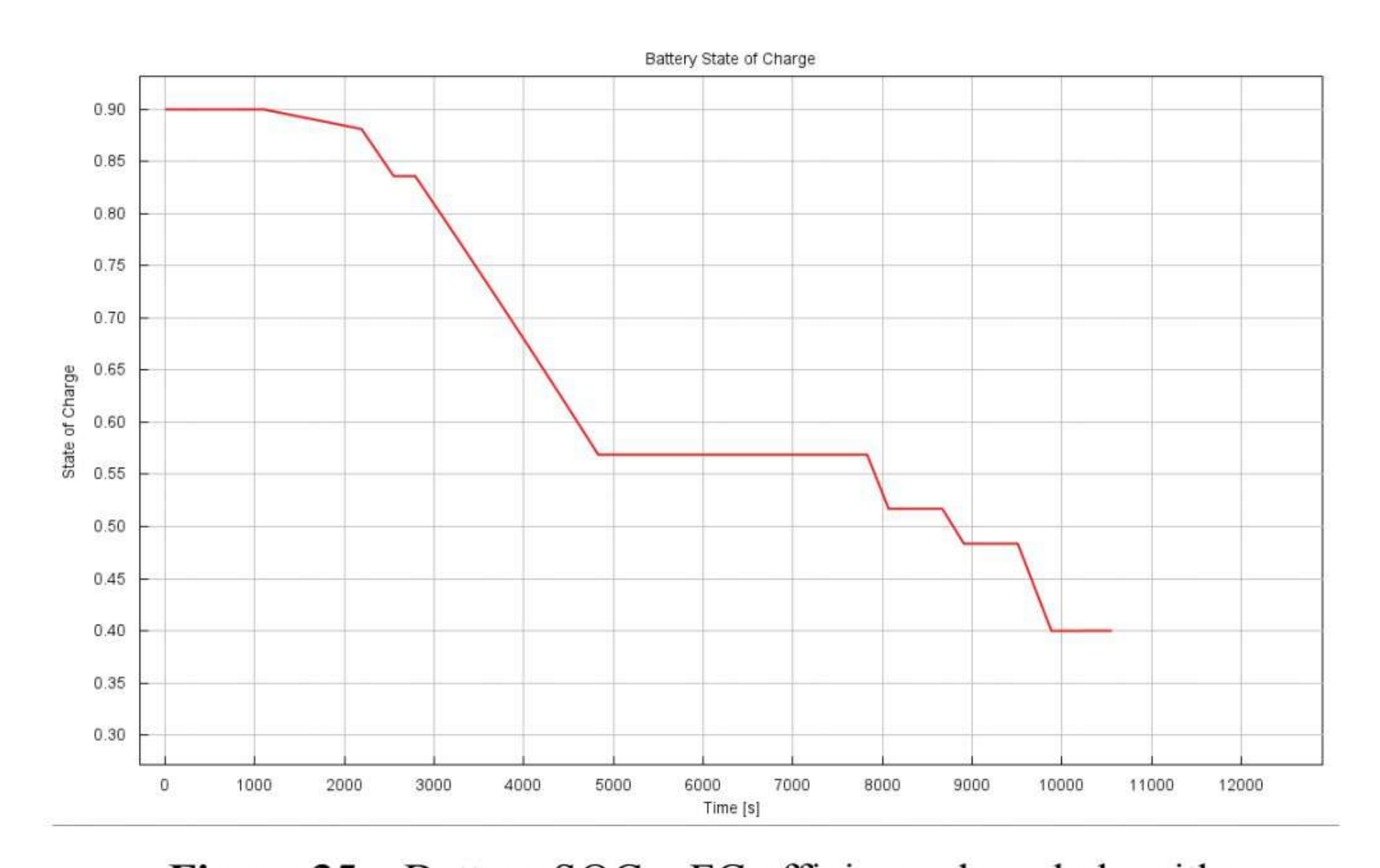


Figure 35 – Battery SOC – FC efficiency-based algorithm

Figure 34 shows the power demand vs power output profile. It can be seen that the power demand is completely met except the last few seconds of the drive cycle wherein the battery SOC reaches to its lower limit due to which it cannot contribute

any further to the power output and the fuel cell is restricted by the efficiency limits leading to a power deficit. Figure 35 depicts the battery SOC profile. It can be observed that the battery is utilized fully as it reaches to its lower limit. There is a step fall in the SOC between 3000 and 5000 seconds where the power demand is very high. Between 5000 and 8000 seconds, the battery SOC is constant which means that there is zero load on the battery. This is because the efficiency of FC between this interval is between the upper and lower limit due to which it is providing the entire power demand.

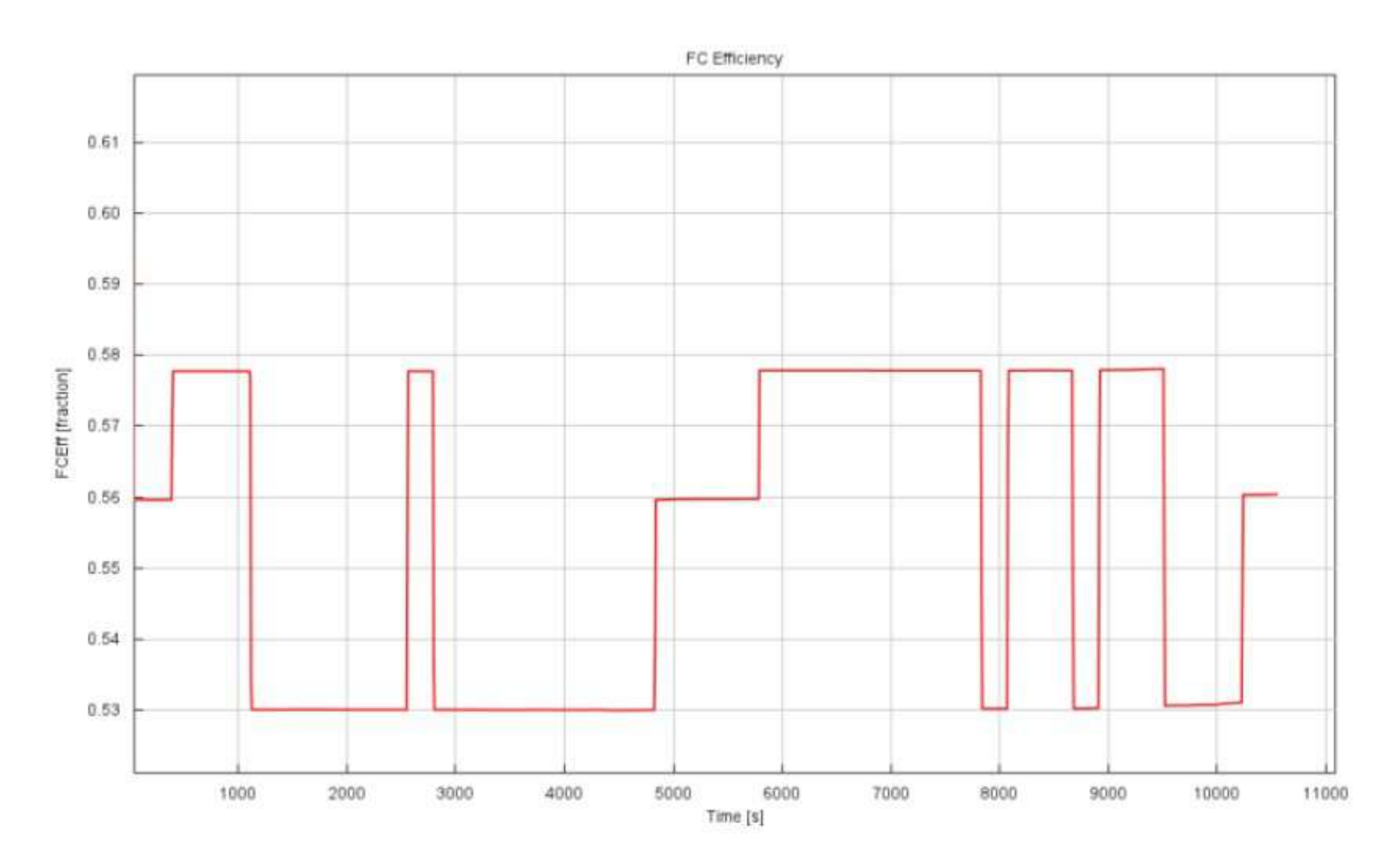


Figure 36 – FC efficiency curve – FC efficiency-based algorithm

The figure 36 above shows the FC efficiency curve. The FC efficiency has been restricted between the upper and lower limit of 60 and 53% respectively. Whenever there is a drop in the power output from the FC, there is a rise in the FC efficiency. This tells us that the FC model is following the polarization curve.

8.3 Results – Battery SOC-based algorithm

Parameter	Value (@T=6°C)	Value (@T=50°C)
Hydrogen consumption	57 kg	61 kg
Hydrogen cost per km	108 Rs/-	116 Rs/-
FC cost per km	65 Rs /-	53 Rs /-
Battery cost per km	41 Rs /-	41 Rs /-
Total energy demand	5811 MJ	5811 MJ
Electricity cost per km	50 Rs /-	50 Rs /-
Percentage of total energy	65.63%	58.04%
delivered by FC		
Percentage of total energy	31.87%	35.02%
delivered by battery		
Percentage energy deficit	2.5%	6.94%

Table 18 – Results - Battery SOC-based

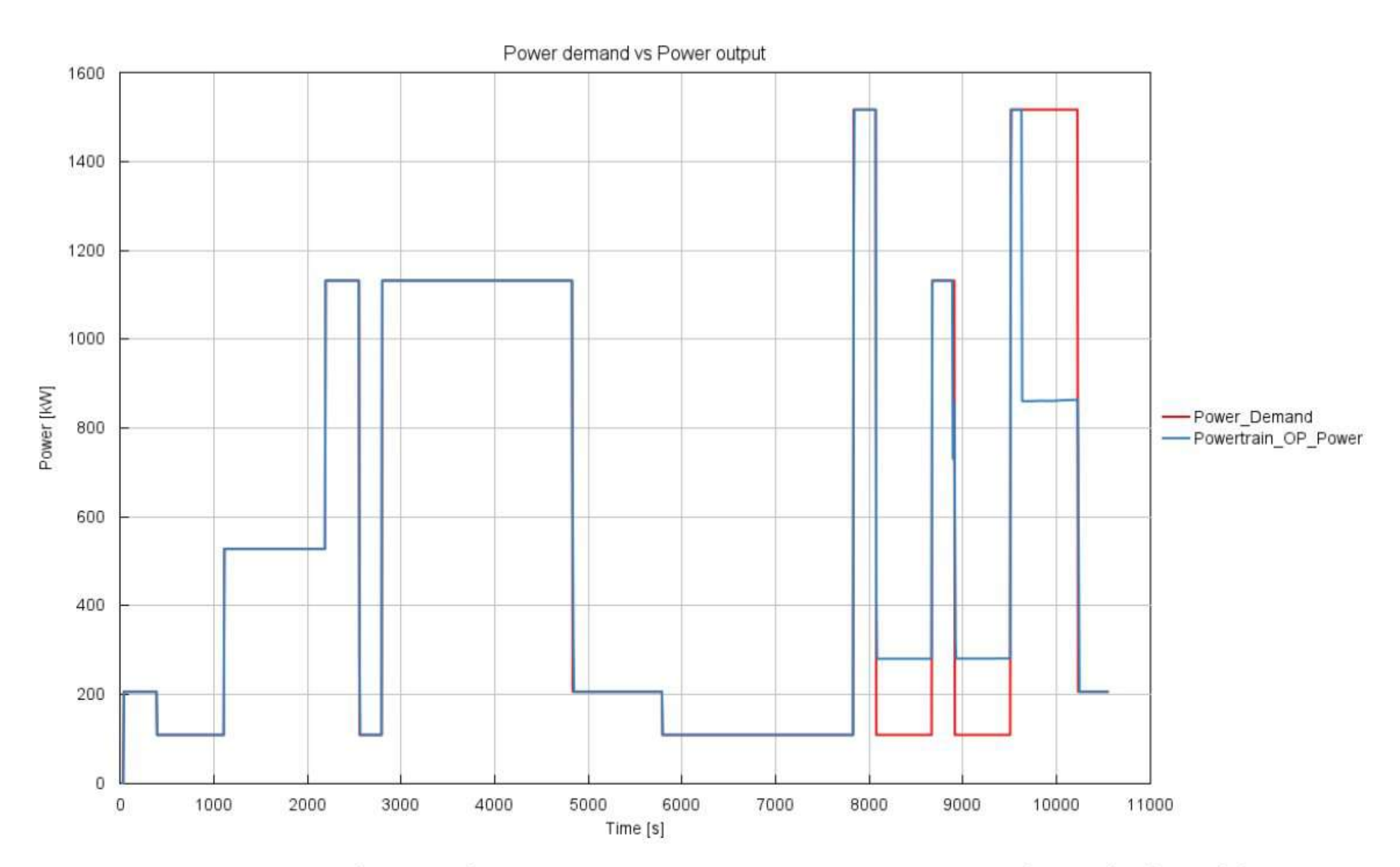


Figure 37 – Power demand vs power output –Battery SOC-based algorithm

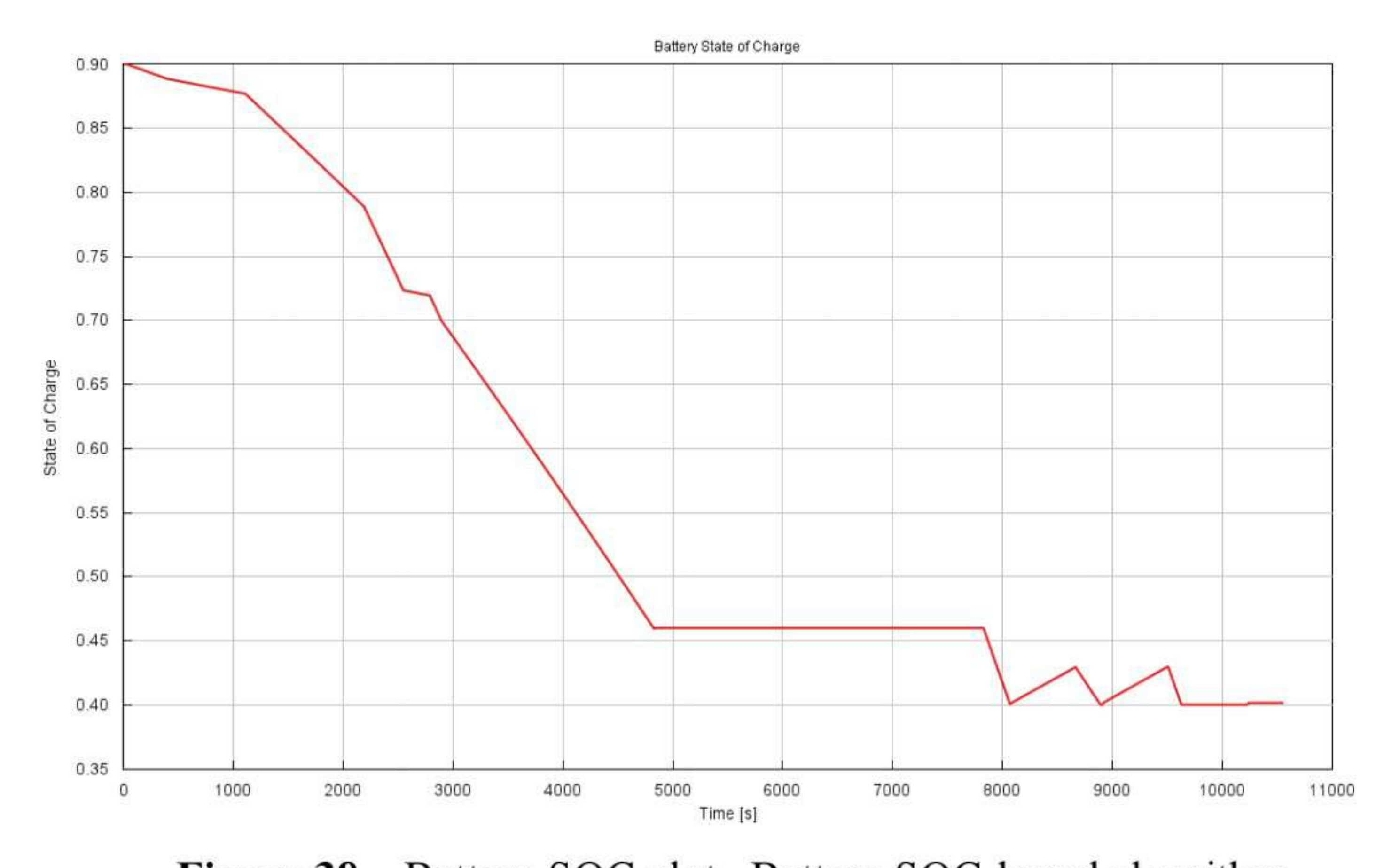


Figure 38 – Battery SOC plot –Battery SOC-based algorithm

Figure 37 depicts the power demand vs power output curve. Apart from the power deficit at last few seconds, we can see that at some instances between 8000 and 9500 seconds, power output is more than what is required. This surplus power can be used to charge the battery.

Figure 38 depicts the battery SOC curve. Between 8000 and 9500 seconds where surplus power is produced, it is seen that there is a rise in the SOC indicating that the surplus power is used to charge the battery.

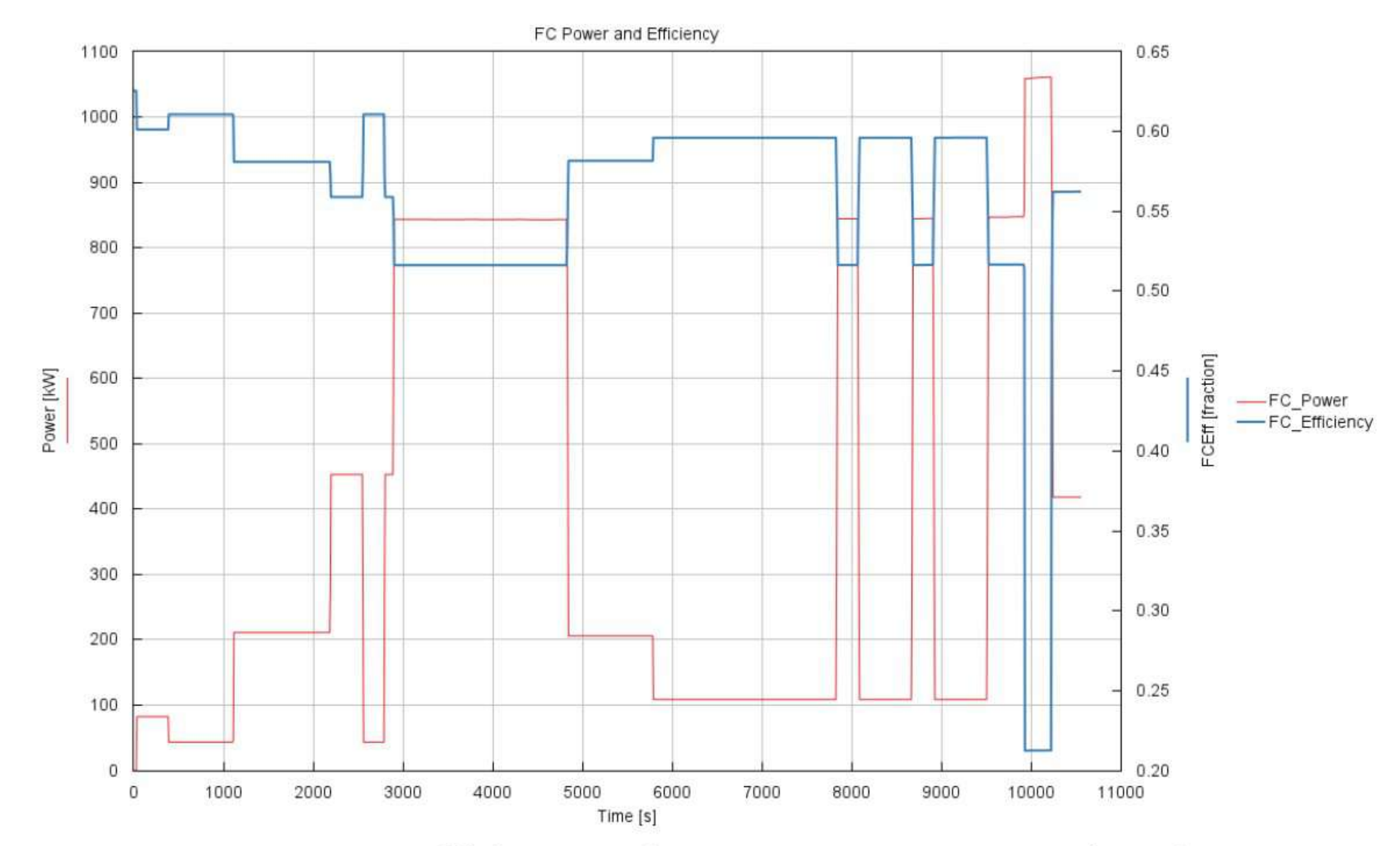


Figure 39 – FC efficiency and FC power–Battery SOC-based

Figure 39 shows FC power output on left Y-axis and FC efficiency on right Y-axis. In the final 500 seconds of the cycle, it can be seen that due to very high power output from the FC, its efficiency has drastically fallen.

8.4 Result comparison

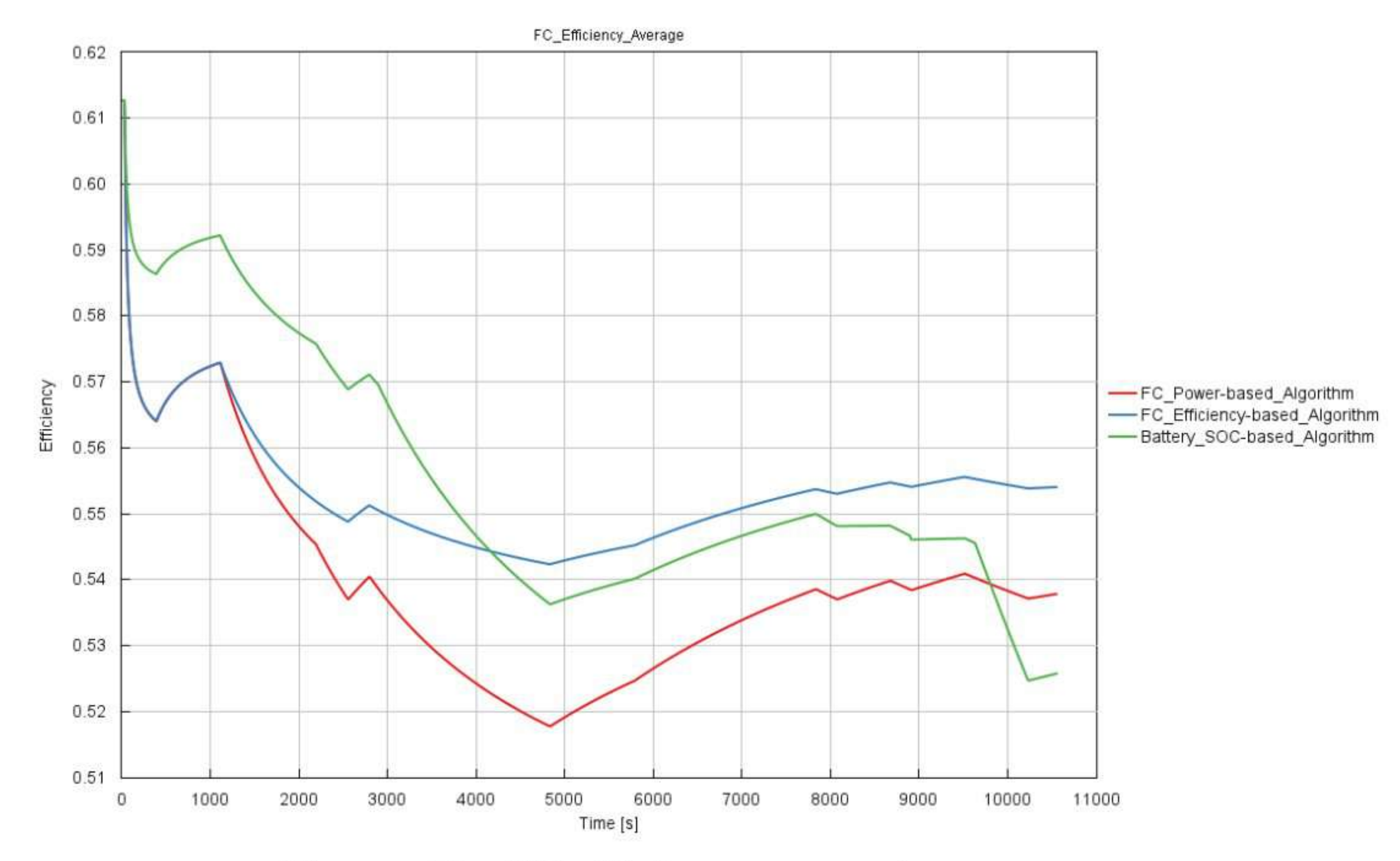


Figure 40 – FC efficiency comparison

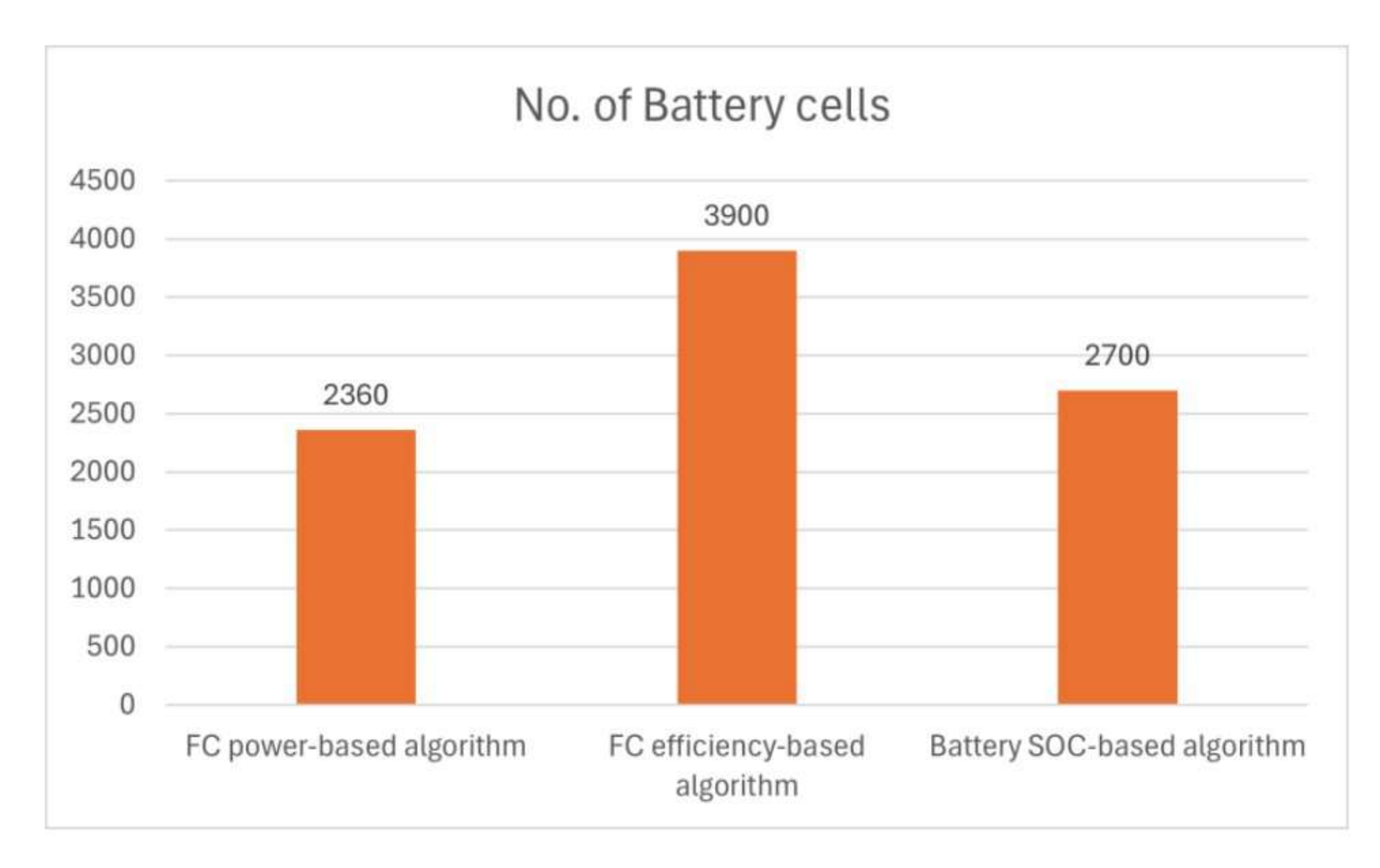


Figure 41 – No. of battery cells comparison

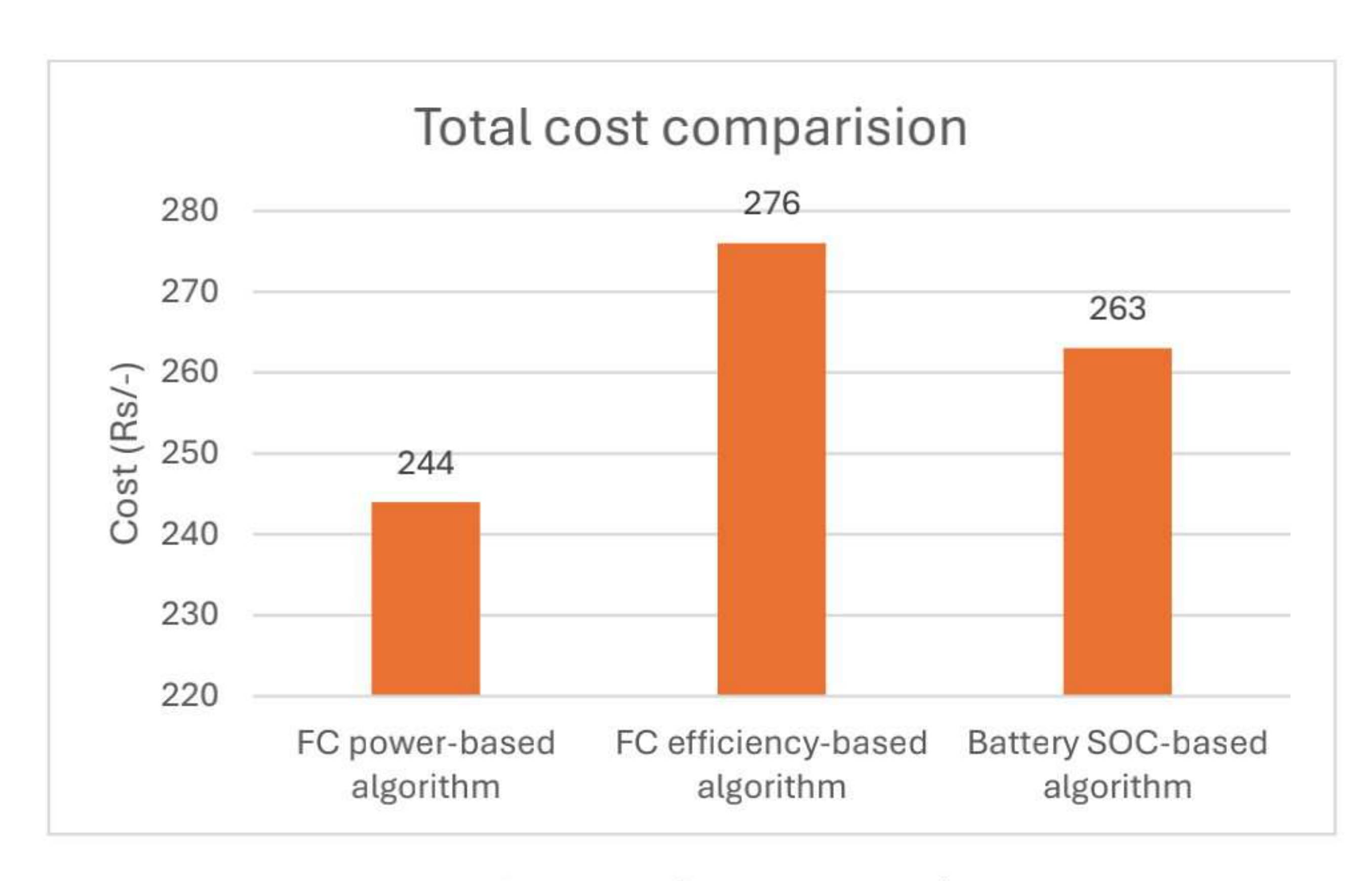


Figure 42 – Total cost comparison

Figure 40 depicts the graphs of average value of efficiency for all the three algorithms. The final average efficiency of the efficiency-based algorithm is the highest followed by the power-based algorithm and the battery SOC-based algorithm. Figure 41 compares the number of battery cells for each algorithm which contributes to the battery cost and the electricity cost. It can be inferred from the Figure 42 that power-based algorithm has the least total cost followed by battery SOC-based algorithm and the FC efficiency-based algorithm in order respectively. This owes to its good FC efficiency and requirement of less battery cells. Based on this observation, FC power-based algorithm can be considered as the best algorithm.

Chapter 9

9. Fuel cell physics-based model

The most optimum algorithm was obtained after running DOE on all the three algorithms with mathematical model of FC as explained in the previous chapter. FC power-based algorithm was this best algorithm. This algorithm was then integrated with the physics-based template of FC which is available in GT-ISE. The main objective was to match the results obtained through FC mathematical model with those obtained from the physics-based model. This chapter explains about this model including its parameters and the results obtained henceforth.

9.1 Fuel cell PEM template

In order to model the chemical and physical properties of a PEMFC (Proton Exchange Membrane Fuel Cell), GT-ISE offers a template named 'Fuel cell PEM'. This template models the flow, mass transfer, heat transfer and electrical power generation of a Fuel Cell. It consists of various folders with each defining specific property of a PEMFC. These folders are mentioned below -

1. Main – Includes following sections-

Electrochemistry and mass transport specification - The reference object that characterizes the electrochemistry and mass transport of the fuel cell. This reference object defines total number of fuel cells in the stack, active surface area of the cell, numeric profile for polarization curve and the loss mechanisms

Load type – defines whether the load is to be given using electrical circuit or using a power request magnitude

Heat rejection method – defines how the heat will be rejected from the fuel cell. One of the options can be using a cooling circuit wherein the heat will be rejected to the coolant which will be cooled by some other means like a radiator. Other option is to provide the heat transfer coefficient value which will determine the convection heat transfer from the fuel cell

- 2.Discretization Option to discretize the flow of cathode, anode, and coolant paths from a single sub volume into a series of sub volumes
- 3.Cathode Used to define the cathode geometry and chemistry and include following sections

Channel – used to define the channel shape and size

Header – used to define the diameter and length of the header

Option – defines the cathode fluid properties and pressure drop in cathode

- 4. Anode includes same option as that of cathode
- 5. Coolant If 'Model coolant circuit' option is enabled in Main folder, this folder defines coolant channel and header dimensions & the coolant fluid properties
- 6. Thermal Option for how to define the primitive thermal mass components and connections that represent the solid components of the fuel cell.

Parameter	Value
No. of cells in the stack	1700
Active surface area	1400
Load type	By electrical connections
Heat rejection method	Using external boundary conditions
No. of cathode channels per cell	6
No. of anode channels per cell	6
Cathode initial temperature	70°C
Anode initial temperature	70°C

Table 19 – FC physics-based model parameters

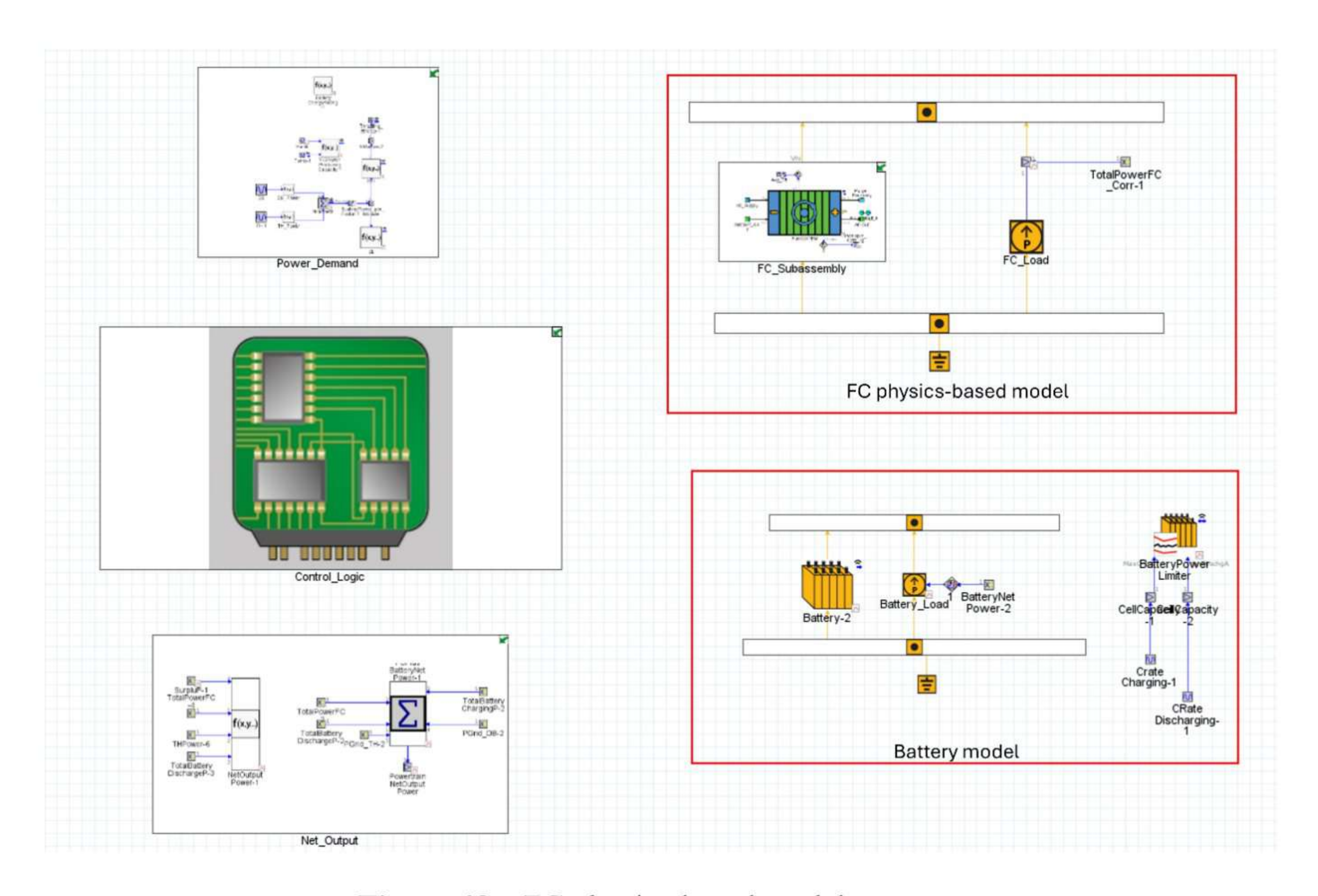


Figure 43 – FC physics-based model

Table 19 above specifies some of the important parameters given as an input in the 'Fuel cell PEM' template. The number of cells and the active surface area were calculated based on the desired total voltage across the fuel cell and the maximum output power required. There were three main assumptions in this calculation -

- 1. Total voltage across the fuel cell = 1300 Volts
- 2. Voltage obtained across each cell = 0.8 Volts
- 3. Current density = 1.5 A/cm^2

Figure 43 shows the model wherein the FC power-based algorithm is integrated with the FC physics-based model and the battery model.

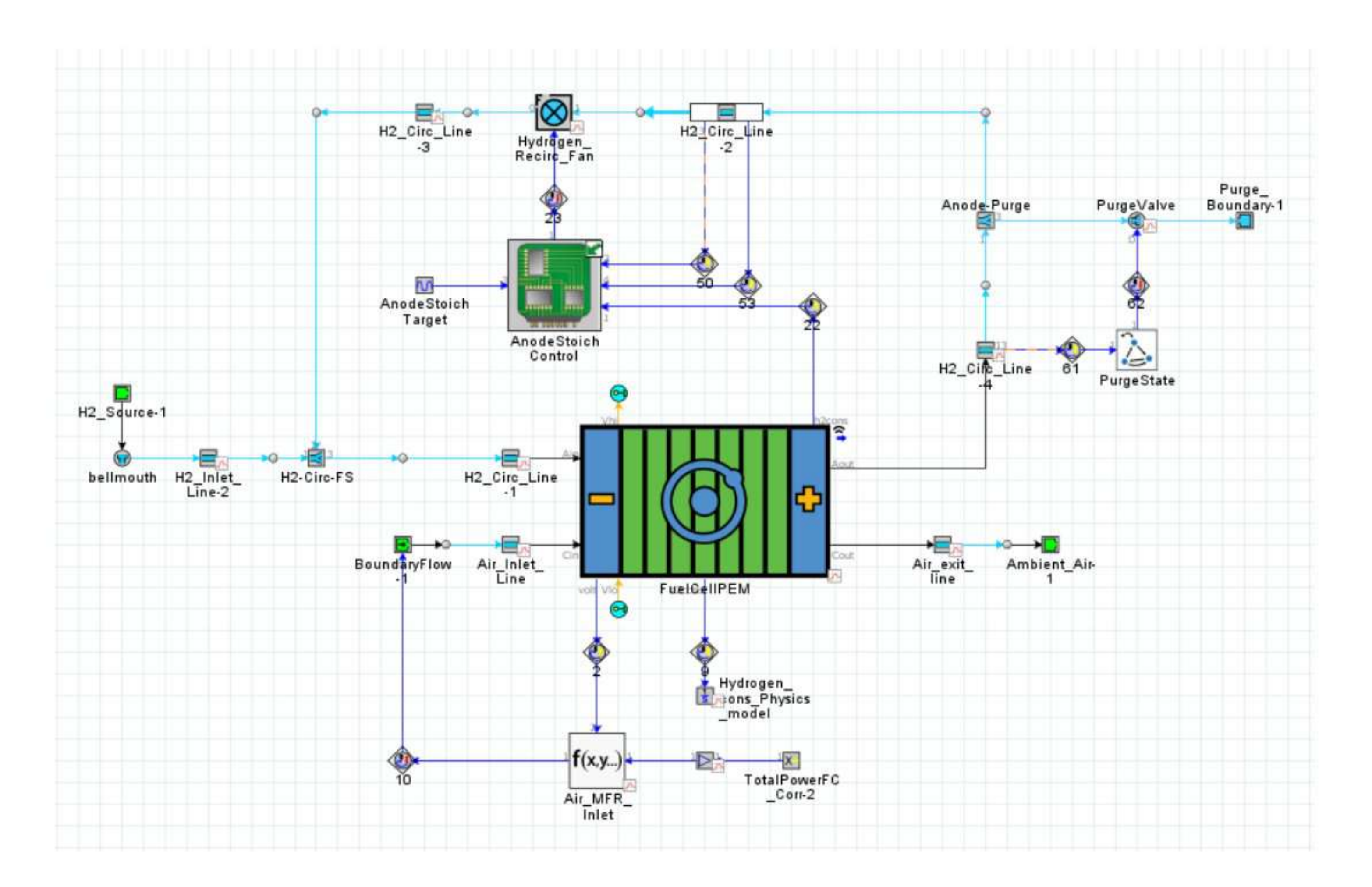


Figure 44 – FC physics-based model flow circuit

Figure 44 shows the flow circuit associated with the FC template. The template required four main physical inputs –

- 1. Anode inlet hydrogen
- 2. Anode outlet unreacted hydrogen
- 3. Cathode inlet oxygen
- 4. Cathode outlet water vapor

A 'boundary pressure' template is used to define the pressure and temperature of hydrogen at the inlet of the pipe which connects to the anode inlet channels. Pipe diameter required can be calculated using the required mass flow rate of hydrogen.

Calculation for hydrogen mass flow rate required

Assumptions -

- 1. Faraday's constant (F) = 96485 Coulombs per mole
- 2. Molar mass of hydrogen = 0.002016 kg per mole
- 3. Anode stoichiometric ratio for a PEMFC = 1.5

Calculations - [14]

Theoretical hydrogen flow rate = $Molar\ flow\ rate \times molar\ mass\ of\ hydrogen$

$$= \frac{Power\ demand}{2 \times F \times voltage\ output\ per\ cell} \times 0.002016$$

Theoretical Hydrogen mass flow rate = $0.002016 \times \frac{Power\ demand}{192970 \times voltage\ output\ per\ cell}$

Actual hydrogen mass flow rate = 1.5 \times Theoretical Hydrogen mass flow rate $\frac{kg}{sec}$

The above equation can be used to calculate the instantaneous mass flow rate of hydrogen required for a given power demand

Calculations for flow pipe diameter -

Using ideal gas equation -

Let

P- Hydrogen pressure in bars

 ρ – Density of hydrogen (kg/m³)

R – characteristic gas constant for hydrogen

T – hydrogen temperature in ⁰C

A – Pipe cross sectional area

Di – Inner diameter of the pipe in meters

V - Velocity of hydrogen in pipe in m/sec

m = Maximum mass flow rate in kg/sec

According to ideal gas equation -

$$\rho = \frac{P}{R \times T}$$

$$m = \rho \times A \times V$$

$$m = \rho \times \frac{\pi}{4} \times Di^2 \times V$$

$$Di = \sqrt{\frac{m \times 4}{\rho \times \pi \times V}}$$

The above equation was used to calculate the diameter of the pipe required to connect the anode channels with the hydrogen storage. Pipe diameter using this equation comes out to be 25 mm. At the exit of the anode, we have the recirculation line of unutilized hydrogen. Hydrogen from the outlet can have one of the two pathways. Either the hydrogen is recirculated back to the anode inlet, or it is purged outside the system through the purge valve. The purge valve is basically an orifice whose state is controlled based on the mass fraction of hydrogen coming through the anode outlet. If it is below the set limit, then the orifice is completely opened, and no recirculation will take place. The flow rate of hydrogen recirculated is controlled through a 'Fan Flow' template which imposes the required flow rate on the fluid flowing across it. The amount of flow rate is given as input to this template using following equation - Let,

m - Mass flow rate of hydrogen (kg/sec)

x - hydrogen mass fraction in the incoming flow

SR - Desired stoichiometric ratio

 ρ – hydrogen density (kg/m³)

Q = Volumetric flow rate (kg/m³)

$$Q = \frac{m}{x} \times \frac{SR - 1}{\rho}$$

9.2 Results comparison – FC Mathematical model & FC physics-based model

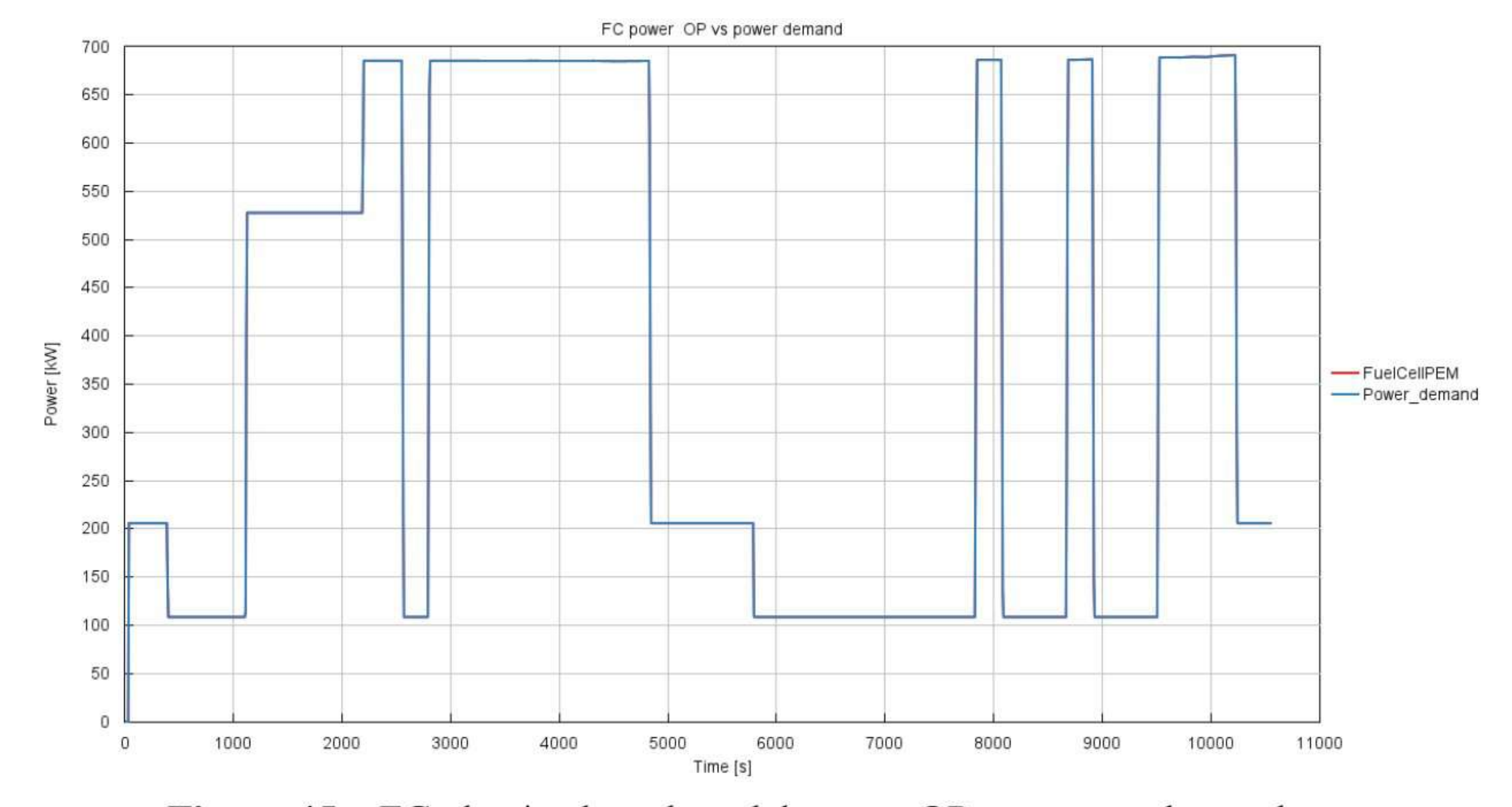


Figure 45 – FC physics-based model power OP vs power demand

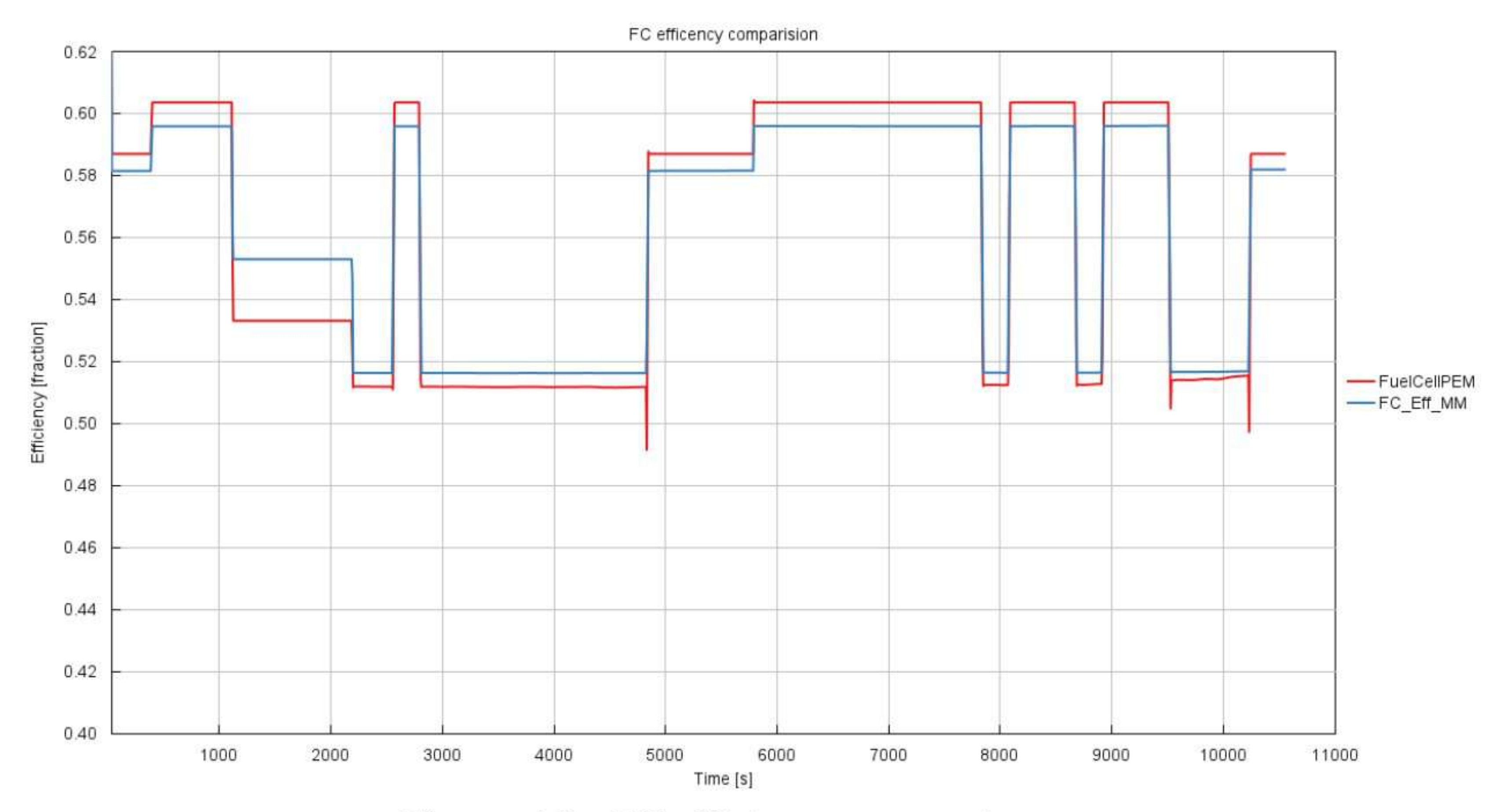


Figure 46 – FC efficiency comparison

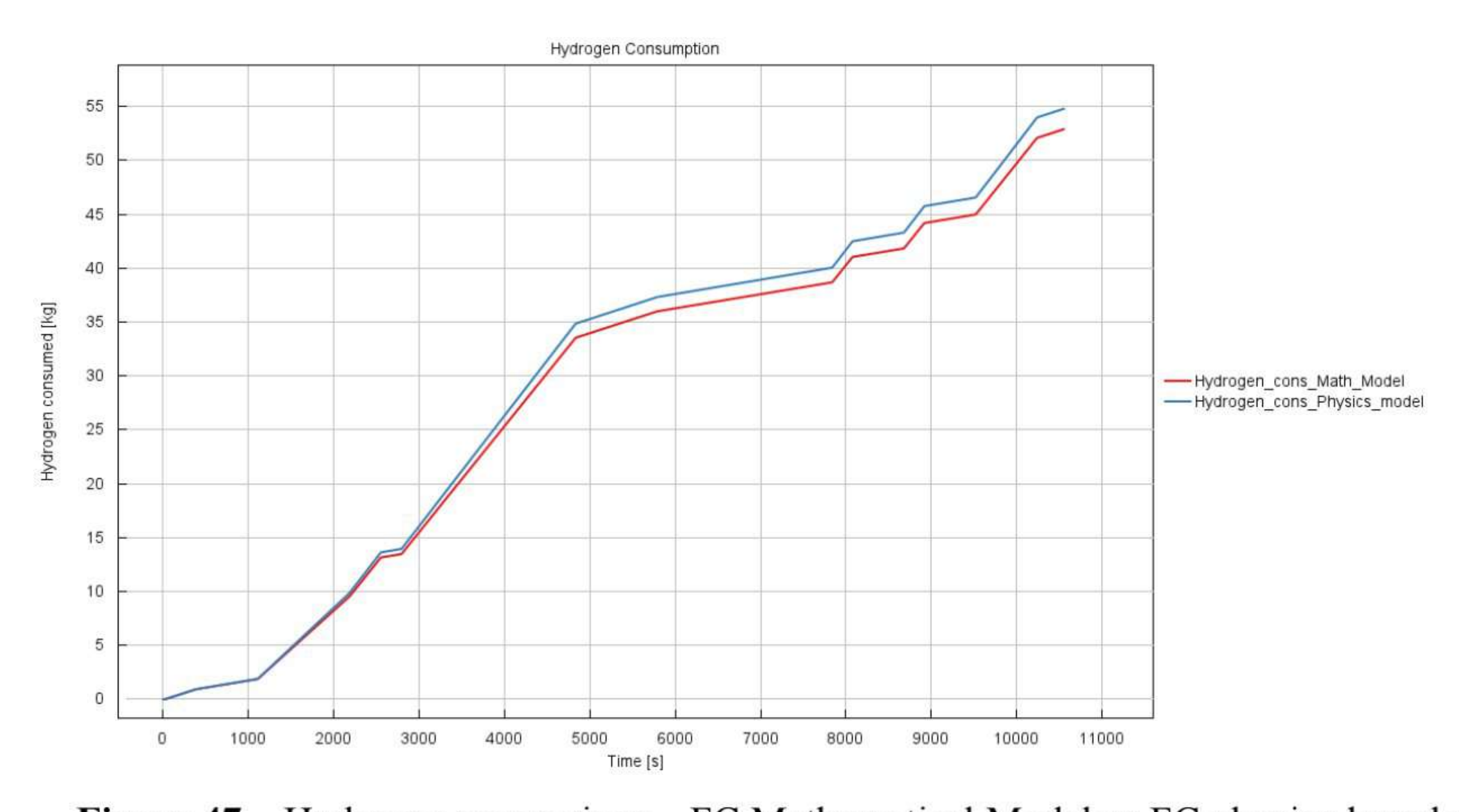


Figure 47 – Hydrogen comparison – FC Mathematical Model vs FC physics-based model

This section includes the results obtained on integrating the FC power-based algorithm with the physics-based template 'Fuel cell PEM'. The main objective behind this integration was to find out the significant parameter values which are required to match the results obtained through the mathematical model with the physics-based model. The significant input parameters, especially the number of fuel cells and active surface area were to be determined such that the FC produces the demanded power with the hydrogen consumption being similar to the one obtained

from the mathematical model. It was observed that the number of cells in the stack and active surface area were the two parameters that were highly affecting the FC efficiency and hydrogen consumption. Hence, various iterations were done on these two parameters in order to get the desired results which are mentioned in this section.

From the Figure 45, it can be seen that the power demand is completely met by the fuel cell. Apart from this, Figure 46 and Figure 47 depicts that there is a very close match between the efficiency and hydrogen consumption of the mathematical model and the physics-based model.

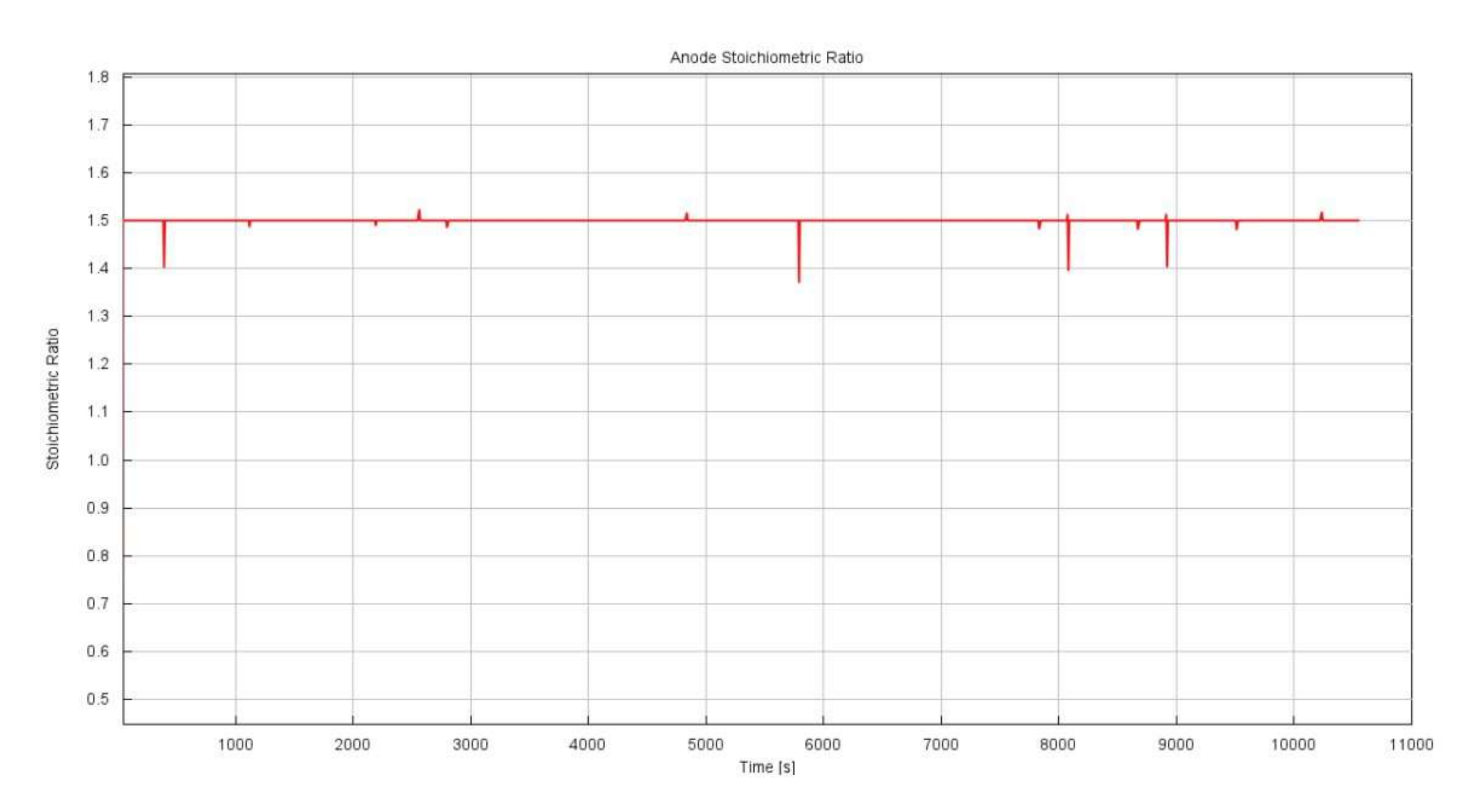


Figure 48 – Anode stoichiometric ratio

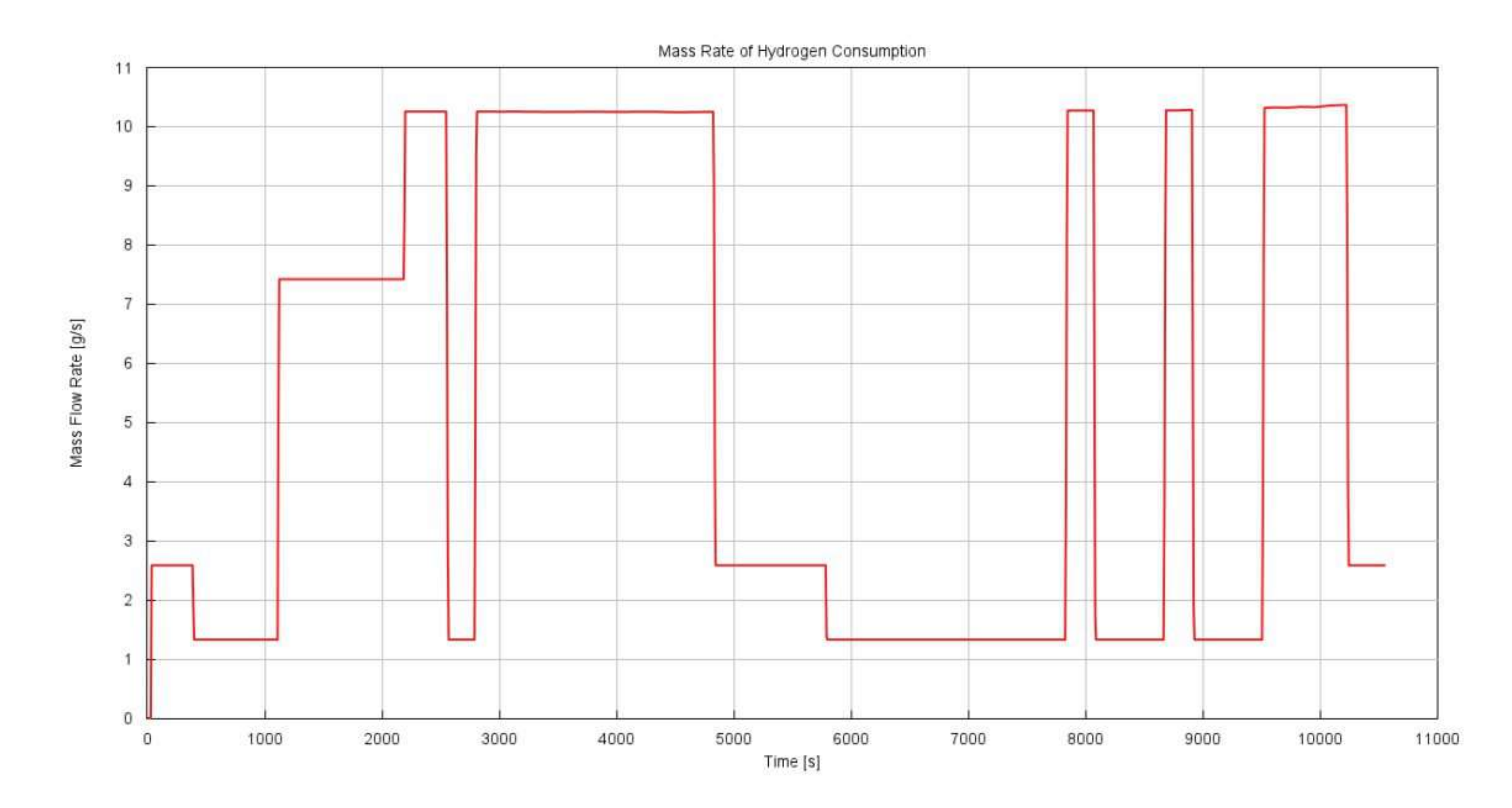


Figure 49 – Hydrogen mass flow rate

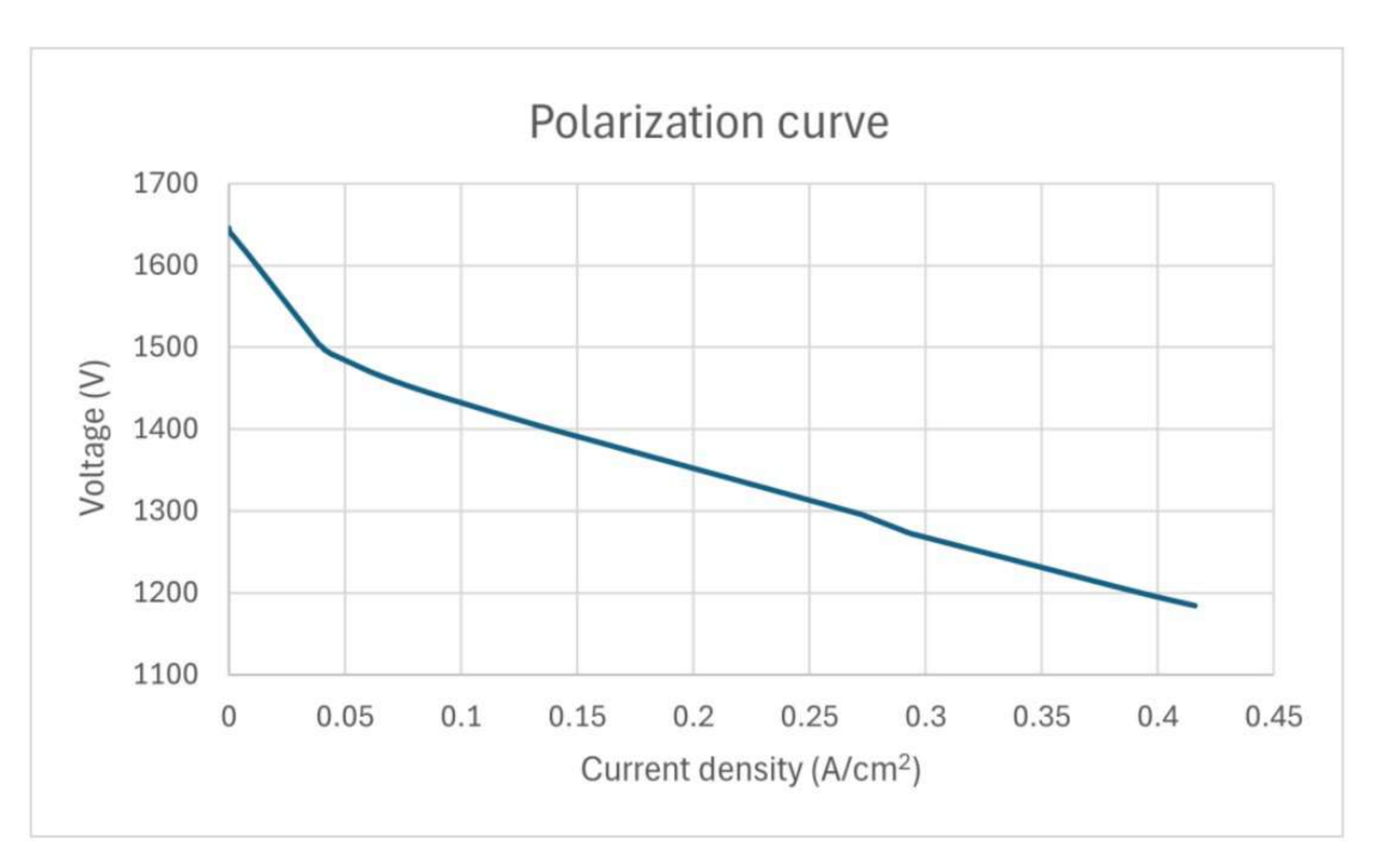


Figure 50 – Polarization curve obtained from the model

From the Figure 48, it can be seen that the anode stoichiometric ratio is maintained at 1.5 which is the standard value for a fuel cell. Figure 49 shows the mass flow rate of hydrogen at the anode which follows a trend similar to the power output from FC. By plotting the FC voltage and current density values obtained from the model, polarization curve is obtained as seen in the Figure 50. This fairly matches with the standard polarization curve of a FC.

Chapter 10

10. Conclusion and future scope

10.1 Conclusion

This thesis formulated a comprehensive framework for the design and simulation of a hybrid locomotive utilizing battery and fuel cell as the power sources. The entire thesis can be summed up into following critical steps-

- Formulating energy balance algorithms Three energy balance algorithms were established for efficient power split between fuel cell and battery. One of them was FC power centric while the other two were FC efficiency centric and battery SOC centric respectively
- Building mathematical simulation models The derived algorithms were implemented in GT-ISE as a simulation model and were integrated with the mathematical model of FC and a battery model
- 3. Performing Design of Experiments On the built mathematical model, DOE was conducted to obtain the optimum hardware configurations and control parameters. Sensitivity analysis identified critical variables influencing efficiency and reliability, guiding further refinements in fuel cell and battery integration. Using total cost as the cost function, best algorithm out of the three was obtained and various plots for this algorithm were plotted which gave deeper insights into the behaviour of the model.
- 4. Design of a FC physics-based model and integrating with the control logic A physics-based fuel cell model was constructed to provide a high-fidelity representation of hydrogen flow, electrochemical reactions, and thermal effects. Efforts were made to keep the model as less complex as possible without compromising with the physics so as to reduce the computational time.
- 5. Calibrating results of mathematical and physics-based fuel cell model Several iterations were made to obtain the values of significant FC physics-based model parameters which gave the desired power, efficiency and hydrogen consumption from the model. The model was also calibrated for desired polarization curve and anode stoichiometric ratio.

10.2 Future scope

Although the proposed hybrid locomotive design demonstrates promising results, several key areas remain open for exploration to enhance efficiency, reliability and further fine tune the design. Some of the key possibilities are mentioned below –

- Feed-forward control to smoothen the FC power profile Currently proposed algorithms focus on the inputs at present time step. Feed forward logic can be prepared wherein the FC output is defined based on the average power demand of few hundreds of future time steps. This will aid in smoothening the FC power output
- Inclusion of other locomotive systems in the model Parts like axles, wheels, vehicle body, brakes along with vehicle dynamics can be added into the model so that factors like inertia can betaken into account and outputs like vehicle velocity and acceleration can be observed
- Addition of cooling circuit in the physics-based model A cooling circuit can be integrated with the current FC model to have a better control over its temperature and make it more practical.
- 4. Inclusion of regenerative braking In the current model, the battery is charged only when there is surplus power produced from FC. Some regions can be determined in the drive cycle where regenerative energy can be used to charge the battery.

References

- 1. http://www.railway-technical.com/trains/rolling-stock-index-l/diesel-locomotives/
- David Murray-Smith, "A Review of Developments in Electrical Battery, Fuel Cell and Energy Recovery Systems for Railway Applications by", A Report for the Scottish Association for Public Transport, 2019, Pg. No.10
- 3. https://www.energy.gov/eere/fuelcells/types-fuel-cells, official website of US Department of Energy
- Vijay Ramani, Russell Kunz, James Fenton, "The Polymer Electrolyte fuel cell", Pg. No. 1
- Alessandro Franco, "Optimum design of bipolar plates for separate air flow cooling system of PEM fuel cells stacks", Table 1
- 6. https://www.fuelcellstore.com/blog-section/fuel-cell-information/fuel-cell-operating-conditions
- Muhammad Tawalbeh, Suma ALarab, Amani Al-Othman, "The Operating Parameters, Structural Composition, and Fuel Sustainability Aspects of PEM Fuel Cells: A Mini Review", MDPI
- 8. Luis Blanco, Luis Ordonez, Sergio Pena, "A Self-Validating Method via the Unification of Multiple Models for Consistent Parameter Identification in PEM Fuel Cells", MDPI, Page 3
- Julakha Jahan Jui, Mohd Ashraf Ahmad, M.M. Imran Molla, Muhammad Ikram Mohd Rashid, "Optimal energy management strategies for hybrid electric vehicles: A recent survey of machine learning approaches", Journal of Engineering Research, 2024, Pg No.457-458
- 10. US Dept of Energy Hydrogen Program Record, Record No 23002, Page No 1
- 11. Thessaloniki, September 21, 2011, Frank de Bruijn 'PEMFC Lifetime and Durability an overview', Page No. 2
- 12. www.sgh2energy.com
- 13. https://www.pnnl.gov/projects/esgc-cost-performance/lithium-ion-battery
- 14. "James Larminie, Andrew Dicks", 'Fuel Cell Systems Explained', Second Edition, 2003 John Wiley & Sons, Ltd., Pg No 398